

**MATHEMATICAL MODELLING AND EXPERIMENTAL STUDY
OF THE KINETICS OF THE ACID SULPHITE PULPING
OF EUCALYPTUS WOOD**

by

EDWARD WATSON

Submitted in part fulfilment of the requirements
for the Degree of Master of Science in Engineering
in the Department of Chemical Engineering of the
University of Natal

SUPERVISOR Professor M. Mulholland

DATE SUBMITTED 15th DECEMBER, 1992

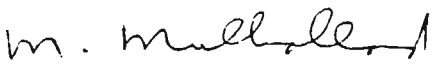
DECLARATION

I Edward Watson hereby certify that this research is a result of my own investigation, has not already been submitted in any substance for any degree, and has not been concurrently submitted in candidature for any other degree.

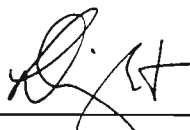


E. Watson

I hereby certify that this research is the result the of candidate's own investigation.



Professor M. Mulholland
SUPERVISOR



D. W. Wright
CO-SUPERVISOR

ACKNOWLEDGEMENTS

This thesis is the result of nearly five years of work and over this period the assistance, advice and support of many people have been sought out. This was always given freely and willingly and all of this input was eventually woven into the fabric of this project both implicitly and explicitly. It is not possible for me to mention by name the huge number of people who have assisted me in this work; however, there are those without which this would never have been completed.

The project relied totally on the financial and technical support provided by Sappi Saiccor. Mr Sinclair Stone and Mr Brian Thomas provided invaluable support and guidance personally, as well as by permitting Sappi Saiccor staff to spend time assisting with various aspects of the project. The design and construction of the Satellite Mini Digester plant was achieved with the assistance of the following people in the areas indicated:

Instrumentation Design and Construction: Sean Smith
Mechanical Design and Construction: Henry Zan
Electrical Design and Construction: Ronnie Palmer

Laboratory equipment and the use of laboratory facilities was arranged by Derek Simpson. In addition to this, he arranged for laboratory staff to assist with some of the analytical procedures - for which I am deeply indebted (a single experimental run required more than 40 different analyses to be performed).

The voluntary assistance of Siphon Zimba with the preparation and loading of cooking liquor was also greatly appreciated.

The untiring support and assistance of my wife Noelene, who married me despite the fact that this work was incomplete at the

time, is most probably the main reason why this thesis has now been completed. Apart from the moral support, she was entirely responsible for the editing and correcting of this document.

Finally, I must acknowledge the support and technical assistance of my supervisors Mr Dave Wright and Professor Mike Mulholland. Dave Wright's efforts led to the original inception of this project, and he was my supervisor for the first two years. He provided a tremendous amount of input at all stages of the project. Mike Mulholland took over as supervisor from Dave and has been extremely patient with me during the period in which it has taken me to complete this work.

ABSTRACT

The chemistry of the batch cooking process at Sappi Saiccor, relating to both the pulp and liquor, was investigated with the aim of using kinetic expressions to develop an improved process control model. The mill produces dissolving pulps using the acid sulphite method.

Three process reactions were identified as important: cellulose hydrolysis, delignification and hemicellulose dissolution. Of these, cellulose hydrolysis is the most important since the primary aim is to achieve a targeted cellulose degree of polymerisation (DP) or viscosity (DP is commonly expressed in terms of this measurement). This is directly determined by the rate of this reaction during the cook, and the acidity of the cooking liquor was found to be the key factor.

As existing equipment was not suitable for obtaining the data required to perform a kinetic analysis, a pilot plant was constructed. A commercially available probe was used for the first time to measure pH directly. The measured acidity is not directly equivalent to hydrogen ion activity at these temperatures and pressures; however, since the conditions of each cook are similar the errors incurred were found to be constant from cook to cook.

The probe was found to be prone to drift due to ageing and this was accounted for by using an 'on line' calibration based on a liquor analysis.

The kinetics of the cellulose hydrolysis reaction were determined using the on-line measurement of acidity and the concept of degradation increase (DI) which relates the reduction in DP value to the rate at which the polymeric chains are split. The kinetics were found to be accurately represented ($R^2=0.98$) by the expression:

$$DI = A_c e^{\left(-\frac{E_c}{RT}\right)} \int_{t=t_0}^{t=t_f} [H^+] dt$$

Delignification and hemicellulose dissolution were examined, since it is beneficial to maximise these reactions to reduce the quantities of chemicals consumed during the bleaching process.

A model for controlling cooks to a set target cellulose DP value within a set time was developed based on the reaction kinetics. This was capable of predicting cooking conditions required with sufficient accuracy to control the cellulose DP value to within ± 6 cp SNIA on the viscosity scale.

TABLE OF NOMENCLATURE

1) GENERAL

<u>SYMBOL</u>	<u>DESCRIPTION</u>
<i>DI</i>	Degradation Increase :- a measure of the number of linkages broken in a polymer ie. a measure of the 'extent of reaction' during a de-polymerisation reaction.
<i>DP</i>	Degree of Polymerisation :- ie. the number of repeating units in a polymeric chain.
<i>DD</i>	Degree of Degradation :- defined as the reciprocal of the degree of polymerisation.
<i>N</i>	Number of linkages between repeating units of a polymer.
\bar{M}	Average molecular mass of a polymer (g/mol).
\bar{M}_μ	Average molecular mass of a cellulose polymer given by the viscometric method (g/mol).
μ	Viscosity of cellulose as determined by the SNIA method (cp SNIA).
<i>t</i>	Time (minutes)
<i>T</i>	Temperature (degrees Celsius or Kelvin where indicated).
<i>R</i>	Universal gas constant (cal/gmol K).
<i>r_c</i>	Number of linkages broken in a cellulose polymer per unit time.
<i>k_c</i>	Arrhenius factor for the cellulose hydrolysis reaction.

A_c	Pre-exponential factor for the cellulose hydrolysis reaction.
E_c	Energy of activation for the cellulose hydrolysis reaction.
r_l	Rate of lignin dissolution.
k_l	Arrhenius factor for the lignin dissolution reaction.
A_l	Pre-exponential factor for the lignin dissolution reaction.
E_l	Energy of activation for the lignin dissolution reaction.
r_h	Rate of hemicellulose dissolution.
k_h	Arrhenius factor for the hemicellulose dissolution reaction.
A_h	Pre-exponential factor for the hemicellulose dissolution reaction.
E_h	Energy of activation for the hemicellulose dissolution reaction.
r_{SA}	Rate of formation of strong acid anions.
k_{SA}	Arrhenius factor for the formation of strong acid anions.
A_{SA}	Pre-exponential factor for the formation of strong acid anions.
E_{SA}	Energy of activation for the formation of strong acid anions.
$[H^+]$	Hydrogen ion concentration (mol/l).

- [HSO_3^-] Bisulphite ion concentration (mol/l).
- [L] Lignin concentration in solid phase (% m/m).
- K Permanganate Number:- measure of the lignin content of pulp.
- [H] Hemicellulose content of pulp:- defined as %S₁₈ (m/m).
- [SO_2^{tot}] Total SO₂ concentration as defined by the Palmrose test and expressed as mol/l.
- [SO_2^{com}] **AVAILABLE** combined SO₂ concentration (mol/l).
- [SO_2^{free}] Free SO₂ concentration as defined by the Palmrose test and expressed as mol/l.
- [SA^-] Concentration of strong acid anions corresponding to completely dissociated acids (mol/l).
- K_{SO_2} Sulphur dioxide protolysis in water (mol/l).
- K_p Sulphur dioxide solubility and protolysis in water
 $(\frac{(mol/l)^2}{bar (absolute)} mol/l)$.
- P_{tot} Total system pressure:- bar (absolute).
- P_{SO_2} Partial pressure of SO₂:- bar (absolute).
- P_{H_2O} Partial pressure of H₂O:- bar (absolute).
- ϕ Liquor-to-wood ratio at start of cooking (dm³/Kg).
- SF 'S Factor' parameter.
- θ 'Chemical-to-wood' ratio.
- E_{el} Electrode potential (mV).

E_o	Zero potential (mV).
pH_i	pH value of the internal buffer.
pH_a	pH value of the measured solution.
S	pH electrode characteristic slope.
J	Cost function.
T_{max}	Maximum cooking temperature.
pH_{calc}	Theoretically calculated pH value.
pH_{meas}	Physically measured pH value.
pH_{corr}	Average pH correction factor.
pH_{act}	pH value corrected for zero point shift.
pH_{err}	Zero point correction factor for an individual cook.

2) GENERAL SUBSCRIPTS

<u>SYMBOL</u>	<u>DESCRIPTION</u>
c	Cellulose.
l	Lignin.
h	Hemicellulose.
SA	Strong acid anions.
$pred$	Parameter as predicted by model.
act	Parameter actually achieved.
kin	Parameter estimated from kinetic model.
o	Parameter value at the start of the process.

tgt Desired value of parameter ie. target value.

3) EXPONENTS AND CONSTANTS

Exponents :- α , β , γ , a , and n .

Constants :- k_1 , k_2 , A , B , C , D , E , F , G , and M .

Table of Contents

CHAPTER 1 INTRODUCTION	1
1.1 The Process	2
1.2 The Origin of the Project	6
1.3 The Objectives of the Project.	6
CHAPTER 2_ WOOD CHEMISTRY IN THE PRODUCTION OF DISSOLVING PULPS	9
2.1 Definitions	9
2.2 Macroscopic Structure of Wood	10
2.3 Microscopic Structure of Wood	13
2.4 Cellulose	14
2.5 Lignin	26
2.6 Hemicellulose	39
CHAPTER 3 LIQUOR CHEMISTRY IN DISSOLVING PULP PRODUCTION	47
3.1 Liquor Composition	47
3.2 Charge Balances and Equilibrium Relationships.	49
3.3 Determination of Acid and Bisulphite Ion Concentrations.	52
3.4 Commonly Used Models for 'Cook End' Determination.	57
3.5 Comparison of Cooking Models	66
CHAPTER 4 EXPERIMENTAL EQUIPMENT DESIGN AND CONSTRUCTION	69
4.1 Summary of Reaction Kinetics to be Investigated.	69
4.2 Equipment Design and Construction.	75
4.3 Experimental Methodology and Results.	86
CHAPTER 5 EXPERIMENTAL RESULTS AND KINETIC ANALYSES	94
5.1 Typical Set of Results.	94
5.2 Discussion of Results.	96
5.3 Calculation of Bisulphite and Strong Acid Concentrations.	105
5.4 Kinetic Analysis of the Cellulose Hydrolysis Reaction.	115
5.5 Kinetic Analysis of Other Reactions.	122
5.6 Chapter Summary.	135
CHAPTER 6 DIGESTER COOKING MODEL DEVELOPMENT	139
6.1 Model Selection.	139
6.2 Model Requirements.	143
6.3 Model Development.	143
6.4 <u>Summary.</u>	162
CHAPTER 7 CONCLUSIONS AND RECOMMENDATIONS	169
7.1 Conclusions.	169
7.2 Recommendations.	179
REFERENCES	184
APPENDIX 1	190
SECTION A : VISCOSITY	190
SECTION B : PERMANGANATE NUMBER (K No.)	192
SECTION C : ALKALI SOLUBILITY OF PULP (S ₁₈)	193
SECTION D : PALMROSE METHOD	195
SECTION E : CHLORINE DIOXIDE BLEACHING	197
APPENDIX 2 SOLUTION OF CORRELATIONS TO OBTAIN EXPRESSIONS FOR [HSO₃⁻] AND [H⁺].	200
APPENDIX 3 MECHANICAL DRAWINGS OF SATELLITE MINI-DIGESTER PLANT	203
APPENDIX 4 DATA COLLECTION PROGRAMME LISTING	206
APPENDIX 5 EXPERIMENTAL RESULTS.	222
A-5.1 Experimental Run CK016.	222
A-5.2 Experimental Run CK017.	224

A-5.3 Experimental Run CK018.	226
A-5.4 Experimental Run CK019.	228
A-5.5 Experimental Run CK020.	230
A-5.6 Experimental Run CK021.	232
A-5.7 Experimental Run CK022.	234
A-5.8 Experimental Run CK023.	236
A-5.9 Experimental Run CK024.	238
APPENDIX 6 SAMPLE CALCULATIONS OF CHEMICAL CONCENTRATIONS	240
APPENDIX 7 DEFINITION OF THE pH VALUE	244

Table of Figures

1.1	Schematic Process Flow Diagram of the SAICCOR mill	3
1.2	Viscosity Deviations from Target for 1989	5
2.1	The Structure of a Cell Wall	11
2.2	Chemical Constituents in the Cell Wall	13
2.3	The Structure of Cellulose	16
2.4	Microscopic and Submicroscopic Structure of Cellulose	17
2.5	Mechanism of the Acid Hydrolysis Reaction	19
2.6	Functional Groups Found in Lignin	27
2.7	Proposed Structure of Protolignin in Spruce	29
2.8	Proposed Mechanisms of Lignin Sulphonation	32
2.9	Proposed Mechanisms of Delignification	33
2.10	Proposed Structures of the Hemicellulose Polymer	41
3.1	Cooking Time Determination Using Liquor Absorbance	65
3.2	Liquor to Wood Ratio Using Liquor Absorbance	65
4.1	Process Flow Diagram of Satellite Mini Digester Plant	79
5.1	Temperature and Pressure Profiles for Run CK016	95
5.2	pH Profile for Run CK016	95
5.3	Temperature and Pressure Profiles Reported by Ingruber	99
5.4	Typical pH Profile Reported by Ingruber	99
5.5	Comparison of Raw and Bleached Pulp Viscosities	103
5.6	Profiles of Chemical Concentrations During a Cook	107
5.7	pH Measurement Errors Caused by Temperature Effects	111
5.8	Corrected Chemical Concentration Profiles During a Cook	114
5.9	DI versus Integrated Hydrogen Ion Concentration	116
5.10	Determination of Parameters For Cellulose Hydrolysis	117
5.11	Comparison of Actual and Calculated Viscosities	121

Table of Tables

2.1	The chemical components of wood.	10
2.2	Typical DP Values for Various Sources of Cellulose	15
2.3	Functional Group Breakdown of Spruce Lignin	28
2.4	Percentages of Pentoses and Hexoses in Hardwoods	40
3.1	Definitions Referring to Liquor Composition	49
3.2	Values of Antoine Correlation Parameters	51
3.3	Decrease in DP for a set number of broken linkages	68
4.1	Instrument Calibration.	85
4.2	Typical Experimental Temperature Profile.	89
4.3	Cook Times at Maximum Temperature	90
5.1	Typical Set of Results From an Experimental Run	94
5.2	Series of Experimental Runs Performed	96
5.3	Effect of Chip Size on Pulp Characteristics	104
5.4	Activation Energies for Acid Hydrolysis of Cellulose	118
5.5	Estimation of Cellulose DP Value at $t = 0$	120
5.6	Kinetic Fit for the Delignification Reaction	124
5.7	Extent of Delignification Covered by Various Studies	127
5.8	Kinetic Parameters for the Delignification Reaction	127
5.9	Kinetic Fit for the Hemicellulose Hydrolysis Reaction	132
5.10	Kinetic Parameters for Hemicellulose Hydrolysis	134
6.1	Plant Temperature Profile	145
6.2	Linear Target Model Regression Results	150
6.3	Quadratic Target Model Regression Results	154
6.4	Standard Errors for Cook Time and Viscosity	156
7.1	Varying Residual Hemicellulose with Fixed Viscosities	177

CHAPTER 1

INTRODUCTION

SAICCOR (the South African Industrial Cellulose Corporation) is situated close to the town of Umkomaas, 48 km south of Durban. It was originally set up in 1953 by Courtaulds (UK), Snia Viscosa (Italy) and the Industrial Development Corporation (SA) to supply dissolving pulp for Courtaulds' viscose rayon fibre and cellophane film processes. By the time SAICCOR was acquired by the SAPPI group in September 1988, it had become the largest mill of its sort in the world, providing in the region of a quarter of the free world's demand for this type of pulp.

Dissolving pulps are used to manufacture a great diversity of products, of which the most important is rayon textile fibre. Rayon products range from clothing fabrics and textiles to non-woven disposables used in surgical and hygiene products. Other products include cellophane film, cellulose acetates, cellulose ethers and nitro-cellulose. In the manufacture of rayon fibres, the pulp is first dissolved using a number of steps involving the addition of alkali and carbon disulphide. It is then re-precipitated by passing the solution through microscopic nozzles and simultaneous neutralisation to eventually form the fibre.

The mill currently uses 1,2 million tons of timber to produce 400,000 tons of dissolving pulp per annum. The timber used at the mill consists of approximately 85% eucalyptus (mostly Eucalyptus Grandis and Eucalyptus Saligna) and 15% wattle (Acacia Molissima). It is necessary at this point to emphasise the differences between the properties of dissolving pulps and the pulps produced for paper, board and tissue products. The important attributes of paper and board pulps are mostly physical properties

such as tear and burst strength, whereas the important properties of dissolving pulps depend primarily on purity (92.5% Alpha Cellulose) and the Degree of Polymerisation (DP) of the cellulose fibres.

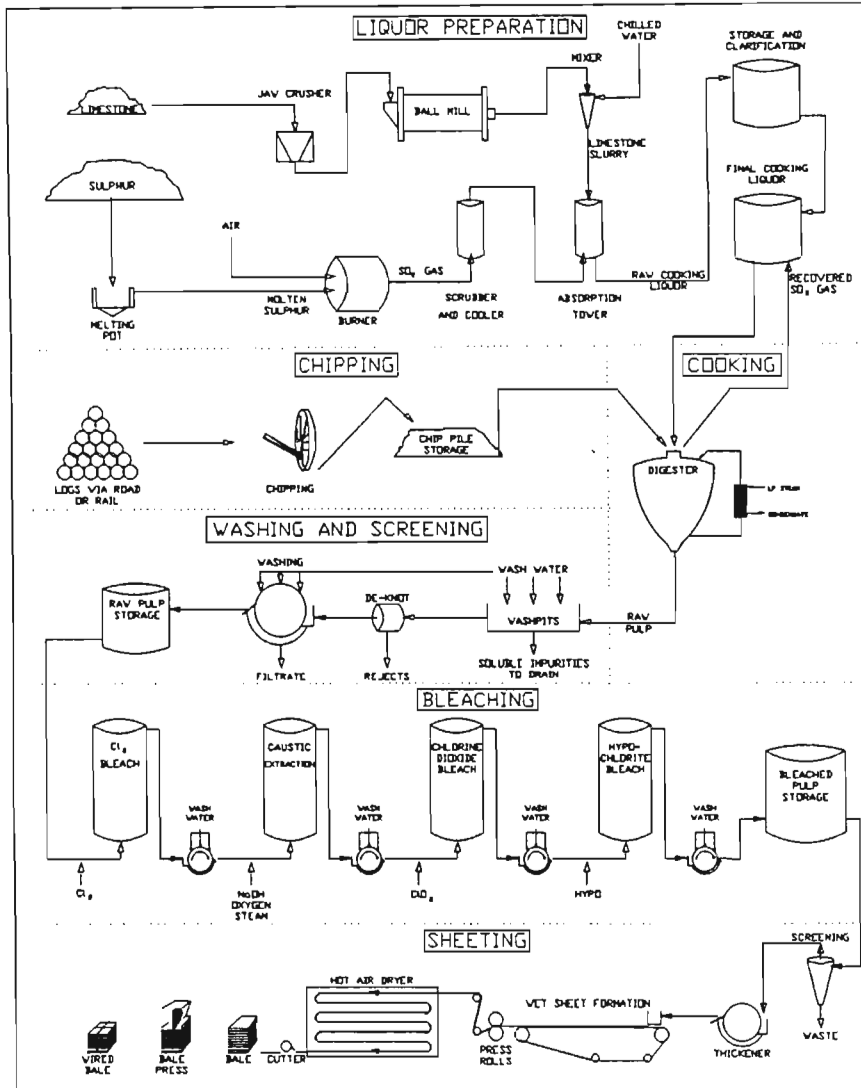
1.1 The Process

The process used at SAPPI SAICCOR centres around the 'acid sulphite' pulping of wood chips. This involves the batch cooking of chips, at temperatures of up to 147°C and at a pressure of 10.4 Barg, in a liquor consisting of approximately 6% to 7% (m/m) dissolved SO₂ gas and 1.2% (m/m) combined SO₂. The combined SO₂ corresponds to the base content of the cooking liquor and is present in the form of a bisulphite. Two bases are used at the SAPPI SAICCOR plant: the older section of the plant (14 digesters) uses calcium-based cooking liquor and the new section (6 digesters) uses magnesium-based cooking liquor. The reason for the change to magnesium-based liquor on the new plant is that it can be recovered and recycled, whilst the spent calcium-based liquor is discarded as effluent.

The initial composition of the chips is roughly 1/3 water, 1/3 cellulose and 1/3 a complex mixture of lignin, resin gums and sugars. During the cooking process, approximately 98% of the lignin is dissolved, around 90% of the hemicellulose is hydrolised, and the degree of polymerisation (DP) of the cellulose fibres is reduced. The final average chain length and the DP distribution of the cellulose are of fundamental importance as these are the characteristics which are vital to the final product. The rest of the process consists of washing, screening, bleaching and drying. (For a more detailed overview of the entire process refer to Figure 1.1.)

FIGURE 1.1

Schematic Process Flow Diagram of SAPPI SAICCOR



Accurate scheduling and control of the cooking process is essential to ensure a steady supply of uniform quality pulp from the batch-run cooking process to the rest of the plant, which operates on a continuous basis. This will ensure that the entire plant runs smoothly and produces a uniform and high

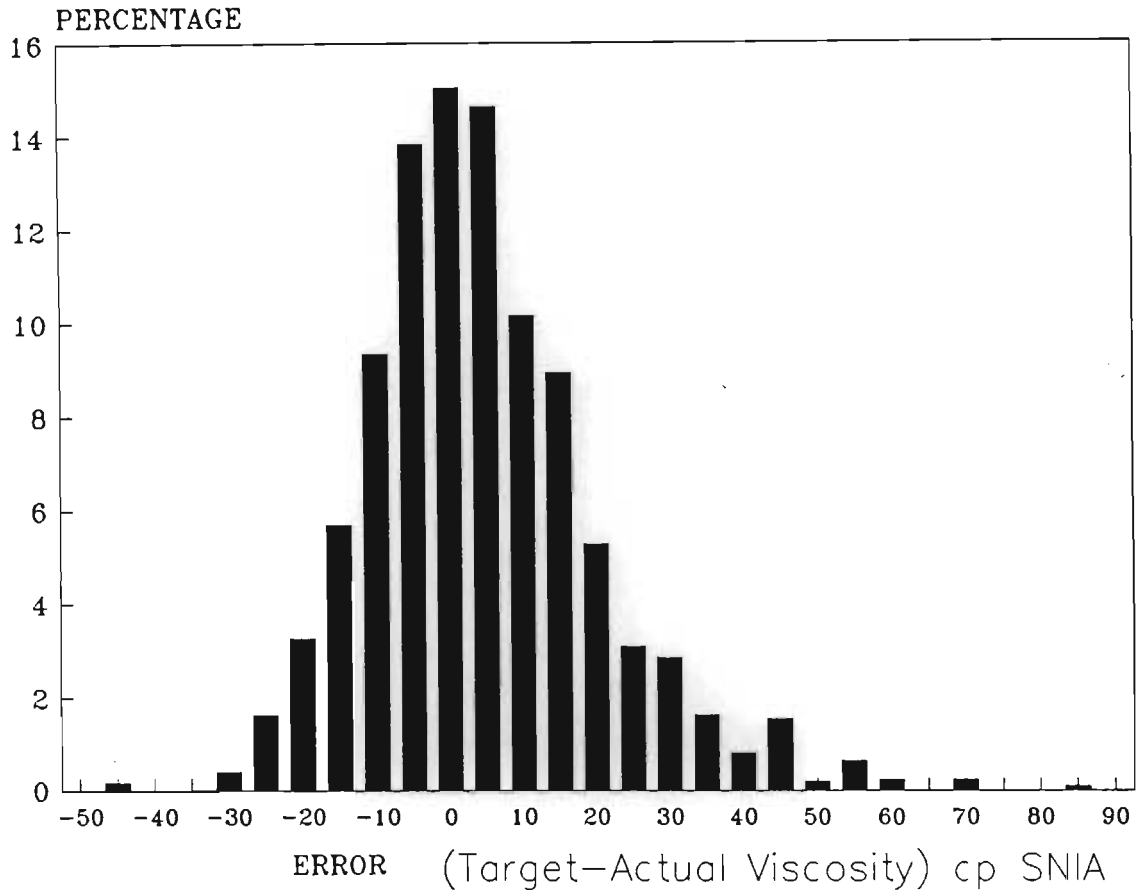
quality product. Final quality control adjustments are made in the bleaching process; although the pulp supplied from the digesters to this process can be made more uniform by blending, the end result will be limited by the uniformity of the pulp which can be achieved in the cooking process.

The cooking process at SAPPI SAICCOR is currently controlled by a computerised model, called the 'S Factor' model. The original form of this was developed by Yorston & Liebergott¹ in the early 1960s. The coefficients of the model are determined statistically from the regression of plant data, which is continuously updated using a feedback process.

This model not only attempts to schedule the digesters but also to control the energy input to them, in order to achieve a target average cellulose DP within the scheduled cook time. The weight average of the cellulose DP is measured by dissolving the cellulose in cuprammonia and then measuring the viscosity of the resulting solution. An idea of the success achieved by the model can be gained from the frequency distribution shown in Figure 1.2.

FIGURE 1.2

Frequency Distribution of Viscosity Deviation from Target
for 1989



It is difficult to separate out deviations caused by disturbed plant operations; however, the above results give some indication of the capabilities of the 'S Factor' model over an extended period.

In the increasingly competitive dissolving pulp market, this degree of variation is beginning to become a problem. The quality variations in the pulp resulting from the cooking process can be reduced by blending and by adjusting the bleaching process. However, both these solutions have their drawbacks.

Blending a high viscosity pulp and a low viscosity pulp may yield the target weight average DP. However, the DP distribution becomes bi-modal and this still causes problems in the tertiary processes (eg. viscose manufacture). Adjusting the bleaching process requires accurate dosing control, which is extremely difficult to achieve in a process which has a long retention time relative to the rate at which the nature of the pulp feed varies.

1.2 The Origin of the Project

A recent investigation² into improving control of the cooking process reviewed the literature available at the time and concluded that a model with a mechanistic basis offered the best probability of not only improving its accuracy but also of increasing understanding of the entire cooking process. Based on the strength of these findings, it was decided to initiate a project which would investigate the important reactions involved in the acid sulphite process used at SAPPI SAICCOR, and then to use these findings to develop a new model to control the digesters.

The important reactions, in order of precedence, have been identified as:

- i) Acid hydrolysis of cellulose.
- ii) Delignification.
- iii) Hemicellulose hydrolysis and dissolution.

1.3 The Objectives of the Project.

The objectives of the project were thus defined as the following:

- i) Investigate the suitability of available experimental equipment and, if none exists, design, construct and commission the required experimental equipment.
- ii) Experimentally measure and calculate the kinetics of the three important reactions identified above with particular reference to the cellulose degradation reaction, as it is the rate of this reaction which determines the average DP at the end of the cooking process.
- iii) Using the data, the correlations and the kinetic model obtained for cellulose degradation, develop a cooking model with the aim of improving viscosity control (ie. cellulose DP at the end of the cook). This model should satisfy the following prerequisites:-
 - a. The model must be able to achieve a target DP (viscosity) in a fixed cook time.
 - b. It should be simple and robust, thus allowing easy integration into an industrial situation.

As mentioned above, SAPPI SAICCOR uses both calcium and magnesium cooking liquors. For the purpose of this study, it was decided to consider only the calcium-based process. The reason for this was due to the fact that a good representative pulp sample for any individual cook on the plant is obtained most easily for calcium-based cooks because of the design of that section of the plant. It was further felt that this would greatly simplify the correlation of results if any work was performed on the actual plant itself. Essentially however, the mechanisms of the reactions should not differ with the base used, although the absolute reaction rates will definitely do so.

The cooking process as a whole can be understood only if the chemistry of both the wood and the liquor is clearly understood.

A brief summary of the chemistry of both was included in the original project²; however it is felt that a far more comprehensive explanation is required to fully understand the cooking process. A comprehensive review of wood and liquor chemistry is therefore presented in the following two chapters.

CHAPTER 2

WOOD CHEMISTRY IN THE PRODUCTION OF DISSOLVING PULPS

2.1 Definitions

Botanically, trees are divided into two main groups:

- Gymnosperms, more commonly called softwoods or conifers, and
- Angiosperms, more commonly called hardwoods or broad-leaved trees.

The designations 'softwood' and 'hardwood' are used merely to distinguish between two different botanical classes and are not otherwise accurately descriptive. As only hardwood species are pulped at SAPPi SAICCOR, the discussion here will concentrate on them, although most common hardwoods and softwoods are much alike in chemical composition.

Due to the complex heterogeneous nature of wood, it is extremely difficult to define chemically or to distinguish between some of the components. It is impossible to separate the various chemical species quantitatively due to the fact that they are mostly of high molecular weight, as well as being intimately mixed and combined in native wood.

The composition of wood can be divided into four broad categories of chemical species. These are briefly outlined in Table 2.1 and are then discussed in detail.

TABLE 2.1

The Chemical Components of Wood

Component	Description ³	Percentage
Cellulose	Linear polysaccharide of sufficient chain length (DP) to be insoluble in water and dilute alkalis or dilute acids at room temperature. Consists only of anhydroglucose units linked together with 1:4-β-glycosidic bonds and possessing a well-ordered structure	45.6 % (45 ± 2%)
Hemicellulose	Non-cellulosic polysaccharides of wood such as glucose, mannose, galactose, xylose and arabinose as well as related substances (such as uronic acids, etc.)	26.5 % (35 ± 5%)
Lignin	Complicated phenolic three-dimensionally branched network consisting of four or more phenylpropane monomers per molecule.	25.7 % (20 ± 4%)
Extractives	Low molecular weight compounds, extractable from wood with either water or organic solvents. Excluding compounds which, by definition, belong to the hemicelluloses or lignins.	0 % (5 ± 3%)

* Typical analysis of Eucalyptus Grandis (used in this study) on an extractive free basis⁴²
(Balance is ash). Values in parentheses are average compositions for hardwoods⁴.

2.2 Macroscopic Structure of Wood

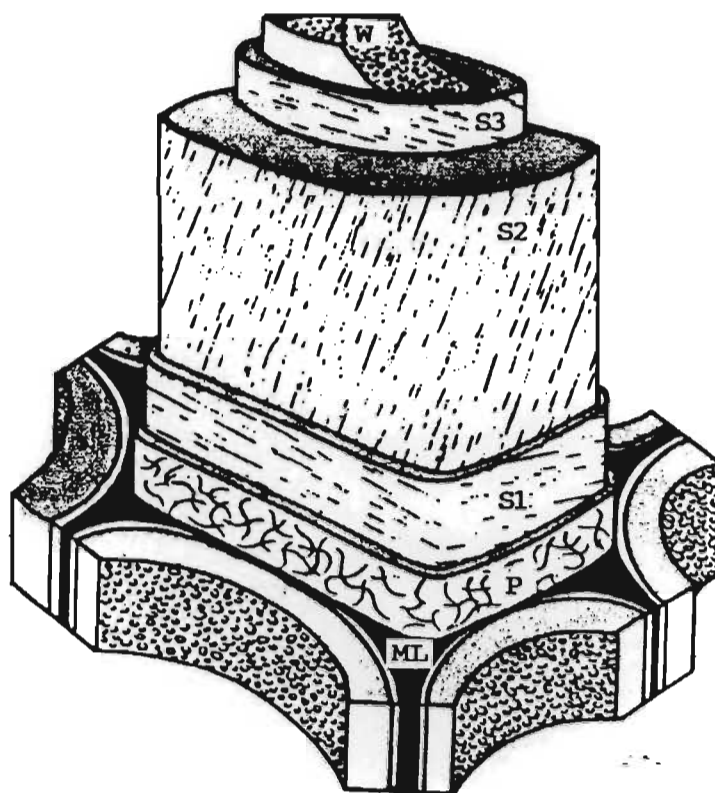
The macroscopic structures of softwoods and hardwoods differ markedly. Softwoods consist of fibres which have average lengths of between 3 and 4 millimetres and are characterised by pits along their radial surfaces. These fibres are called tracheids and they serve to conduct fluids in the sapwood of a growing tree. The fibres in hardwoods are called libriform fibres and do not conduct fluids; instead they are mixed with a proportion of relatively wide vessels with extremely thin walls (often called pores) which are responsible for conducting the fluids. The fibres in hardwoods have an average length of 1 to 1½ millimetres and are more slender and solid than those of

softwoods. In both softwoods and hardwoods, the fibres are bonded together by a layer called the middle lamella which is composed almost entirely of lignin⁵.

Despite the fact that the macroscopic structures of softwoods and hardwoods differ in gross dimensions, the structures of their cell walls are remarkably similar. Figure 2.1 shows a schematic representation of the various layers which make up a libriform fibre cell wall.

FIGURE 2.1

Schematic Representation of the Structure of a Cell Wall⁵

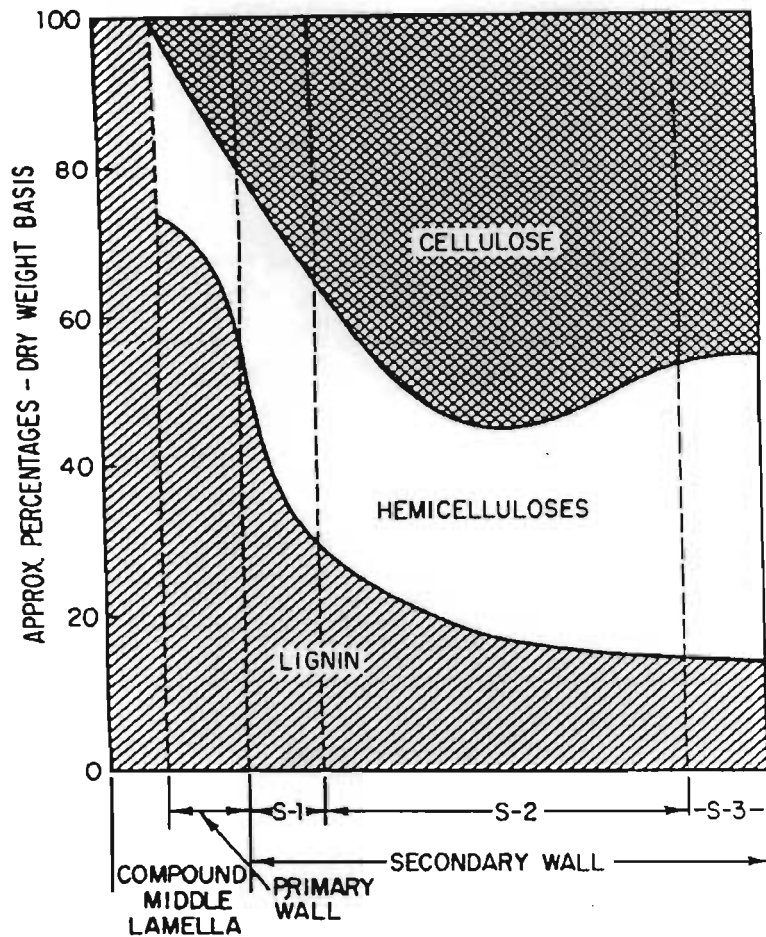


As can be seen from the above diagram, a fibre is composed of several distinct layers. Surrounding the fibre is the heavily lignified and stiff middle lamella (ML), which is shared with the adjacent fibres. The outermost layer is the primary wall (P). The secondary wall is not homogeneous and can be subdivided into the outer layer of the secondary wall or transition lamella (S1), the main secondary wall (S2), and the inner layer of the secondary wall or tertiary wall (S3 or T). The three layers of the secondary wall are characterised by different alignments of the fibrils to the axis of the fibre. The fibrils consist of 'bundles' of microfibrils, which in turn consist of aggregates of cellulose molecules. The primary and secondary walls consist of a varying number of microfibrillar layers (laminae). In the centre of the fibre is a void called the lumen (W).

The distribution of celluloses, hemicelluloses and lignins varies from layer to layer and, as mentioned previously, they are intimately mixed in with each other. Figure 2.2 shows the approximate distribution of these chemical constituents in the cell walls.

FIGURE 2.2

Distribution of Chemical Constituents in the Cell Wall^{3,6}



2.3 Microscopic Structure of Wood

The nature of the lignin-carbohydrate complex is a subject of considerable interest in that native wood behaves very differently from its constituents. This is evident from the fact it is extremely difficult to extract the different wood components using solvents in which they are normally soluble as isolated products. For example, lignin preparations are soluble in alkali or dioxane but cannot be separated from native

wood by these solvents. Similarly, carbohydrates are soluble in cuproxam solutions but cannot be completely extracted from wood without additional chemical treatments. These observations raise the question as to whether the association between the carbohydrates and lignins is chemical, mechanical or a combination of both³.

The structure of the fibre wall has been studied with the use of electron micrographs, and these have shown that lignin and hemicellulose occur amorphyously in the fibre wall. In contrast to this, the cellulose is present as a distinct separate crystalline phase³. These findings indicate that while a chemical association between cellulose and lignin is unlikely, bonds between hemicellulose and lignin cannot be ruled out. Further research^{17,18} has established that the hemicellulose-lignin linkage is a glycosidic bond. The lignin-carbohydrate complex differs between hard and softwoods, as the lignin concentration tends to be greater at the middle lamella in hardwoods. In addition to the chemical linkages, the intimate physical association between the various components is also thought to result in a significant mechanical hindrance to the separation of the various components¹⁹.

Now that the physical nature of wood has been discussed, the detailed chemistry of the three major components, namely cellulose, hemicellulose and lignin, is discussed in the following sections.

2.4 Cellulose

2.4.1 Structure

The basic building unit of cellulose is D-glucose and the polymer is formed by condensation reactions between the D-glucose molecules. As defined in Table 2.1, cellulose is thus a polysaccharide which consists of large numbers of

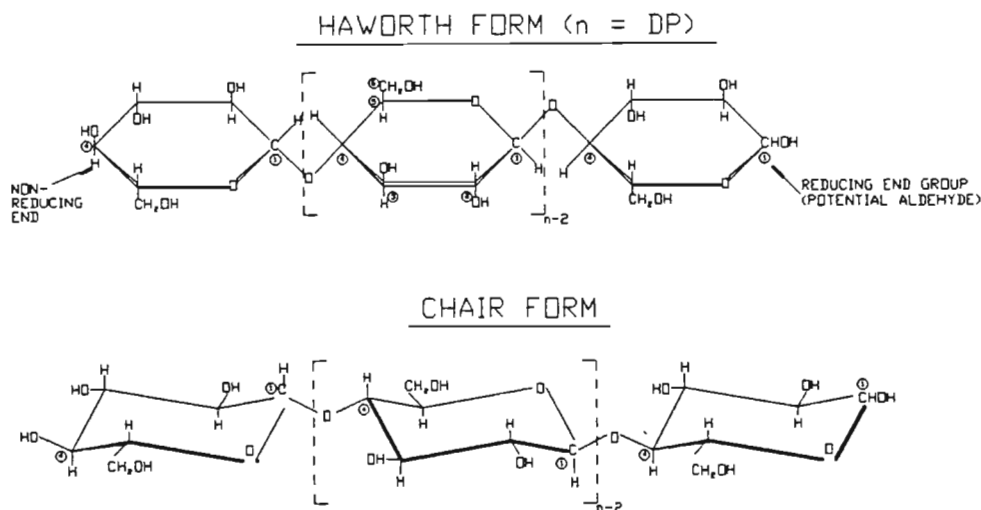
repeating anhydroglucose units. The chemical formula for cellulose is $(C_6H_{10}O_5)_n$, where 'n' is the number of repeating sugar units or the degree of polymerisation (DP). The DP value of cellulose varies depending on the source and on how it was isolated, treated and purified. Typical values have been included in Table 2.2.

TABLE 2.2	
<u>Typical DP Values for Various Sources of Cellulose</u>⁴	
(Weight averages)	
Source	Typical DP
Native cellulose (in situ)	3500
Purified cotton linters	1000 to 3000
Commercial wood pulps	600 to 1500
Regenerated cellulose (eg. rayon)	200 to 600

The molecular structure of cellulose is shown in Figure 2.3. From this it can be seen that the recurring unit is actually two consecutive anhydroglucose units (called a cellobiose unit). Of specific significance is the fact that the D-anhydroglucose units in cellulose are joined by 1,4- β -glucosidic bonds. Starch is a 1,4- α polymer of D-anhydroglucose, thus both cellulose and the linear fraction of starch (amylose) are polymers of D-anhydroglucose. However, their completely different structures and characteristics are caused by the differences between their associated 1,4 linkages which bond the individual glucose units together.

FIGURE 2.3

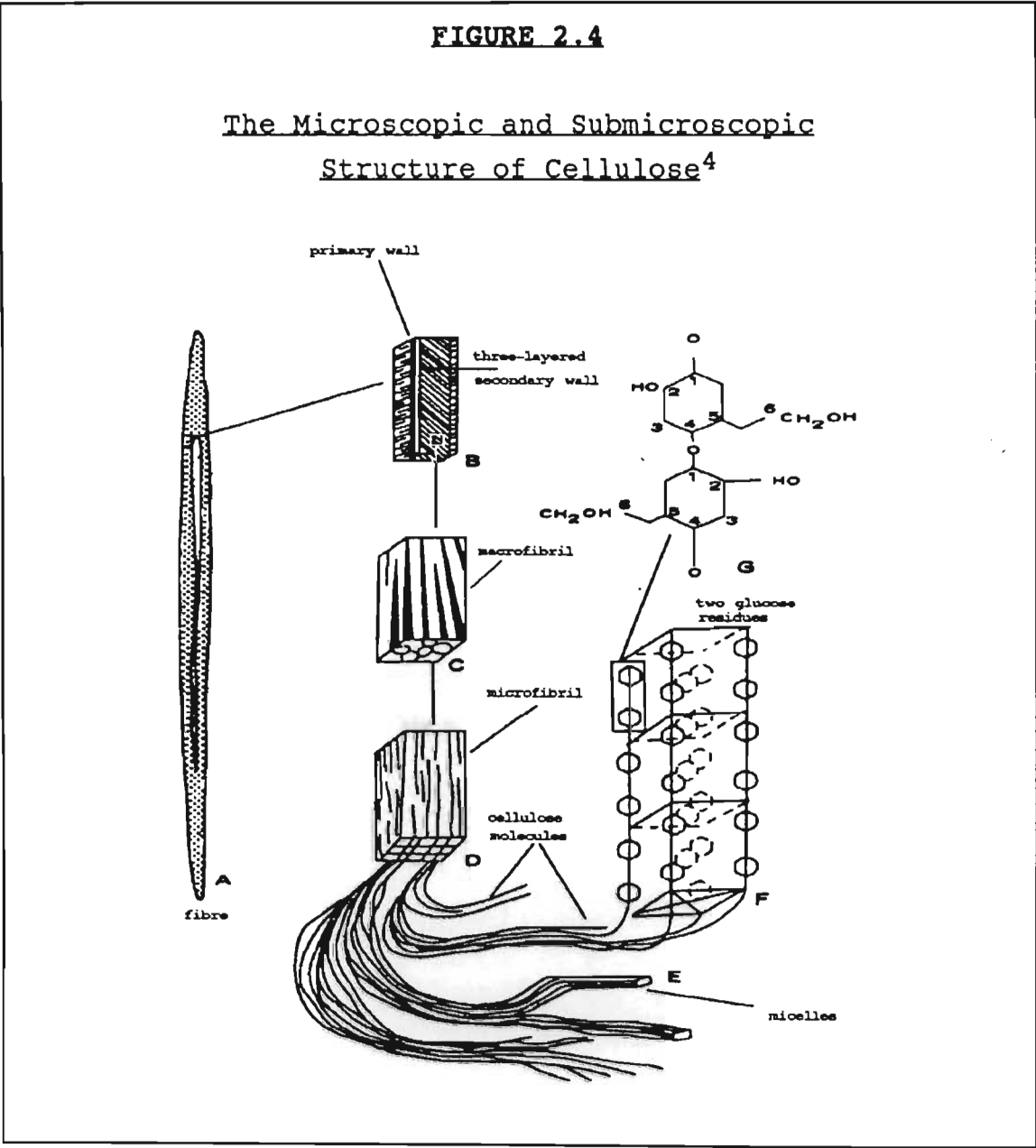
The Structure of Cellulose⁵



The β linkage results in a 180° rotation of the plane of the alternate glucose units. This alternation causes the cellulose molecules to form as a straight chain of indefinite length, in contrast to the non-alternating structure of starch which results in a helical or spiral construction⁶. The linear-chain structure of cellulose allows the molecules to fit compactly together over long segments which result in hydrogen bonds forming between the adjacent molecules. These associative forces allow regions of crystallinity to develop.

The cellulose molecules in plant fibres have varying levels of ordered orientation, ranging from very ordered crystalline structures to amorphous regions. The crystalline regions are difficult to penetrate by means of solvents and reagents, and are consequently more resistant to hydrolysis reactions when

compared with the more amorphous regions. The microscopic and sub-microscopic structure of cellulose is further illustrated in Figure 2.4.



2.4.2 Reactions of Cellulose

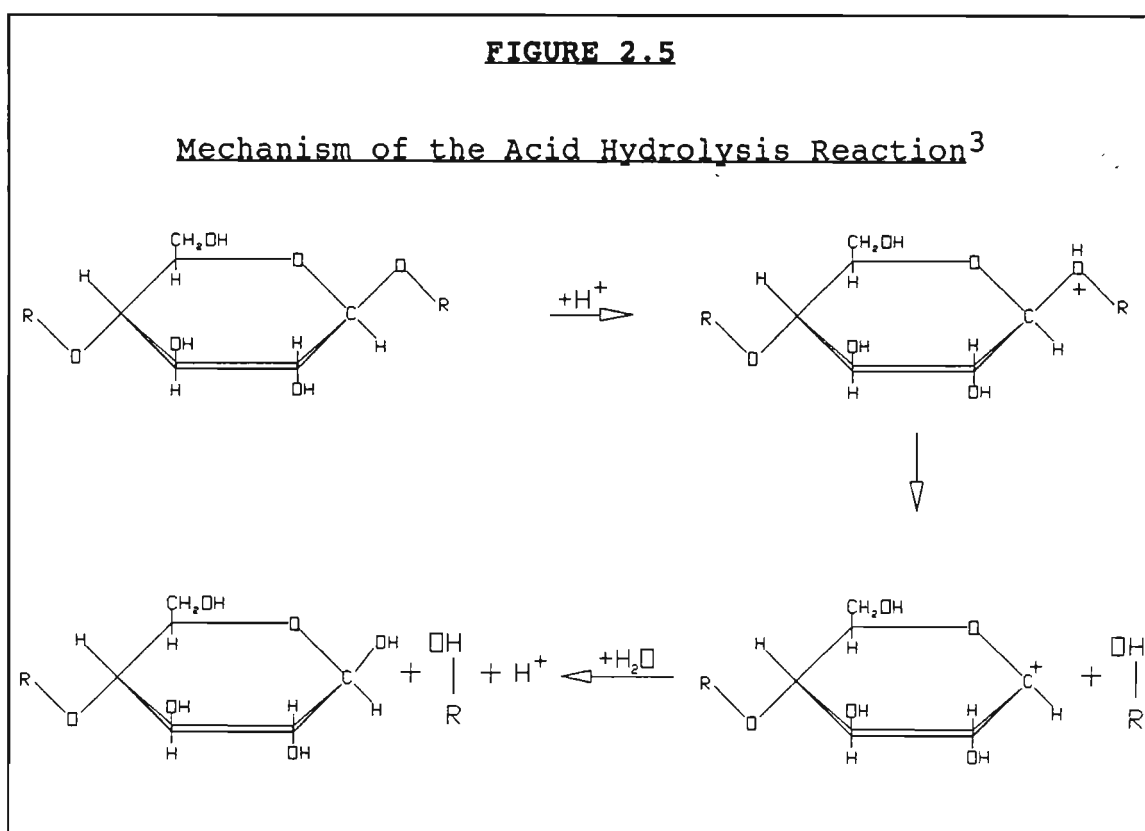
The hydroxyl and acetal groups as well as the aldehydic end groups, associated with the cellulose molecule, are reactive³. A brief summary of the reactions relevant to each group has been included below:

- Hydroxyl groups react with substitution, addition and oxidation agents.
- Acetal groups undergo hydrolysis in acid as well as in alkaline mediums.
- Under the influence of an alkali, aldehydic end groups can be reduced to alcohol groups, oxidised to carboxyl groups or rearranged to form alcohol or carboxyl end groups.

Of the above reactions, substitution and addition reactions are only of importance in the tertiary processing of purified dissolving pulps. The REDOX and rearrangement reactions are important only during bleaching, when extreme oxidative and hydrolytic modification of the carbohydrates occur. The only reaction of importance in acid sulphite cooking is the acid hydrolysis reaction, which causes chain scission of the cellulose molecules and thus reduces the average DP values of these molecules.

The rate of the acid hydrolysis reaction is affected by electrophilic groups present in the individual monomers making up the extended cellulose molecule. These effects are of no real significance during the cooking process however, as it is now generally accepted that wood cellulose in its native state does not contain carbohydrate monomers other than D-glucose or linkages other than 1,4- β -glucosidic bonds⁶. (These effects do become significant during and after the bleaching processes, during which some of the sugar monomers are modified by introducing electrophilic groups.)

A probable mechanism for the acid hydrolysis of an acetal bond was developed by Clermont & Schwartz⁷. They considered the mechanism to be as follows: A proton is added to the acetal oxygen and heterolysis results in the formation of an intermediate carbonium ion, which finally reacts with water to re-form the proton. The reaction mechanism is illustrated in Figure 2.5, from which it can be seen that the ultimate result of the reaction is that the cellulose molecule is split into two.



The supermolecular structure of wood cellulose does exert some influence on the rate of the hydrolysis reaction, with the more amorphous areas (which are the most accessible) being degraded first. The result of this is that the DP of the main fraction of cellulose decreases more rapidly at the start of

the hydrolysis. Subsequent hydrolysis rates have been found to become constant once the degree of accessibility becomes more homogeneous throughout the fibre³.

A stage is eventually reached where the hydrolysis rate drops right off. This point is thought to occur when the DP corresponds to the average length of an elementary fibril fragment (crystalline segment). The DP at which this occurs is commonly of the order of 100 to 200, and thus this phenomenon is of no further importance here as final DP values after the cooking process range between 900 and 1200.

2.4.3 Reaction Kinetics and Analytical Methods

From the description of the acid hydrolysis reaction given above, it can be seen that the kinetics of the cellulose degradation reaction should be directly related to the hydrogen ion concentration of the cooking liquor and to the temperature. This relationship cannot be directly obtained because of three complicating factors, namely:

- The reduction in cellulose DP has to be directly related to the number of hydrolysis reactions (cellulose chain scissions) that have occurred, in order to develop a valid kinetic expression.
- A direct measure of cellulose DP is not practical.
- The degradation of cellulose molecules, while they are still an integral part of a fibre, forms a heterogeneous reaction system.

For the purpose of this study these factors were handled as follows:

1) Calculation of Extent of Reaction.

The hydrolysis reaction causes random cleavages of the cellulose polymer resulting in a reduction in DP of the cellulose molecules. However, this reduction cannot be used directly in a kinetic model. Matthus^{8,9} developed the concept of the 'degree of degradation' (DD), which ultimately allows the DP reduction to be directly related to the number of cleavages and thus to the extent of the reaction. The degree of degradation is defined as the reciprocal of the DP. The advantage of this concept lies in the fact that the reduction in DP from DP_0 to DP_f can be related to the number of linkages broken, which is defined as the degradation increase (DI):

$$DI = \frac{1}{DP_f} - \frac{1}{DP_0} = DD_f - DD_0 \quad (2-1)$$

The rate of hydrolysis can be related to the rate of change in the number of linkages, or $-dN/dt$, where N is equal to the fraction of remaining linkages (1-DI). Using this concept the hydrolysis reaction rate can then be written as:

$$r_c = -\frac{dN}{dt} = \frac{d(1-DI)}{dt} = \frac{-d(DI)}{dt} \quad (2-2)$$

This concept provides a much clearer picture of the degradation process than the DP value or the viscosity because it represents a linear relationship with the extent of reaction. The DP value provides an extremely distorted and non-linear response when used to measure the extent of reaction and the viscosity measurement introduces further non-linearities.

2) Estimation of Cellulose Degree of Polymerisation.

Cellulose, like most polymers, consists of a mixture of molecules which differ widely in size. The value reported for the molecular weight of a sample is thus an 'average' value, the nature of which depends on the measuring technique used. A number of techniques are available, and include osmometry, ultrafugation, light scattering measurements and viscometry. The first three methods, although capable of giving a specific break down of DP distribution, require highly specialised equipment and are extremely time-consuming. They are thus used only for specialised studies of DP distribution or as a once-off exercise to calibrate viscosity measurements in terms of average DP. In contrast to this, the viscometry method is simple and relatively quick; consequently, the DP value is most commonly estimated from viscosity measurements.

The solvents most often used in the viscometric methods are cuprammonium (Cuam) or cupriethylene diamine (CED). These solvents are powerful swelling and complexing agents, capable of completely disrupting the crystal lattice of the cellulose fibres and then complexing with the cellulose hydroxyl groups to prevent the molecules from re-associating. The resulting gel-type solution will then exhibit a viscosity which can be related to the average DP value of the cellulose molecules. The actual average obtained from the viscometric method, given in terms of average molecular weight (\bar{M}), is shown in equation 2-3 and is very close to the weight average as the constant α has been found to be close to 1³:

$$\bar{M}_\mu = \frac{\sum n_i \cdot M_i^{\alpha+1}}{\sum n_i \cdot M_i} \quad (2-3)$$

The viscosity measurement technique used for quality control at SAPPI SAICCOR is based on the SNIA standard (See Appendix I Section A) which uses cuprammonium as the solvent. This method was thus used for all viscosity measurements reported in this study as this enabled the results to be compared directly to actual measurements made at the factory. The correlation between the DP value and viscosity was determined by a non-linear regression performed on standard conversion tables available from literature¹⁰. The resulting correlation is shown as equation 2-4:

$$DP = 285.4 \cdot \mu^{0.345} \quad (2-4)$$

$R^2 = 0.997$ over range $20 < \mu < 150$, μ based on SNIA standard.

3) Kinetics of the Cellulose Hydrolysis Reaction.

Due to the heterogeneous nature of the reaction system, the influence of diffusion on the reaction rates must be considered. A tremendous amount of research on the penetration of acid sulphite cooking liquors into wood chips and the effects of diffusion on reaction rates has been conducted. All the early research work^{11,12} concluded that once the capillary system of the wood has become completely penetrated, the diffusion paths are very short and thus the influence of diffusion on the overall reaction rates is negligible. These conclusions were based on a comparison of reaction rates for wood meal and for well-penetrated wood chips, as well as the strong temperature dependence of the reactions.

A more recent study investigating the rate limiting reactions during acid sulphite cooking¹³ found that during the early part of the cook the rate of carbohydrate dissolution (ie. hemicellulose dissolution) was limited by the outward diffusion

of reaction products. Towards the end of the cook, however, the rate limiting reaction reverts to the chemical reaction step at the surface. The nature of the reactions causing hemicellulose dissolution are very similar to the acid hydrolysis reactions which lead to cellulose degradation. In comparison with the hemicellulose reactions, however, the cellulose degradation reaction is a simple chain scission that does not produce a large molecule which needs to diffuse away from the reaction site. These findings confirm the fact that diffusion effects can be disregarded for the cellulose degradation reaction.

In addition to the above factors, the cooking process has been designed to maximise the 'penetrability' of the wood chips. Measures taken include:

- Pre-steaming of the chips to remove as much air as possible.
- Stringent control of chip quality and dimensions.
- 2-hour hydraulic pressurisation to 10.4 Bar at the start of the cook.

From the mechanism of the hydrolysis reaction, it can be seen that the reaction rate should be directly proportional to the hydrogen ion concentration. This has been confirmed by a number of studies³ performed on cellulose from various sources (cotton, wood, regenerated cellulose, etc.) A logical model for the rate of reaction would therefore be:

$$r_c = k_c [H^+]^a \quad (2-5)$$

where:-

- $r_c = -\frac{dN}{dt}$ = the average number of links broken in the cellulose chains at any instant in time, and N is the number of remaining linkages.

- Temperature dependence has been included using the Arrhenius relation:

$$k_c = A_c e^{-E_c/RT}, \text{ where :-}$$

A_c - pre-exponential factor for cellulose reaction

E_c - energy of activation for cellulose reaction

R - gas constant

T - temperature in Kelvin.

- The hydrolysis rate has been found to follow first order kinetics, ie $\alpha=1$ in equation 2-5¹⁴.

The use of homogeneous kinetics is appropriate here as the reaction can be considered as being of pseudo-zero order in terms of the number of linkages broken, ie. the number of linkages broken is extremely small relative to the reduction in the DP value.

The kinetic expression represented in equation 2-5 can be combined with the expressions developed for the DI concept. This eventually yields the expression shown in equation 2-6 which can be used to directly calculate the DP of cellulose at any point, providing an estimate of the original DP (DP_0) can be made and enough information is available to calculate the reaction rate (ie. temperature and $[H^+]$):

$$DP_t = \frac{1}{\frac{1}{DP_0} - \int_{t_0}^{t_t} k_c [H^+] dt} \quad (2-6)$$

Equation 2-6 was the basic form used for calculation of the DP value at any point during the cook. While the results during the initial stages of the cook are questionable due to diffusion effects, the results during the latter part of the cooking process - which were of importance in this study - should be accurate.

2.5 Lignin

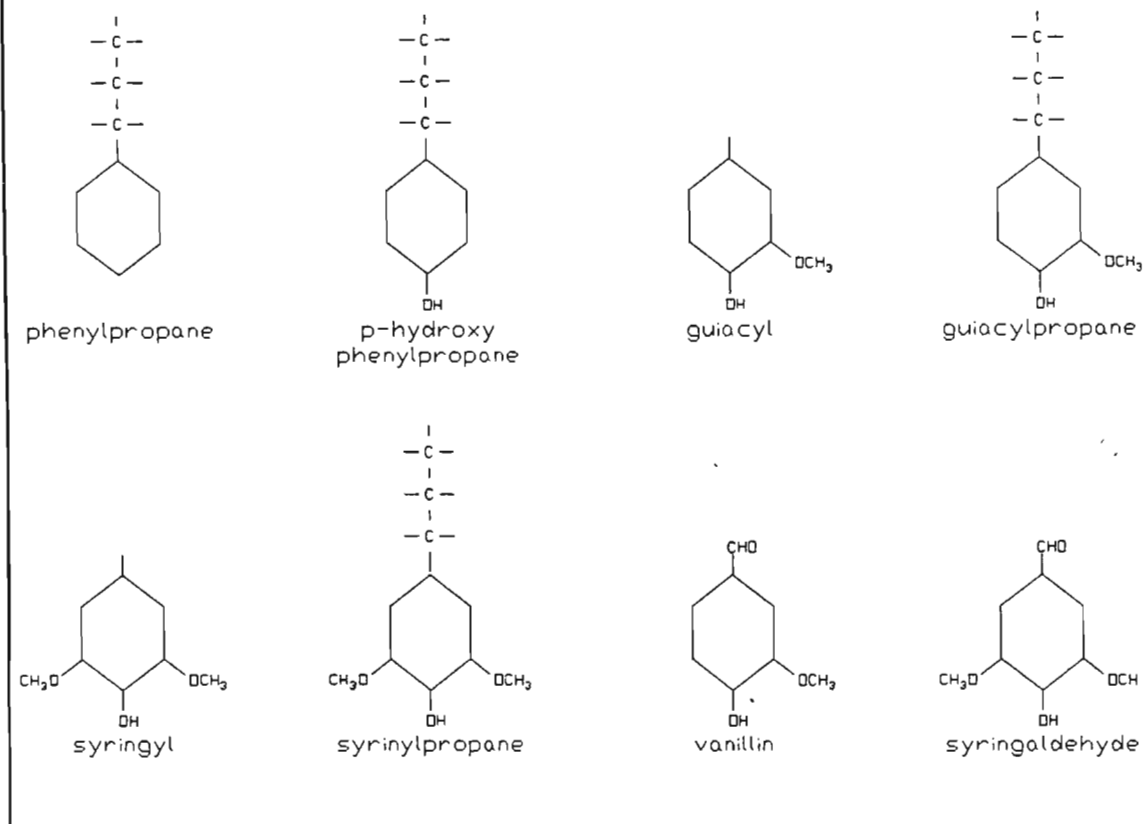
2.5.1 Structure

Lignin is the major non-carbohydrate fraction of wood and accounts for approximately 20% of the total mass. It is lignin which is primarily responsible for giving the fibres their rigid character. From the distribution of lignin in the wood fibre as shown in Figure 2.4 above, it can be seen that it is intimately mixed with the other components. As mentioned previously, it is practically impossible to isolate just the lignin without severely re-arranging it; consequently, detailed knowledge of the structure of lignin in situ, known as protolignin, is not available.

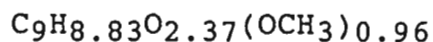
What has been determined is that lignin exists basically as an aromatic polymer with an amorphous nature, and consists of a heterogeneous network system with no evident simple repeating unit. The basic structural units of which lignin is thought to comprise can be found in Figure 2.6. The composition of lignin tends to vary in basic structure, composition and rate of growth with species (ie. from softwoods to hardwoods), and thus should be considered as a class of related materials rather than as a specific compound. These are shown in Figure 2.6.

FIGURE 2.6

Functional Groups found in Lignin¹⁵



Some idea of how these groups combine to form lignin was obtained from an elementary and functional group analysis¹⁵ of a milled wood, spruce lignin. This study yielded the following empirical formula for spruce lignin:



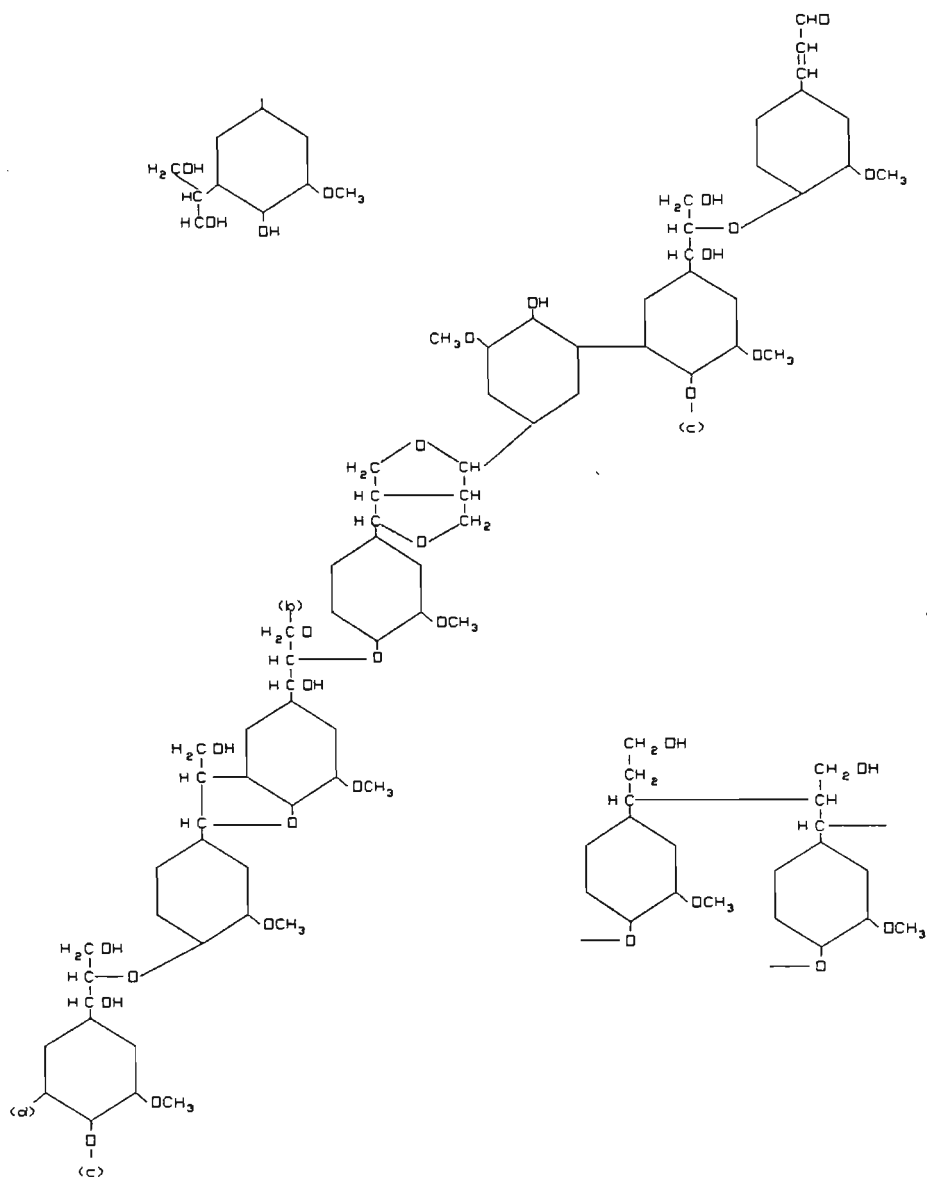
The formula was constructed using the phenylpropane group, C₉, as the basic building unit. A more detailed functional group breakdown of the lignin has been included in Table 2.3.

TABLE 2.3	
<u>Functional Group Breakdown of</u> <u>Spruce Lignin</u> ¹⁵ (Using C ₉ as basic unit)	
FUNCTIONAL GROUP	ATOM RATIOS
Carbon	9.00
Hydrogen	7.68
Methoxyl (OCH ₃)	0.96
Phenolic OH	0.30
Aliphatic OH	0.85
Carbonyl O	0.18
Alkylaryl ether O	0.70
Dialkyl ether O	0.34

From the above work and other chemical studies, a schematic and speculative structure for spruce lignin was constructed by Adler et al¹⁶ and has been included as Figure 2.7. This proposed structure, despite its inconsistencies when compared with the values given in Table 2.3, has been widely accepted as the closest prediction of the structure of protolignin currently available.

FIGURE 2.7

Proposed Structure of Protolignin in Spruce¹⁶



Bonds are 'open' at positions a, b, c and d to indicate other possible bonding points.

It can be seen from the proposed structure that all the phenylpropane structures are methoxylated and that the individual structural elements are linked by carbon-carbon

bonds as well as dialkyl and alkylaryl ethers. In addition to this, the proposed structure emphasises that there is no evident pattern in the sequence of the linkages.

The actual bonds involved in the lignin-carbohydrate complex, mentioned in section 2.3, are thought to consist of phenylglycosidic bonds at the 3-carbon atom of the lignin¹⁸ or of the benzyl ether bonds¹⁷. Of the two, the benzyl ether bonds are considered more likely¹⁷.

Most of the information presented above is specific to spruce which is a softwood. There is still some doubt, however, as to the specific composition of hardwood lignins. It has been generally accepted that in hardwood lignins the ratio of guaiacyl to syringyl units is roughly equal, ie. every second guaiacyl unit in Figure 2.7 must be replaced by a syringyl unit. Hardwood lignins also contain a small proportion of p-hydroxy phenylpropane units. There is still some doubt as to whether hardwood lignin consists of a mixture of two polymer types, one consisting of mainly guaiacyl units and one of mainly syringyl units, or if it consists of a single polymer containing both⁶.

2.5.2 Reactions of Lignin

Due to the diverse nature of lignin, it is understandable that it is subject to a tremendous variety of reactions. The only reactions of significance in this study are those which occur during the acid sulphite cooking process. These include the lignin condensation reaction and the reactions which separate the lignin from the carbohydrate fraction, eventually resulting in the lignin becoming soluble in the form of a liginosulphonate.

It has been generally accepted that the mechanism of delignification consists of two stages²⁰. The first stage is the sulphonation of lignin while still in the solid phase to produce a solid insoluble lignosulphonic acid. The lignin is then rendered soluble by either sulphitolysis or hydrolysis. The susceptibility of the various phenylpropane constituents of lignin can be broadly divided into two groups:

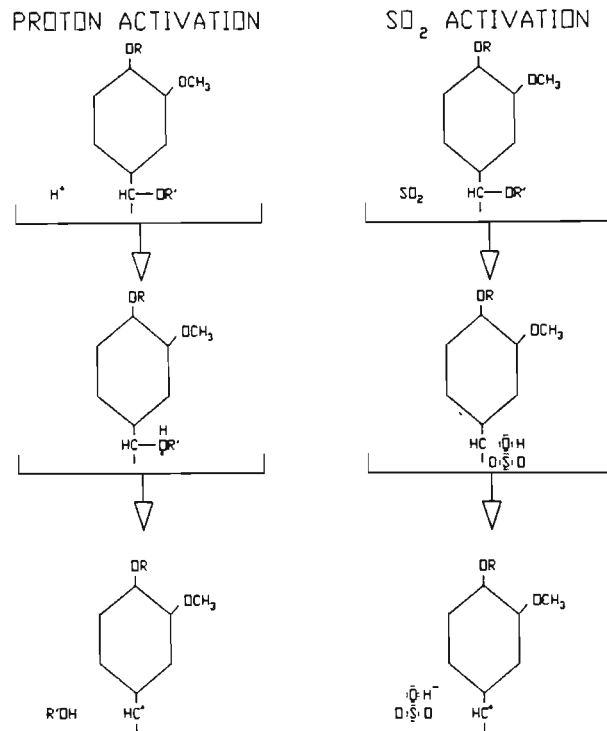
A groups: 'easily' sulphonatable monomers, defined as those groups which are sulphonated when the wood is treated with a neutral sulphite solution. These groups are thought to be benzyl alcohol or alkyl ether groups in monomers activated by a free phenolic hydroxyl.

B groups: the remaining monomers which can only be sulphonated in an acid medium. These groups are most probably unactivated benzyl alkyl ether groups. After hydrolysis these groups are converted to benzyl alcohol or carbonyl groups (B' groups). (These groups appear to require two stage sulphonation).

The initial sulphonation reaction involves the sulphonation of the A groups to form the solid lignosulphonic acid mentioned above. These groups cannot diffuse into the liquid phase as their hydrolysable groups, which form the bonds between the lignin and the carbohydrates, are still intact. There is still some doubt as to whether the actual sulphonating agent is sulphur dioxide or a proton³. Figure 2.8 illustrates the proposed mechanisms for both reactions.

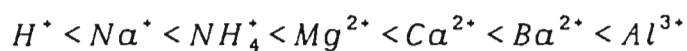
FIGURE 2.8

Proposed Mechanisms of Lignin Sulphonation²⁰



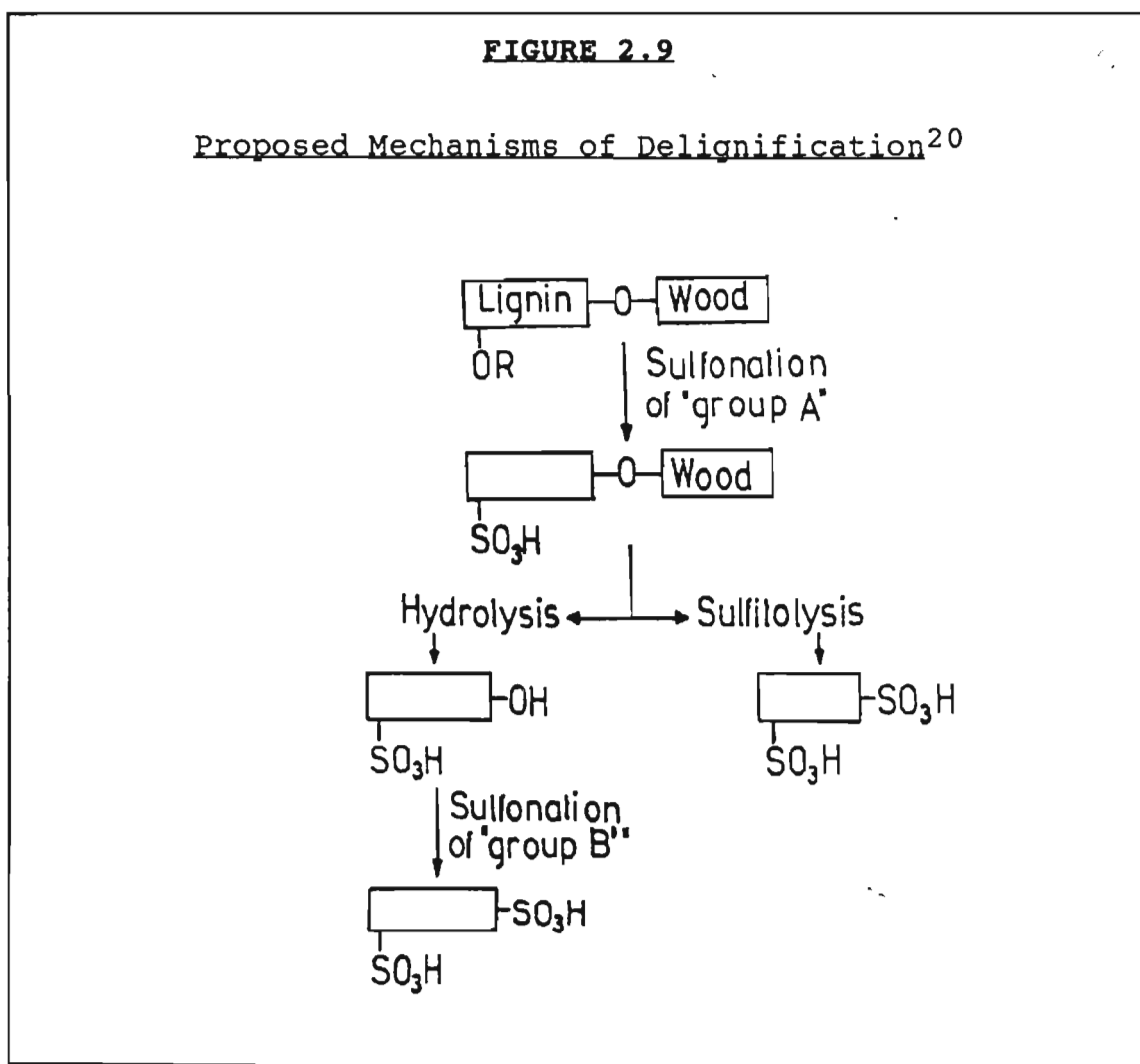
- | | |
|-----|---|
| i) | Proton activation: primary reaction is a proton addition to the benzyl ether oxygen |
| ii) | SO ₂ activation: here the SO ₂ accepts electrons from the α-carbon oxygen (analogous to hydration of SO ₂ to sulphurous acid). |

The high concentration of the lignosulphonic acid groups in the solid phase results in the formation of an ion exchange surface which obeys the **Donnan law**⁴¹. In the presence of other cations (the base used in the cooking liquor), the acidity of the solid phase is reduced. This acidity will be proportional to the cations attached to the surface and the lower the acidity, the slower the delignification. This phenomenon is thought to explain the different reaction rates exhibited by the various bases. The affinity for the solid phase in all cases of ion exchange is, in increasing order:



The above trend, with the exception of H^+ , agrees with the reaction rates found in practice. With only hydrogen ions in the solid phase, lignin dissolution is retarded by lignin condensation.

The second stage of the delignification reaction, in which the lignin-carbohydrate bonds are broken to form the soluble liginosulphonate, can be achieved by either hydrolysis or sulfitolysis. The proposed mechanisms for both reactions have been illustrated in Figure 2.9.



The only other important reaction relating to lignin is the lignin condensation reaction which occurs in both the solid and liquid phases²⁰. This reaction is undesirable as it results in the formation of large lignin polymers which retard the delignification reactions by blocking the sulphonatable groups, as well as making the lignin and carbohydrates more difficult to separate physically. Lignin condensation involves the benzyl alcohol, and possibly alkyl ether and carbonyl groups, especially in those monomers containing a free phenolic group.

The mechanism of the condensation reaction is similar to the sulphonation reaction; consequently, the rate of the condensation reaction is dependent on the acidity of the solid-liquid interface. The rate of lignin condensation during the early stages of the cook is restricted by the high bisulphite concentrations: as the bisulphite concentration drops, the rate of condensation increases. If the initial bisulphite concentration was high enough, then the lignin is further protected from condensation as most reactive benzyl alcohol and carbonyl groups will have been already sufficiently sulphonated to ensure dissolution. The unsulphonated groups and benzyl alcohol groups formed by hydrolysis are still susceptible to condensation; however this will occur mostly in solution.

Conditions favouring excessive condensation in the solid phase include a combination of low initial bisulphite concentration, high acidity and high temperature. The ultimate result of excessive condensation is a 'burnt cook' in which the pulp becomes very dark in colour and is unbleachable because of the large lignin polymers, resistant to hydrolysis, which have formed in the fibres.

2.5.3 Reaction Kinetics and Analytical Methods

The delignification reactions during the cooking process may be both heterogenous and homogeneous in nature. However, most of the kinetic studies to date have ignored this and the analyses have been based on homogeneous kinetics^{3,20,21,22,23}. While this assumption greatly simplifies the resulting kinetic expression, as well as the data required to develop the model, it severely limits the mechanistic interpretations which can be made. Researchers have continued to make the assumption of homogeneous kinetics even after the development of the theory of heterogeneous kinetics. There are many reasons for this, of which some of the more important include:

- i) The precise nature of the lignin-carbohydrate structure is still to be determined, thus an extremely simplified geometry would have to be assumed (for example, a spherical geometry) and this would introduce further inaccuracies. In addition to this, the structure of the wood fibre changes dramatically during the cooking process.
- ii) As mentioned previously, lignin should be considered as a class of related compounds which will obviously exhibit a range of reactivities. The delignification reaction will consequently consist of a large number of similar and independent parallel reactions taking place simultaneously. The reaction will thus be characterised by a wide range of rate constants.
- iii) The influence of diffusional aspects, either of reactants to the surface or products from the surface, have yet to be accurately defined. The effect of diffusion has been ignored in most of the studies reported in the literature. This has been justified by the strong tem-

perature dependence of the rate of delignification as well as the negligible difference between the rates for well-impregnated chips and wood meal.

- iv) The assumption of homogeneous reaction kinetics yields perfectly adequate results when used for simulations or for control in paper pulps, where the residual lignin is an important factor.

The incorporation of all the complexities of the delignification reactions into a rigorous kinetic model results in an extremely complex expression. The theory for such a model has been developed by Schön²⁴, who introduced frequency functions to account for the distribution of rate constants and the distribution of particle sizes (spherical geometry assumed). The resultant model is a set of complex differential equations which require extensive data throughout the cooking process if they are to be solved. Schön concluded that while the heterogeneous model provides a more accurate mechanistic insight to the delignification reaction, the use of homogeneous kinetics provides just as accurate results and is far more functional.

A homogeneous-type rate equation, incorporating mechanistic and empirical considerations, was selected for use in this study as opposed to the more complex rigorous solution²⁴. This simpler model was chosen as it provided a sufficiently accurate simulation of the reaction while still being simple enough to apply in the actual plant situation. In the context of dissolving pulp manufacture, the residual lignin at the end of a cook is important in that it directly affects the downstream bleaching process. Controlling cooking conditions to achieve an average target DP value mutually excludes achieving a target

residual lignin content. However, an understanding of the lignin chemistry provides a greater understanding of the cooking process as a whole.

The earliest delignification reaction rate studies found the rate to be proportional to the vapour pressure of SO₂ in the cooking liquor¹², where the partial pressure of SO₂ also corresponds to the product [HSO₃⁻].[H⁺]. Later studies found the delignification rate to be dependent on the degree of delignification^{25,21}. In addition to this, they found the reaction order with respect to lignin to be dependent on the degree of delignification. The resulting form of the rate of reaction was then written as shown in equation 2-7:

$$r_l = k_l [L]^{\alpha} [H^+]^{\alpha} [HSO_3^-]^{\beta} \quad (2-7)$$

where:-

- $r_l = -\frac{dL}{dt}$ = rate of lignin removal at any instant in time

- [L] - lignin in solid phase

α, α, β - exponents representing order of reaction

- Temperature dependence has been included using the Arrhenius relation:

$k_l = A_l e^{-E_l/RT}$, where:-

A_l - pre-exponential factor for lignin

E_l - energy of activation for lignin

R - gas constant

T - temperature in Kelvin.

The work performed by Hagberg & Schöön²¹ covered a wide range of delignification. They found that the model had to be broken into two regimes depending on the extent of delignification, and that the transition point corresponded to 12.4% lignin on wood. There are a number of possible reasons as to why this transition point occurs; these include variation in

accessibility, different susceptibilities of various components to reaction and change in the dominant reaction from sulphitolysis to hydrolysis. The actual cause cannot be precisely established as the kinetic model used does not provide enough of a mechanistic insight into the nature of the reaction.

A later study by Sloan²² found that a single expression was adequate. The reason for this is most probably because the range of delignification covered was smaller and concentrated on conditions toward the end of the cook. Sloan also found that reasonable results were obtained by assuming first order behaviour with respect to all the reactants.

A number of standard methods for determining residual lignin in pulp are in general use. These include direct methods such as the Klason lignin determination and indirect methods such as the chlorine (or Roe) number, permanganate (or K) number and Kappa number determinations. The Klason lignin determination is not well-suited to acid sulphite pulps, while both the indirect methods give fairly accurate repeatable results. Since SAPPI SAICCOR have standardised on the permanganate number method, it was used in this study (a copy of the procedure can be found in Appendix I section B.)

One of the disadvantages associated with the indirect methods is that they are not linearly proportional to the actual lignin content of the pulp³. Earlier delignification studies²¹ used linear correlations to estimate the residual lignin content from Kappa number and permanganate number determinations. However, recent work²² has used non-linear correlations which are accepted as a better representation of the

actual relationship. The correlation between the permanganate number (K) and actual lignin content given in equation 2-8 was developed by ITT Rayonnier²² and was used here:

$$\% \text{lignin on pulp} = 0.055 * K^{1.47} \quad (2-8)$$

A point of general disagreement between the various delignification studies has been whether the lignin content should be adjusted from a lignin content on pulp to a lignin content on wood, using the yield. No justification for using this correction has been found in the literature; however, for the purpose of a kinetic study, it was felt that the lignin content of the solid phase is the more correct value and therefore the lignin on pulp percentage was used in this study.

2.6 Hemicellulose

2.6.1 Structure

As mentioned in Table 2.1, a substantial proportion ($\pm 35\%$) of the total carbohydrate fraction present in wood is not in the form of cellulose and is collectively referred to as hemicellulose. The hemicellulose fraction consists of polysaccharides made up mainly of five different sugars, namely:

Hexoses : glucose, mannose and galactose

Pentoses : xylose and arabinose.

Various combinations of these sugars occur as polymers in association with glucuronic acid and methoxyl and acetyl groups. A breakdown of the percentages of these sugars in a typical hardwood can be found in Table 2.4. As shown in Figure 2.2, hemicellulose occurs throughout the cell wall although the detailed composition has been found to vary with locality.

TABLE 2.4

Percentages of Pentoses and
Hexoses in a Typical Hardwood⁵

FUNCTIONAL GROUP	PERCENT
Glucan	50
Mannan	3
Galactan	1
Xylan	15
Araban	0.5

Due to the complex nature of hemicellulose, the exact structures of the polymers have yet to be determined. Estimates of the more important polymers which occur in hardwoods have been included in Figure 2.10.

which is easily hydrolysable (mainly softwoods). Hardwood xylans contain a large number of acetate ester groups attached to the 2- or 3-hydroxyl group by a pyranosidic linkage which is also resistant to acid hydrolysis. The DP values of the xylan chains in hardwoods range from 80 to 270 (average ± 190).

III Galactoglucomannans are considered to be mixed straight chain monomers, consisting of mannose and glucose in the main chain linked by 1,4- β -glycosidic linkages. All the mannose present in wood is thought to occur in these polymers. The DP values of these compounds range from 70 to 140.

While hemicellulose occurs in close association with cellulose and lignin, it is now generally agreed that no covalent bonds exist between cellulose and hemicellulose. By contrast hemicellulose is thought to be linked chemically with lignin, most probably by a small number of easily hydrolysable bonds. The hemicellulose-lignin bonds are also thought to provide the link between the different types of hemicellulose. In its original form (in wood), hemicellulose is almost completely amorphous in nature; during cooking, however, some of the components tend to form a closer association with cellulose. This is caused by the polymers becoming increasingly linear during the cooking process until a point is reached where the polymer is able to attach itself to a cellulose crystallite by hydrogen bonding⁶.

2.6.2 Reactions of Hemicellulose

Since the structure of hemicellulose is closely related structurally to that of cellulose, the reactions of both are very similar. The dominant reaction for hemicellulose in an acidic medium is the acid hydrolysis of the glycosidic bonds.

This hydrolysis causes depolymerisation and the eventual dissolution of the low molecular carbohydrate compounds, especially hemicellulose. The compounds in solution then degrade further forming sugars, and ultimately sugarsulphonic acids (polymers containing sulphonate and carboxyl groups) and low-molecular aldonic acids. As with cellulose, the rate of hemicellulose degradation depends on the acidity of the cooking liquor. In comparison with cellulose however, the rate of hemicellulose dissolution has been found to be very dependent on the hemicellulose content of the pulp.

The susceptibility of the different constituents of hemicellulose to hydrolytic degradation varies. The action of sulphite cooking liquors on hardwoods results in arabinose appearing in the liquor first, owing to the hydrolysis of the arabinofuranose groups in the xylan-type hemicelluloses. The acetyl groups are dissolved simultaneously. Next, the galactose is lost from the galactoglucomannan polymer which is then degraded and dissolved itself. Xylose and mannose follow and eventually, towards the end of the cook, glucose appears in the liquor.

2.6.3 Reaction Kinetics and Analytical Methods

The problem of formulating a kinetic expression for the dissolution of hemicellulose is very similar to that discussed for lignin. For the purpose of developing a model to simulate hemicellulose dissolution, it is not practical to attempt separate treatments of the different compounds which make up hemicellulose. There are many reasons for this, of which some of the more important are:

- i) The exact structure of the polymers involved have still to be determined.

- ii) The methods of analysis for the different polymers in the solid phase are specialised and extremely time-consuming.
- iii) Analyses of the cooking liquor to determine reaction residues is not very instructive, as all the polymers eventually degrade to very similar compounds.

As in the case of lignin, a rigorous solution incorporating frequency functions (to account for the distribution of rate constants and the distribution of particle sizes) can be used. As mentioned previously, this leads to a complex set of differential equations which require extensive data to solve successfully. As in the case of lignin, since the residual hemicellulose content is of secondary importance compared to the cellulose DP, the use of a single kinetic expression to characterise the group as a whole was considered adequate for the purpose of this study. As mentioned previously, it must be accepted that a kinetic expression of this form severely limits the detailed mechanistic conclusions that can be drawn from the results. Most of the kinetic studies reported in the literature^{21,26} used this approach with a fair degree of success, as their models were capable of predicting the hemicellulose on pulp percentage to within $\pm 8\%$.

The general form of the rate expression is as shown in equation 2-9:

$$r_h = k_h [H]^a [H^+]^a \quad (2-9)$$

where:-

- $r_h = -\frac{dH}{dt}$ = rate of hemicellulose removal at any instant in time
- $[H]$ - hemicellulose in solid phase

- α, α - exponents representing order of reaction
- Temperature dependence has been included using the Arrhenius relation:
 $k_h = A_h e^{-E_h/RT}$, where:-
 A_h - pre-exponential factor for hemicellulose
 E_h - energy of activation for hemicellulose
 R - gas constant
 T - temperature in Kelvin.

The S₁₈ method was used to characterise the residual hemicellulose content of the pulp, and consists of measuring the carbohydrate fraction soluble in an 18% caustic solution. This method has become so widely accepted in the pulping industry that hemicellulose is now defined in terms of the S₁₈ analysis, ie. the percent carbohydrate soluble in 18% caustic at room temperature. It must be accepted that this definition is by no means precise as small quantities of the lower DP fractions of cellulose are also soluble in cold caustic. Despite this, the use of S₁₈ values in the above model has given better results²⁶ than when more elaborate methods were used²¹. The procedure for this analysis has been included in Appendix I Section C.

In order to perform the S₁₈ analysis, the residual lignin has to be removed from the sample. This can be achieved using either chlorite or chlorine dioxide extraction methods. Since it is known that chlorite extraction has a greater tendency to attack the carbohydrates³, the chlorine dioxide method was chosen (See Appendix I Section E).

The chemistry of all the above reactions (cellulose, lignin and hemicellulose) relies entirely on the nature of the cooking liquor, ie. on the acid and bisulphite ion concentrations. In addition to this, the high temperatures and pressures which

characterise an acid sulphite cook make it extremely difficult (if not impossible) to obtain representative pulp samples during cooking. These factors have resulted in most of the models developed for process control being based on various types of liquor analyses. The chemistry of the cooking liquor is thus just as important as the wood chemistry, and is discussed in detail in Chapter 3.

CHAPTER 3

LIQUOR CHEMISTRY IN DISSOLVING PULP PRODUCTION

3.1 Liquor Composition

As mentioned earlier, the cooking liquor consists of a solution of bisulphite containing an excess of sulphur dioxide. Initial charge liquor always contains small quantities of organic and inorganic impurities due to the nature of the cooking cycle, which involves returning a small portion of the digester charge liquor back to the liquor storage system after impregnation is complete. From the chemistry of cellulose, hemicellulose and lignin presented in Chapter 2, it is clear that the most important aspects of the cooking liquor are its acidity and the concentration of bisulphite ions. Most of the effort in the study of the cooking liquor is thus directed at determining the acid and bisulphite ion concentrations and understanding how and why they vary during the cooking process.

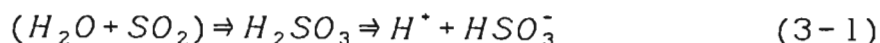
The composition of the cooking liquor has always been described historically by the total and combined SO_2 concentrations. The total SO_2 is defined as the iodine-reducing components of the liquor, while the combined SO_2 corresponds to the 'base content' of the liquor and is defined as the amount of SO_2 bound as neutral sulphite (CaSO_3). The analytical method used to measure combined and total SO_2 is the Palmrose test, and a copy of the procedure has been included in Appendix I Section D. Sometimes the concept of free SO_2 is used; however this is directly related to the total and combined SO_2 by subtraction (see Table 3.1).

Changes in liquor acidity are caused by changes in temperature and the appearance of acidic by-products in the liquor. Initially, the increase in temperature reduces the solubility

of SO₂ and decreases the degree of dissociation of the sulphurous acid resulting in a decrease in acidity. As the cook progresses however, acidic by-products are produced. These compounds result from three main sources namely:

- i) Delignification reactions, which form lignosulphonic acids.
- ii) Hemicellulose dissolution reactions, which form the sugarsulphonic acids.
- iii) Liquor decomposition reactions, which result in the formation of polythionates, thiosulphuric acid and sulphuric acid.

Not all these acids will exist in the completely dissociated form and consequently it is necessary to make a distinction between the acids and the anions formed, where the latter corresponds to the completely dissociated acids. The anions formed are then grouped and referred to collectively as 'strong acids'. The presence of these acid anions eventually causes an increase in acidity. Towards the end of the cook, the concentration of reacting bisulphite ions decreases to a point where new ions are thought to form from a reversal of the sulphurous acid (SO₂) equilibrium³:



which causes a rapid increase in the acidity. During depressurisation at the end of the cook, the acidity decreases again due to the loss of SO₂ and the decomposition of the α -hydroxysulphonic acids³⁶.

A summary of the commonly used definitions referring to liquor composition has been included as Table 3.1.

TABLE 3.1**Commonly Used Definitions Referring to Liquor Composition**

Component	Description³
Total SO ₂	Refers to the iodine-reducing components of the cooking liquor, ie. the total content of the SO ₂ taken up by the liquor.
Combined SO ₂	Refers to the base content of the liquor and is defined as the amount of SO ₂ bound as neutral sulphite (CaSO ₃ in this case).
'Strong Acids'	Corresponds to the formation of lignosulphonic, α-hydroxysulphonic, sugar-sulphonic, sulphuric aldonic, formic, acetic and carbonic acids during the cook. This definition is in general use without regard to the degree of dissociation of the various acids. It has been used here with specific reference to the anions formed, corresponding to completely dissociated acids.
Available combined SO ₂	Corresponds to the initial combined SO ₂ less the strong acid anions formed. This concentration decreases as the cook progresses and the strong acid anions are formed. It will eventually become negative toward the end of the cook.
Free SO ₂	Total SO ₂ - Combined SO ₂

Due to the ease of obtaining liquor samples during a cook, the models used in industry for predicting the end of a cook have been based on liquor analyses. A summary of the most commonly used models reported in the literature was included in the previous report²; an updated summary has been incorporated as section 3.4 for the sake of completeness. One of the problems highlighted by these methods is that they completely disregard actual concentrations of the various species in the cooking liquor. The charge balances and equilibrium relationships which govern the concentrations of acidic and bisulphite ions have thus been developed in the following section (3.2).

3.2 Charge Balances and Equilibrium Relationships.

Although the models for the cooking process in general use have been based on the concentrations of total and combined SO₂,

they do not provide a direct indication of the chemical and ionic concentrations which actually exist in the liquor during the cook. These analytical results can however be related to the actual chemical concentrations of $[H^+]$ and $[HSO_3^-]$, by using the following charge balances and equilibrium relationships:

i) The electroneutrality condition:-

$$[H^+] + 2[Ca^{2+}] = [HSO_3^-] + [SA^-] \quad (3-2)$$

where $[SA^-]$ = strong acid anions formed. ($[SA^-] = 0$ at start of cook).

ii) Relationship between combined and available combined SO_2 :-

$$[Initial\ combined\ SO_2] = [Ca^{2+}] \quad (3-3)$$

$$[Available\ combined\ SO_2] = [Ca^{2+}] - \frac{1}{2}[SA^-] \quad (3-4)$$

iii) Sulphur dioxide protolysis:-

$$K_{SO_2} = \frac{[H^+].[HSO_3^-]}{[total\ SO_2] - [HSO_3^-]} \quad (3-5)$$

iv) Sulphur dioxide solubility:-

$$K_p = \frac{[H^+].[HSO_3^-]}{P_{SO_2}} \quad (3-6)$$

Neglecting partial pressures of all other gases except SO_2 and water, then:

$$P_{tot} = P_{SO_2} + P_{H_2O} \quad (3-7)$$

(Quantities of CO_2 formed during the cooking process are very small and can be ignored.)

Mathematical correlations are available from the literature²⁷ for the temperature dependence of the parameters K_{SO_2} , K_p , and P_{H_2O} , in the form of the Antoine equation (equation 3-8):

$$\text{Log}_{10} A = B + \frac{C}{T} \quad (3-8)$$

where the temperature T is in Kelvin and A represents K_{SO_2} , K_p and P_{H_2O} . The values of the parameters for these correlations have been included in Table 3.2.

TABLE 3.2				
Values of Parameters for Equation 3-8²⁷				
A	Temperature Range °C		B	C
	From	To		
K_{SO_2}	20	80	-5.077	1045
	80	120	-6.916	1700
	120	150	-7.971	2113
K_p	20	80	-9.430	2392
	80	120	-10.208	2665
	120	150	-10.948	2960
P_{H_2O}	20	150	5.882	-2198

Units of temperature, pressure & concentration are Kelvin, Bar & mol/l respectively.

A number of different sets of values for K_{SO_2} are available in the literature, although two of the most commonly reported sets differ markedly. One set was originally constructed by Schön & Wannholt²⁸ and the other by Maas et al²⁹. The latter set of data was later extrapolated to higher temperatures^{30,31}. The difference between the two sets may have originated from the correction made to account for inter-ionic effects and the method used to calculate the parameters. Ingruber³² calculated

K_{SO_2} using actual pH measurements made at the various temperatures and pressures and his result agree closely with those reported by Maas et al²⁹ and Rydholm³.

The more recent study performed by Schöön & Wannholt²⁸ was also based on a direct potentiometric determination of the hydrogen ion concentration. However, the measurements were made at specific ionic strengths (0.25 to 3 M). A more important difference between the two sets of measurements is the method Schöön & Wannholt used to estimate the hydrogen ion concentration in the equilibrium SO_2 solution. This was done by comparing the emf of the equilibrium solution with the emf of a solution of known hydrogen ion concentration, where both were at the same temperature in order to account for the temperature dependence of the constant in the Nernst equation. The standard calomel electrode used as a reference was however kept at constant temperature ($23 \pm 1^\circ C$)²⁸ and joined to the equilibrium solution via a salt bridge. This contrasts directly with Ingruber's³² pH measurement in which the reference electrode was at the same temperature as the measuring electrode.

Since recent studies use both sets of values without justifying the choice, it was decided to test both here. An interesting observation is that the values given by Schöön & Wannholt²⁸ are almost exactly double those reported by Rydholm³, which may also indicate that an error was made in one of the methods of calculation.

3.3 Determination of Acid and Bisulphite Ion Concentrations.

3.3.1 Indirect Methods.

Equations 3-2 to 3-8 can be used to obtain expressions for $[H^+]$ and $[HSO_3^-]$ in terms of the total and combined SO_2 and

either K_{SO_2} or K_p . The actual solutions of these equations have been presented in Appendix 2 and the resulting expressions are presented as equations 3-9 to 3-12:

i) $[H^+]$ and $[HSO_3^-]$ as functions of total SO_2 , combined SO_2 and K_{SO_2} :-

$$[HSO_3^-] = [SO_2^{com}] - \frac{1}{2}K_{SO_2} + \left\{ \frac{(2[SO_2^{com}] - K_{SO_2})^2}{4} + K_{SO_2}[SO_2^{tot}] \right\}^{\frac{1}{2}} \quad (3-9)$$

$$[H^+] = K_{SO_2} * \left\{ \frac{[SO_2^{tot}] - [HSO_3^-]}{[HSO_3^-]} \right\} \quad (3-10)$$

where:-

$[SO_2^{com}]$ - available combined SO_2 concentration,

$[SO_2^{tot}]$ - total SO_2 concentration.

ii) $[H^+]$ and $[HSO_3^-]$ as functions of total SO_2 , combined SO_2 and K_p :-

$$[HSO_3^-] = [SO_2^{com}] + \{ [SO_2^{com}]^2 + K_p P_{SO_2} \}^{\frac{1}{2}} \quad (3-11)$$

$$[H^+] = \frac{K_p * P_{SO_2}}{[HSO_3^-]} \quad (3-12)$$

where:-

P_{SO_2} - partial pressure of SO_2 .

A serious drawback associated with these two sets of equations is that they require the concentration of strong acids at any point to be known in order to allow calculation of the $[H^+]$ and $[HSO_3^-]$. This situation was handled by Hagberg & Schön²⁷ by using the same potentiometric measurements used in the development of the K_{SO_2} correlation to estimate the acidity of the liquor during a cook. They then back-calculated the strong acid concentration and eventually developed an empirical model to describe the formation of strong acids during the

cook³³. The model which they eventually decided best represented the formation of strong acids was based on a standard Arrhenius form, and incorporated the liquor-to-wood ratio at the start of the cook as well as the concentrations of $[H^+]$, $[HSO_3^-]$ and strong acid ($[SA^-]$). The form of the kinetic model developed was as follows:

$$r_{SA} = \frac{k_{SA}}{\phi} [SA^-]^\alpha [H^+]^\beta [HSO_3^-]^\gamma \quad (3-13)$$

where:-

- $r_{SA} = d \frac{[SA^-]}{dt}$ - rate of strong acid formation at any instant in time

- ϕ - liquor to wood ratio at the start of the cook
- α, β, γ - exponents representing order of reaction

- Temperature dependence has been included using the Arrhenius relation:-

$$k_{SA} = A_{SA} e^{-E_{SA}/RT}, \text{ where:-}$$

A_{SA} - pre-exponential factor for strong acids

E_{SA} - energy of activation for strong acids

R - gas constant

T - temperature in Kelvin.

Hagberg & Schöön used this model very effectively²⁷ to simulate paper grade acid sulphite cooks (sodium-based liquor on spruce). More recently, Sloan (ammonia-based liquor on hemlock) used the same model to simulate cooking liquor acidity in order to determine the kinetics of the delignification²², hemicellulose dissolution²⁶ and cellulose degradation³⁴ reactions. The basis for **general** use of the correlation given in equation 3-13 is not strong however, as the nature of the cooking liquor (ie. the base used) and the type of wood being

pulped play a pivotal role in the formation of the strong acids. This can be seen from the chemistry of delignification, hemicellulose dissolution and the composition of wood.

3.3.2 Direct Methods.

The reason why these elaborate correlations have been developed to model the acidity and bisulphite ion concentrations during cooking is because pH measurement at cooking temperature and pressure (150°C and 10.5 Barg) is extremely difficult. Measurements of pH on cooled samples bear no relation to the values at actual cooking temperature and pressure^{35,3}, as the equilibriums of all the components involved change dramatically with temperature and pressure. In addition to this, some of the compounds (especially the sugarsulphonic acids) tend to decompose with depressurisation³⁶. The complications associated with measuring pH at elevated temperatures and pressures include:

- i) The design and operation of the reference electrode.
- ii) Glass membranes of pH probes age rapidly at high temperatures.
- iii) Calibration (this is discussed in detail in Section 5.3.2).

Ingruber developed a probe with a pressurised reservoir feeding the reference electrode and this innovation enabled the pH of the cooking liquor to be continuously measured during a cook. This instrument was used in a series of studies on the effect of pH on 'cooking rate'^{35,37,38}. However, despite the access to direct measurements, no attempt was made to develop kinetic expressions for the various reactions. The main emphasis of

these studies was on controlling pH during a set temperature profile in order to achieve the desired pulp characteristics at the end of the cook.

Recent developments in the design of pH probes include gel-type reference electrodes, porous impregnated reference electrodes and improved glass for membranes. These specialised pH probes are now easily available and cover a range of temperatures up to 150°C and pressures up to 17 bar and they thus make direct measurements of cooking liquor pH far more feasible than before. In addition, the extended periods that these probes will operate under harsh conditions offer more alternatives than before. If the probes do not last long enough to be useful on the actual plant, they will at least enable the development of a strong acid model.

It must be mentioned at this point that all of the above measurements and correlations give values for the CONCENTRATION of H^+ and HSO_3^- ions and not for their activities. This argument is dealt with by Ingruber³² and he concludes that for solutions with a pH less than 4, the only error that will result from assuming a constant activity coefficient will be due to the temperature dependence of the coefficient. The correction for activity was also ignored by Maas et al²⁹, Rydholm³¹ and Schön & Wannholt²⁸ in their determinations of K_{SO_2} . Another aspect to be considered here is that the commercial cooking process consists of a repetitive cycle where conditions, including the temperature profile and ionic strengths, do not vary greatly from cook to cook; consequently, the errors incurred by ignoring the correction for activity for this specific process are likely to be negligible. (A theoretical justification for this has been included as Appendix 7.)

Now that the chemistry of the cooking liquor has been dealt with in some detail, it is instructive to discuss the basis of the more commonly used cooking models.

3.4 Commonly Used Models for 'Cook End' Determination.

A survey of the literature revealed that two main methods are commonly used in industry to predict the end of the cook for the dissolving pulp process. The first - the so-called 'S Factor' method - was developed originally by Yorston & Liebergott¹ in 1965, and is based on an extension of the 'H Factor' method used to control paper grade cooks. The second method, developed specifically for controlling dissolving pulp cooks, is based on the rate of change of the absorbance of the cooking liquor. This particular process is the subject of a United States Patent¹⁴ and a Canadian Patent³⁹.

Many other methods for controlling rayon cooks to a desired end point have been investigated at SAPPI SAICCOR. These methods include measurements of liquor refractive index, liquor U.V. absorption, liquor viscosity and liquor conductivity. None of these methods, however, have been found to provide a sound basis for a control model⁴⁰.

3.4.1 The 'S Factor' Models

The 'S Factor' model was developed from the kinetics of the delignification reaction, and was based on the assumption that a relationship existed between the lignin content of the solid phase and the pulp viscosity.

Yorston & Liebergott¹ developed a correlation for the rate of sulphite pulping using the relationship reported by Hagberg

& Schön²¹, viz. that the delignification rate is proportional to the product $\{[H^+].[HSO_3^-]\}^n$, from which the following rate equation was developed:

$$-\frac{d[L]}{dt} = K_1 [L]^a \{[H^+].[HSO_3^-]\}^n \quad (3-14)$$

where:-

$[L]$ - Residual % lignin

Yorston & Liebergott then determined the product $\{[H^+].[HSO_3^-]\}^n$ to be proportional to the partial pressure of SO₂. The power 'n' was found to be less than unity, with the most acceptable value being 0.75. The rate equation then became:

$$-\frac{d[L]}{dt} = K_1 [L]^a \{P_{SO_2}\}^{0.75} \quad (3-15)$$

They then graphically integrated their experimental rate data to arrive at a 'degree of cooking'. The temperature dependence of K_1 was assumed to follow an Arrhenius-type equation of the following form:

$$K_1 = A_0 e^{\left\{B - \left(\frac{E_0}{RT}\right)\right\}} \quad (3-16)$$

where:-

- A_0 - pre-exponential factor
- E_0 - energy of activation
- R - gas constant
- T - temperature in Kelvin
- B - normalising factor (usually $\frac{E_0}{373}$ which normalises the equation to 100°C.

Substituting 3-16 into 3-15 (making the assumption that the order of delignification with respect to [L] is unity) and integrating then yielded the 'S Factor' model:

$$SF = - \int_{L_0}^{L_f} \frac{1}{A_0[L]} d[L] = \int_{t_0}^{t_f} e^{\left(B - \frac{A}{kT}\right)} (P_{SO_2})^n dt \quad (3-17)$$

where:-

- SF - S Factor
- L_0 - % lignin at cook start ($t=t_0$)
- L_f - % lignin at time $t=t_f$.

Integrating the left side of equation 3-17 yields:

$$[L_f] = k_1 e^{(-A_0(SF))} \quad (3-18)$$

Then, assuming that the residual lignin concentration is directly proportional to the cuprammonium viscosity of the pulp:

$$\text{Viscosity} = k_2 e^{(-A_0(SF))} \quad (3-19)$$

where k_1 and k_2 are constants.

Equation 3-19 thus forms the basis of the 'S factor' model. From the above explanation, it is immediately apparent that the weakness of the model arises from the assumption that at any point in time the residual lignin content is proportional to the cellulose DP. This proportionality is likely to be extremely weak in view of the different reaction kinetics exhibited by the delignification reaction and the cellulose degradation reaction.

Individual mills have developed their own forms of the 'S factor' model in an attempt to adapt it to their respective processes and hence improve control. Only two versions of the

model are discussed here, the model in use at SAPPI SAICCOR and the most recent form of the model reported in the literature⁴¹ (1986).

i) The SAPPI SAICCOR Version of the 'S Factor' Model.

Studies carried out at SAPPI SAICCOR led to the conclusion that using the partial pressure form of the model (equation 3-17) was undesirable, and that a more accurate model would be obtained if the actual SO₂ concentration of the liquor was measured. They consequently adjusted the equation to the form:

$$SF = - \int_{L_0}^{L_f} \frac{1}{A_0[L]} d[L] = \int_{t_0}^{t_f} e^{\left(B - \frac{A}{kT}\right)} [SO_2^{free}]^n dt \quad (3-20)$$

However this method of measuring SO₂ concentrations also introduces a further complication in that SO₂ is present in two forms, viz. 'FREE' SO₂ and 'COMBINED' SO₂ (in the form of bisulphite). As can be seen from equation 3-20, this model was initially based on the 'FREE' SO₂ concentration in the liquor. Later investigations eventually resulted in the value of 'n' being set to zero, effectively removing the dependence of the model on the free SO₂ altogether.

The use of a direct measure of the SO₂ concentration, instead of the SO₂ partial pressure, now made the 'S Factor' directly dependent on the base concentration in the liquor. The relationship between the base concentration and the target 'S Factor' was initially assumed to be of the form:

$$\text{Target SF} = M * \{\%Base\} + C \quad (3-21)$$

where M and C are constants and were determined by regression of data. The base percentage (referring to %CaO in this case) is calculated from the combined SO₂ using the following relationship:

$$\%Base = 1.143 * \text{Combined } SO_2 \quad (3-22)$$

(This can be derived using molar masses of the compounds.)

Later investigations indicated that this relationship was not linear and this led to the development of the following form of the model, which is currently in use:

$$\text{Target SF} = A * [SO_2^{free}]^2 + B * [SO_2^{free}] + C * (\%Base) + D \quad (3-23)$$

where A, B and C are all constants, and D is a constant which is updated continuously by means of a feedback system.

The manner in which the model works is as follows:

- (1) From the analysis of a liquor sample after one hour of cooking, the target 'S factor' is calculated using 3-23.
- (2) From the time that the digester temperature reaches 110°C, the 'S factor' values begin to accumulate and are calculated according to the following equations:-

$$\text{Reaction Rate} = e^{\left(B - \frac{A}{RT}\right)} \quad (3-24)$$

and

$$\text{Accum S's} = \frac{\text{Reaction rate}}{2} + \text{Previously accum S's}$$

These calculations are performed every 30 seconds. (Units of time used in the model are minutes.)

- (3) A four-hour liquor sample is taken and the original target 'S factor' is then adjusted if the SO₂ consumption is considered too high or too low.

- (4) Once the cook is complete, the resulting viscosity is measured and the average for the last 7 cooks is compared against the target viscosity. The difference between the two is then used to increase or decrease the constant D in equation 3-23 by increments of 200. This is done on individual digesters after a minimum of 7 cooks, and on all digesters 60 cooks after the last update.

An additional factor involved in the control of cooks at SAPPI SAICCOR is the amount of liquor removed from the digester after chip impregnation is complete. This operation is called 'side relief' and is performed once the cook temperature reaches 110°C. Until recently, the amount of liquor to be removed was calculated to ensure a constant base concentration-to-wood ratio after side relief, as this ratio was thought to exert a considerable influence on the cooking rate. When the amount of liquor removed during side relief was made constant, no noticeable deterioration in cook quality control was observed. The side relief has thus now been set to a constant volume, as this not only smooths the demand for cooking liquor but also improves temperature control of the liquor in the storage vessels.

The results of the SAPPI SAICCOR model are not satisfactory, with the Coefficient of Variation (COV) for the viscosities commonly varying between 15 and 30 on the target viscosity of 55 (this target value is also occasionally altered). The 'S factor' constant 'D' varies continuously and often has to be manually adjusted to bring viscosities back into specification. Apart from illustrating the weakness of the model, this trend indicates that the model is most probably being driven primarily by the feedback system.

ii) Tembec Mill's Version of the 'S Factor' Model.

Marr & Bondy⁴¹ presented a paper in 1986 in which they developed an updated version of the 'S Factor' model for use at the Tembec Mill in Quebec (Canada). They used an equation of the following form on which to perform a regression analysis

$$\text{Viscosity} = A + B * e^{(-A_0 SF)} + C * \theta + D * \theta * e^{(-A_0 SF)} \quad (3-25)$$

where:-

- A_0 - pre-exponential factor
- θ - **chemical** to wood ratio*1
- SF - S factor
- A, B, C, D - constants determined by regression analysis.

*1Marr & Bondy do not fully define this parameter in terms of which chemical concentration was used.

The regression analysis indicated a strong interdependence of the variables being correlated. In addition to this, they eventually concluded that the term $D * \theta * e^{-A_0 SF}$ should be eliminated because of a contradiction in the functionality. This was based on the reasoning that the larger the 'S factor' the smaller the value of $e^{-A_0 SF}$, which corresponds to the expected result of a lower viscosity (ie. $D > 0$). By comparison, an increase in the chemical-to-wood ratio (ie. the stronger the nett formation of acidic by-products) would be expected to result in a decrease in the viscosity. The constant 'D' determined from their regression analysis was negative. From this reasoning it would appear that the 'chemical' referred to in the chemical-to-wood ratio is the free SO_2 , because if combined SO_2 had been used the functionality of the term would be correct.

At the time at which this paper was presented (1986), the model was still in the process of being developed and no results were presented. Marr & Bondy were, however, apparently aiming at being able to predict 95% of the viscosities to within 20% of their actual values. There has been no subsequent publication of results since then.

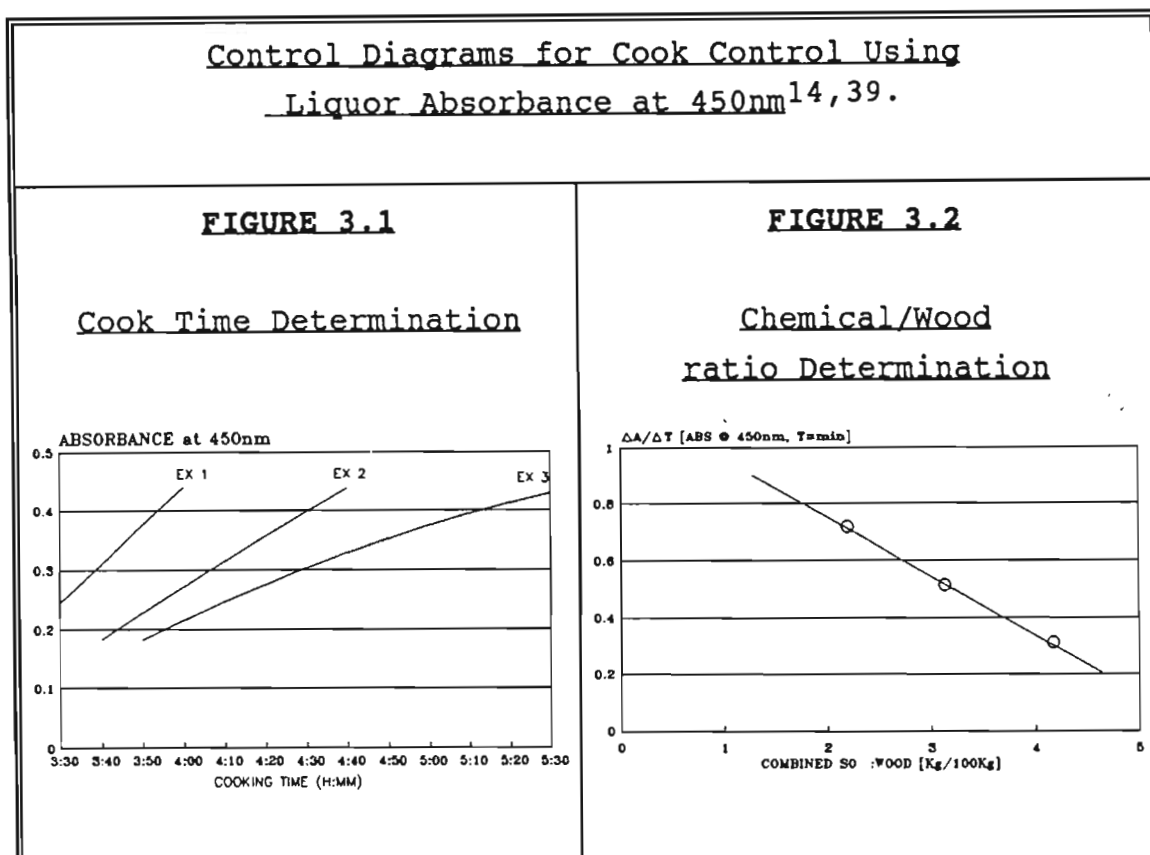
3.4.2 Liquor Absorbance Method^{14, 39}

This patented method of cook control is based on the observation that the initial weight ratio of combined SO₂ to wood (in a sulphite digestion process) may be determined fairly accurately by measuring the rate of change of absorbance in the digestion cooking liquor. A given rate of change in absorbance has been found to be characteristic of a certain initial chemical-to-wood ratio, which in turn may be directly correlated with the cooking time, temperature or pressure required to obtain a given pulp viscosity (ie. cellulose DP value).

This method requires the measurement and construction of a standard set of curves, consisting of (1) absorbance vs time and (2) rate of change of absorbance vs initial combined SO₂. This could be achieved by running a series of cooks in which all factors are constant, with the exception of the initial combined SO₂ and the total cooking time. The liquor absorbance is then measured during the cook and the time when the target viscosity is achieved is noted. From this data, a set of curves (similar to those shown in Figure 3.1) can be constructed. The initial slope of these curves is then used to construct the curve given in Figure 3.2.

The method of control involves the measurement of the rate of change of absorbance during the cook. This value is then used

to determine the combined SO₂-to-wood ratio, using Figure 3.2, which in turn defines the applicable curve in Figure 3.1 to predict the total cook time required to achieve the target viscosity.



According to the literature^{14,39}, apparently this method can also be used to control a cook to achieve a required target viscosity within a set time in order to facilitate scheduling. This is achieved by adjusting the temperature and pressure to obtain the required rate of change of absorption necessary to yield the target viscosity in the specified time.

Open references in literature to mills using this method of control have not been found. However, it is likely that the method is used at some of ITT Rayonnier's mills as the model

was developed by them. (Due to the lack of data, the effectiveness of the method cannot be assessed accurately at this stage.)

3.5 Comparison of Cooking Models

The vagaries and shortcomings of the two models explained above can be seen in the light of the chemistry of the wood and liquor reactions. The assumption on which the 'S factor' model is based, namely that the degree of delignification is proportional to the viscosity, is clearly incorrect due to the different kinetics of the delignification and the cellulose degradation reactions. In addition to this, during the latter part of an acid sulphite dissolving pulp cook the delignification reaction slows down considerably but the cellulose degradation reaction accelerates. Thus, at best, the model will be insensitive to the rate of change of the DP value. The model also does not take into account the strong dependence of the SO₂ solubility on temperature. Apart from these drawbacks, the form of the model is also undesirable in that the parameters are extremely interdependent, which is understandable when the actual kinetics are known.

The model based on the rate of change of liquor absorbance essentially makes the same assumption as the 'S Factor' model, ie. that there is a direct correlation between the degree of delignification and the degree of cellulose degradation, because the absorbance of the liquor changes due to the dissolved lignin. An additional problem with this model is that lignin condensation is not accounted for; however, these condensed products have a significant effect on the liquor colouring and hence on the absorbance measurement. A further drawback associated with this model is the large number of experimental measurements which have to be made. In addition to this, it is a known fact at

SAPPI SAICCOR that the correlation between results from laboratory cooks and plant cooks is weak. The primary reason for this is most probably the vast difference in liquor-to-wood ratios between the two, a factor which will play a major role in the colouration of the liquor due to the varying dilution of reaction products. The timber used at SAPPI SAICCOR also contains a coloured 'heartwood' which tends to cause an additional liquor colouration.

Another problem associated with all models which rely on the pulp viscosity as a primary regression parameter is the fact that it is a non-linear measurement of the cellulose DP. Apart from this, the drop in viscosity (or for that matter in the DP value) is by no means a direct measure of the number of linkages broken in a cellulose polymer and thus does not offer a direct measure of the reaction rate. This can be clearly illustrated using the concept of degree of degradation, presented in section 2.4.3, to calculate the lowering of the DP value corresponding to the splitting of a set number of linkages. An illustration of this concept has been included in Table 3.3 where the decrease in DP corresponding to 0.022% of the linkages being broken has been calculated for different initial DP values. The viscosities relating to the DP values have also been included.

TABLE 3.3**Decrease in DP and Viscosity Corresponding to 0.022% of
Cellulose Linkages Being Broken**

Initial		Final		Drop in	
DP	Viscosity	DP	Viscosity	DP	Viscosity
800	19.8	680	12.4	120	7.4
1000	37.9	820	21.3	180	16.6
1200	64.3	950	32.6	250	31.7
1400	100.5	1070	46.1	330	54.3
1600	147.9	1180	61.7	420	86.2

In the light of the existing models in use, it can be seen that a more direct mechanistic approach as proposed here offers many advantages, especially with respect to controlling the cellulose degradation reaction to achieve a target DP value. Using the chemistry and correlations presented in chapters 2 and 3 as a basis, the various reaction kinetics and correlations can be used to derive a comprehensive cooking model. This then clearly defines the data necessary to develop the model and the experimental procedures and requirements can then be set up accordingly.

CHAPTER 4

EXPERIMENTAL EQUIPMENT DESIGN AND CONSTRUCTION

4.1 Summary of Reaction Kinetics to be Investigated.

In view of the many kinetic expressions and correlations presented in chapters 2 and 3, it is helpful at this stage to give a brief synopsis of the actual reactions targeted for investigation. The form of the kinetic expression considered to be most appropriate, the use of any additional correlations required and the specific analytical methods chosen are also identified for each of the reactions. Having formalised these aspects, the data required for the determination of the kinetics of each reaction can then be identified easily. A prerequisite common to all the investigations, however, is that a number of cooks must be performed over a range of constant maximum temperatures. It should be noted that all the methods used for determining kinetic expressions in this work are for batch reactors. The additional data required to determine the individual kinetic expressions are specified in the following sections.

4.1.1 Cellulose Degradation Reaction

The form of the kinetic equation to be used for modelling the rate of cellulose degradation was given as equation 2-5 which is of the form:

$$r_c = k_c [H^+] \quad (2-5)$$

where the kinetics of the reaction rate have been accepted as being of first order with respect to $[H^+]$ and $k_c = A_c e^{-\frac{E_c}{RT}}$.

The data required from each constant temperature run would then include:

- i) Temperature profile followed on the rise to the maximum temperature.
- ii) Hydrogen ion concentration during the cook.
- iii) A number of pulp samples taken after increasing lengths of time at maximum temperature. The viscosity of each of the pulp samples can then be determined and the average DP of the sample calculated using the correlation:-

$$DP = 285.4 \cdot \mu^{0.345} \quad (2-4)$$

Since the native DP value of eucalyptus wood is not available from the literature, it is necessary to select a value for DP_0 to be used as an initial reference point for calculating the degradation increase of subsequent samples. These data are then sufficient to determine the kinetics of the reaction, using the following procedure:

- i) Using the reference value of DP_0 , the degradation increase of subsequent samples is calculated using the expression:-

$$DI = \frac{1}{DP_f} - \frac{1}{DP_0} \quad (2-1)$$

- ii) Plotting DI versus $\int_{t_0}^{t_f} [H^+] dt$ for each constant temperature run yields a straight line with slope k_c .
- iii) Plotting the values of $\log(k_c)$ against $\frac{1}{T}$ yields a straight line with slope $-\frac{E_c}{R}$ and Y intercept $\log(A_c)$.

The viscosity test used is based on the SNIA standard (See Appendix I section A).

4.1.2 Delignification Reaction.

The form of the kinetic equation to be used for modelling the delignification rate was given as equation 2-7 and is of the form:

$$r_l = k_l [L]^a [H^+]^a [HSO_3^-]^\beta \quad (2-7)$$

where the order of reaction with respect to residual lignin $[L]$, $[H^+]$ and $[HSO_3^-]$ has to be determined.

The data required from each constant temperature run would then include:

- i) Temperature profile followed on the rise to the maximum temperature.
- ii) Hydrogen ion and $[HSO_3^-]$ concentrations during the cook.
- iii) A number of pulp samples taken after increasing lengths of time at maximum temperature. The permanganate number (K No.) of each of the pulp samples can then be determined and the percentage lignin on pulp calculated using the correlation:-

$$\% \text{lignin on pulp} = 0.055 * K^{1.47} \quad (2-8)$$

The lignin content of Eucalyptus Grandis is typically of the order of 25.7%⁴². Using this value as the lignin content at the start of the cook (ie. $[L]_0$) and the calculated residual lignin of subsequent samples, the extent of the reaction can be calculated. These data are then sufficient to determine the kinetics of the reaction.

If the kinetic expression is to be solved as given in equation 2-7 to obtain A_l , E_l , a , α , β , then a least squares

regression analysis will have to be used. A simpler approach would be to use the results reported in the literature as a starting point and improve on that if necessary.

The work of Hagberg & Schöön²¹ and that of Sloan²² found the order of reaction with respect to $[H^+]$ and $[HSO_3^-]$ to be close to 1 ($\alpha \approx 0.8$ and $\beta \approx 1.0$). The reaction orders with respect to residual lignin ($[L]$) reported in the literature were more variable, with Hagberg & Schöön reporting $\alpha = 0.65$ for $[L] > 12.4\%$ and $\alpha = 1.8$ for $[L] < 12.4\%$ and Sloan reporting $\alpha = 1.0$ for all $[L]$.

Based on these results, it was decided that setting α and β to 1 and testing the fit for a varying order of reaction ($\alpha = 0, 1, \text{ and } 2$) with respect to $[L]$ would provide a good starting point. This considerably simplifies the determination of the various parameters as standard methods for batch reactors can be applied, namely:

- i) Zero order reaction with respect to residual lignin.
Plot $[L]_0 - [L]_t$ versus $\int_{t_0}^{t_f} [H^+].[HSO_3^-]dt$ for each constant temperature run to yield a straight line with slope k_t .
- ii) First order reaction with respect to residual lignin.
Plot $\ln\left(\frac{[L]_0}{[L]_t}\right)$ versus $\int_{t_0}^{t_f} [H^+].[HSO_3^-]dt$ for each constant temperature run to yield a straight line with slope k_t .
- iii) Second order reaction with respect to residual lignin.
Plot $\frac{1}{[L]_t} - \frac{1}{[L]_0}$ versus $\int_{t_0}^{t_f} [H^+].[HSO_3^-]dt$ for each constant temperature run to yield a straight line with slope k_t .

Plotting the values of $\log(k_t)$ against $\frac{1}{T}$ for each set (zero, first and second order) yields a straight line with slope $-\frac{E_t}{R}$

and Y intercept $\log (A_1)$. The regression results of these curves will then indicate which set provides the best solution. If an adequate fit is not provided by any of the above solutions, then the parameters from the best fit could be used as starting estimates for a least squares regression analysis on the entire equation.

Permanganate number analyses were performed according to the standard method included in Appendix I Section B.

4.1.3 Hemicellulose Dissolution Reaction.

The form of the kinetic equation to be used for modelling the rate of hemicellulose dissolution was given as equation 2-9 and is of the form:

$$r_h = k_h [H]^a [H^+]^a \quad (2-9)$$

where the orders of reaction with respect to residual hemicellulose $[H]$ and $[H^+]$ have to be determined.

The data required from each constant temperature run would then include:

- i) Temperature profile followed on the rise to the maximum temperature.
- ii) Hydrogen ion concentrations during the cook.
- iii) A number of pulp samples taken after increasing lengths of time at maximum temperature. The hemicellulose percentage (S_{18} value) of each of the pulp samples can then be determined directly.

The hemicellulose content of Eucalyptus Grandis is typically of the order of 26.6%⁴². Using this value as the hemicellulose

content at the start of the cook ($[H]_0$) and the measured hemicellulose content of subsequent samples ($[H]_f$), the extent of reaction can be calculated. This data is then sufficient to determine the kinetics of the reaction.

As the mechanism of the hemicellulose dissolution reaction is the same as that of cellulose degradation, the reaction order with respect to $[H^*]$ can safely be assumed to be one ($\alpha=1$). The reaction order with respect to residual hemicellulose, however, must be determined. As with lignin, the analysis of the kinetics is considerably simplified by testing the fit for a varying order of reaction with respect to $[L]$ in discrete steps (ie. $\alpha=0, 1, \text{ and } 2$) as this enables the determination of the various parameters using standard methods, namely:

i) Zero order reaction with respect to residual hemicellulose.

Plot $[H]_0 - [H]_f$ versus $\int_{t_0}^{t_f} [H^*] dt$ for each constant temperature run to yield a straight line with slope k_h .

ii) First order reaction with respect to residual hemicellulose.

Plot $\ln\left(\frac{[H]_0}{[H]_f}\right)$ versus $\int_{t_0}^{t_f} [H^*] dt$ for each constant temperature run to yield a straight line with slope k_h .

iii) Second order reaction with respect to residual hemicellulose.

Plot $\frac{1}{[H]_f} - \frac{1}{[H]_0}$ versus $\int_{t_0}^{t_f} [H^*] dt$ for each constant temperature run to yield a straight line with slope k_h .

Plotting the values of $\log(k_h)$ against $\frac{1}{T}$ for each set (zero, first and second order) yields a straight line with slope $-\frac{E_h}{R}$ and Y intercept $\log(A_h)$. The regression results of these curves will then indicate which set provides the best solution.

If an adequate fit is not provided by any of the above solutions, then the parameters from the best fit could be used as starting estimates for a least squares regression analysis on the entire equation.

S_{18} analyses were performed according to the standard method included in Appendix I Section C.

4.2 Equipment Design and Construction.

4.2.1 Equipment Requirements.

Once the nature of the data necessary to evaluate the kinetic expressions had been determined, the experimental equipment was designed to fulfil the requirements. From the preceding section, it is evident that an ideal equipment configuration would enable:

- i) Accurate temperature profile control to allow repeatable temperature profiles for each cook.
- ii) In-process liquor samples to be taken.
- iii) In-process pulp samples to be taken
- iv) Incorporate on-line pH measurement.
- v) Allow continuous collection of temperature, pressure and pH data.

In addition to the above experimental requirements, there were practical necessities such as gas absorption during pressure release to prevent excessive SO_2 gas emissions during depressurisation and the incorporation of safety aspects such as over-pressurisation protection.

4.2.2 Options Available

i) Existing Equipment

A 30-litre laboratory digester was available at SAPPI SAICCOR. This unit consisted of a single vessel which could be sectioned to hold different wood samples, and incorporated rudimentary temperature and pressure controls as well as a facility for taking liquor samples.

A major disadvantage was that the unit was not capable of allowing pulp samples to be taken during the cook. Use of this unit would have required that data for each constant temperature run be collected by charging the digester, running up to cooking temperature, and then stopping the cook to obtain a pulp sample. Subsequent pulp samples would then have had to be obtained by repeatedly re-loading the digester with wood and liquor, starting the cook in the same fashion as before, and stopping after increasingly longer periods at cooking temperature.

Apart from being extremely time-consuming, this method of data collection was undesirable in that it would have introduced significant errors due to the difficulties involved in exactly reproducing cooking conditions, such as:

- i) Temperature and pressure profiles.
- ii) Homogeneous wood samples.
- iii) Liquor concentrations.
- iv) Liquor-to-wood ratio.

for each subsequent cook.

The disadvantages associated with using this equipment resulted in alternative equipment configurations being considered.

ii) Satellite Mini Digester Plant.

A satellite mini digester plant was designed to meet the experimental requirements specified above. This configuration consisted of a number of small individual digesters with common liquor distributed through each and enabled isolation and depressurisation of any specific digester at any time during the cook.

Two options existed as to the method of plant operation:

- i) It could be run as a totally independent unit.
- ii) It could be incorporated into the existing laboratory digester circulation line and run simultaneously.

The second option offered the following distinct advantages:

- i) Larger liquor-to-wood ratios would be achieved.
- ii) The impact of isolating mini digesters on the liquor-to-wood ratio would be dramatically reduced due to the wood load of the main lab digester.
- iii) In this format the plant was more flexible since the unit could be connected to plant digesters should the need have arisen.

The efficiency with which data could be collected using this configuration, as well as its flexibility, made it the natural choice. A detailed description of the plant design can be found in section 4.2.3

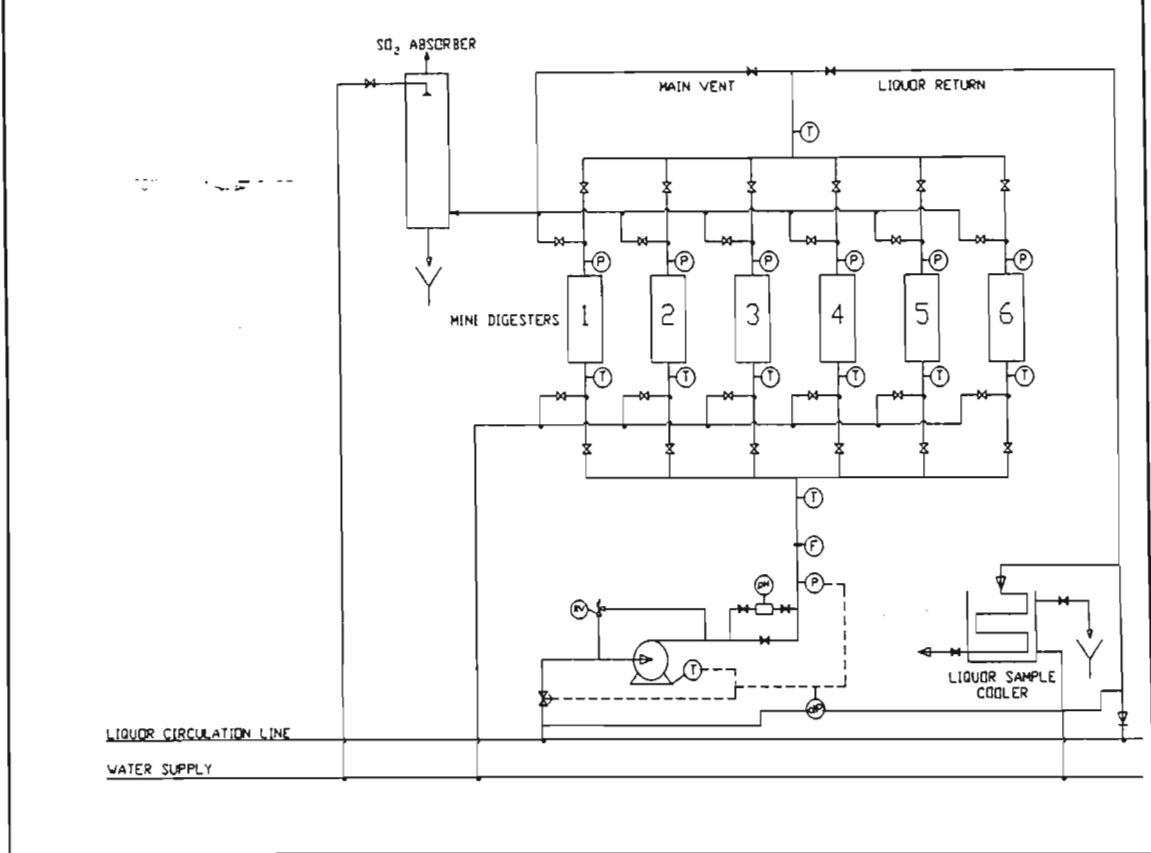
4.2.3 Detailed Equipment Design and Construction.

A process flow diagram of the final plant configuration can be found in Figure 4.1. The plant was designed to operate at a maximum temperature of 150°C and a working pressure of 11 Barg and consisted of the following major components:

- i) Liquor circulation system (and water distribution system).
- ii) Six 2-litre digesters.
- iii) Liquor sample cooler.
- iv) SO₂ absorption column.
- v) Electrical panel with hard-wired interlocks for start-up, shut-down and emergency shut-down procedures.
- vi) Instrumentation, an instrument panel and communication to a remote computer programmed for data collection.

FIGURE 4.1

Process Flow Diagram of Satellite Mini Digester Plant



All vessels, tubing and pipe fittings were constructed from 316 and 316L stainless steel. Plant experience is that 317 stainless steel is better suited to digester conditions; however, 317 piping and pipe fittings are not commonly available in the size range that was required. In addition to this, the plant was to be used only on an experimental basis and consequently would not be exposed to anything like the corrosive conditions found on the plant; thus 316 stainless steel was considered to be adequate.

The construction of all vessels was carried out in accordance with the welding codes applicable at SAPPI SAICCOR⁴³. Although none of the vessels involved were classified as pressure vessels (due to their dimensions), all welds were subjected to 100% x-ray testing as well as a Lloyds inspection. All pipework, valves and fittings were assembled using compression-type fittings which, apart from providing leak-free seals, were also quick and easy to remove thus making blockages easy to clear. The entire plant was constructed on a self-contained framework mounted on castors to allow mobility. A drawing of the plant configuration has been included in Appendix 3 (Figure A3-1). Details of the design and structure of the individual components are discussed in the following sections.

i) Liquor Circulation System.

The liquor circulation system consisted of an intake sourced from an external digester and eventually returned to it. The actual connections on the external digester included an automatic isolation valve on the liquor intake, a non-return valve on the liquor return, and a differential pressure switch connected between the two. This was necessary from a safety aspect because any accidental depressurisation of the satellite digester plant (as a result of a burst gasket, for example) would be accompanied by large SO₂ gas emissions making manual isolation of the plant extremely difficult. The differential pressure switch was connected to ensure immediate isolation of the plant from the external digester if a larger than normal pressure difference between the liquor inlet and return was detected.

Liquor circulation was achieved with the use of a small centrifugal pump rated for 40 litres/min at a 2-bar head. The pump was rated to achieve a similar relative liquor flow

rate through the chips as occurs in the plant digesters at the start of a cook. Since pump packings had proven to be a major problem in the past, both in the laboratory and on the plant, a completely sealed magnetic-drive pump was used on the experimental plant.

The main liquor circulation line consisted of 20mm tubing with the following instrumentation connected in-line:

- i) Duplex RTD temperature transmitters before and after the liquor distribution manifolds.
- ii) Magnetic flow meter.
- iii) Pressure transmitter.
- iv) pH probe, with a by-pass should this need to be isolated during a cook, and connections to enable water flushing.

A pressure relief valve set at 12 Barg and connected to the absorption column was also included as an additional safety precaution against accidental over-pressurisation.

ii) Mini Digesters.

The six 2-litre mini digesters were designed according to the British Standard for pressure vessels - BS 5500. Each of the mini digesters was constructed using a 220mm length of 100mm diameter schedule 40 pipe, an ellipsoidal bottom and a blank flange as a lid (see Appendix 3 Figure A3-2 for drawing). Removable chip baskets consisting of 2mm aperture stainless steel mesh were constructed for each unit. These were necessary to prevent fibre carryover during the latter part of the cook, as this is known to cause severe blocking especially with small bore tubing.

Isolation valves were included at the top and bottom manifolds to enable the digesters to be individually isolated. Depressurisation of the digesters was achieved through a pressure release valve on the outlet routed to the absorption column. A quench water connection was provided at the inlet of each digester to enable the hot liquor to be displaced and for rapid cooling of the sample. A local pressure gauge and RTD temperature probe were provided on each digester so that depressurisation and quenching could be monitored.

iii) Liquor Sample Cooler.

In order to enable liquor samples to be taken during a cook, the sample had to be cooled to below 25°C and depressurised. The design of the liquor sample cooler was based on the standard unit used at SAPPI SAICCOR. The unit consisted of 12 metres of 6mm tubing wound into a coil and immersed in a reservoir of cooling water. After each sample, the cooling coils were flushed with fresh water to prevent blockages forming. A sample was then taken by cracking the outlet valve and waiting until the fresh water had been displaced before collecting the liquor.

iv) SO₂ Absorption Column.

All gas emissions during depressurisation as well as the spent liquor were routed to the SO₂ absorption column. This unit consisted of an acid accumulator which vented to atmosphere through an absorption column 1.5m high, packed with 12.5mm ceramic saddles and fed with cold water.

The design of the column was based on a maximum flow of 50 l/min (@STP) of SO₂ gas. This was equivalent to completely removing all the gas from a single digester while the liquor

was still at full strength. No rigorous absorption calculations were performed; instead the water flow required was estimated on achieving 50% saturation of SO₂ in water at 25°C at atmospheric pressure. This provided an estimate of 5 litres/min of water, so double this quantity was provided for.

v) Control and Instrumentation.

An on-board electrical control panel was built for the plant to provide hard-wired interlocks for start-up, shut-down and emergency shut-down procedures. The panel was wired to accept a 3-phase 380 volt supply which was ultimately used to power the pump. Two of the phases were then converted, through a transformer, to a single-phase 220 volt supply and this was used to power the individual instruments, transmitters and the displays in the instrument panel.

On start-up the interlocks were wired to open the control valve on the supply line and start the pump, and to reverse the procedure on shut-down. Two additional interlocks were included to ensure plant isolation in the event of a dangerous situation developing. These were provided by an over-pressurisation relay on the pressure transmitter and the differential pressure switch connected between the liquor inlet and return. The activation of either of these interlocks would automatically stop the pump, shut the isolation valve on the liquor supply line and send an alarm signal to the remote computer used for monitoring the plant.

The instrument panel on the plant provided a local display of the liquor flow, pressure, pH, and any one of eight temperature readings including the inlet and outlet or any one of the digester temperatures. The instrument panel was

also designed to include data transmission to a remote computer. The following readings were transmitted as 4-20 mA signals: liquor pH, liquor flow, pressure, inlet and outlet temperature and the temperature currently selected on the display.

The remote computer was fitted with a multi-channel analogue-to-digital conversion card and was programmed for data collection. (A listing of the Pascal programme written for data collection has been included as Appendix 4).

Since the method of temperature control on the existing laboratory digester was not considered adequate, it was also upgraded by the inclusion of a programmable temperature controller. This unit made accurate and highly repeatable temperature control possible. Pressure control on the existing laboratory digester was left as a manual operation as this proved to be difficult and costly to automate safely.

4.2.4 Calibration of Instruments.

Calibration of the RTD temperature, pressure and flow transmitters was performed in the usual manner, with the spans being set as shown in Table 4-1.

TABLE 4.1			
<u>Instrument Calibration</u>			
Reading	Units	4 mA	20 mA
Temperature	°C	0	200
Pressure	kPa	0	1600
Flow	l/min	0	40
pH	pH	1	5

Calibration of the pH probe proved to be more complex because of the wide temperature span over which the pH value was being measured, as well as the complex nature of pH measurement. In order to obtain the absolute $[H^+]$ concentration at all temperatures, the temperature dependence of the constant in the Nernst equation had to be accounted for in the calibration. This would have required a re-calibration to be performed during the cook as the temperature increased; eg. as the temperature rose, the probe should have been re-calibrated at predetermined temperature intervals. This constant re-calibration proved impractical, and so the probe was calibrated at room temperature using standard pH 4 and pH 7 buffers. This same method of calibration was used by Ingruber⁵⁷ who reported a reproducibility of ± 0.05 pH between probes (ignoring the effects of electrode aging, which are not a function of the calibration).

The significance of this calibration method and its effect on the absolute accuracy of the pH measurement at all temperatures are discussed in detail in section 5.3.2. It is sufficient at this point to note that this was not expected to compromise

the comparability and reproducibility of the measurements from cook to cook, since the errors incurred were constant for all cooks.

4.3 Experimental Methodology and Results.

4.3.1 Methodology.

A series of cooks was planned, using the satellite digester plant in conjunction with the laboratory digester. An initial set of cooks were performed with the purpose of commissioning the equipment, as well as determining the cooking conditions necessary to yield pulp with viscosities in the range of interest, namely from 20 to 120 cp (SNIA). These results were then used to construct the series of cooks required to develop the kinetic models.

i) Wood.

Random 'grab' samples of eucalyptus chips were obtained from the bulk stock piles over a three-month period. This was done in order to get a realistic estimate of the results that can be achieved with wood of varying characteristics such as age, geographical origin, moisture, chip size, etc. The chip size and shape are well controlled at SAPPi SAICCOR (with over 90% of chips falling in the range 13 to 18 mm). Chip moistures averaged approximately 34% ($\pm 5\%$) with all except two sets falling outside this range at 26% and 51%.

Digester wood loads were kept as high as possible to try and keep the liquor-to-wood ratio down; this was done in an attempt to get closer to plant conditions. On the plant, the liquor:wood ratio is of the order 3:1 kg liquor per kg O.D. wood (Oven Dried wood), whereas in the laboratory the best liquor:wood ratio that could be achieved was of the order of 10:1 kg liquor per kg O.D. wood. Actual wood loads used

were 5.2kg in the main laboratory digester and 0.3kg in each of the mini digesters. The net effect of the high liquor-to-wood ratio was to slow down the cooking rate because of the increased dilution of acid by-products. This was compensated for by using a more rapid rise to temperature and higher free SO₂ concentrations than those typically used on the plant.

ii) Liquor.

Raw cooking liquor was drawn from the Liquor Plant. Usually, this liquor had total and combined SO₂ concentrations of the order of 6% and 1.4% respectively. This relatively high concentration of combined SO₂ not only slowed the cooking process down by depressing the acidity of the liquor, but also tended to cause excessive scaling because of the high liquor-to-wood ratio characteristic of this equipment. Liquor concentrations were consequently adjusted to 1.25 ± 0.05% combined SO₂ by dilution, and then the total SO₂ boosted to 8.00 ± 1% using SO₂ gas. Load liquor concentrations of this order were found by experience to give cook times comparable to those on the plant (±6Hr30 for a pulp viscosity of 55 cp SNIA at a cooking temperature of 145°C). The entire experimental plant required a liquor charge of 46 litres.

iii) Cook Cycle.

A complete cook cycle can be divided into the following phases:

1) Wood loading.

The main laboratory digester was charged with 5.2kg of chips, and each of the mini digester chip baskets was charged with 0.3kg of chips and loaded into the mini digesters. All digester lids were fastened. The chips

were then steamed using a direct 5 Barg steam injection. This ensured the removal of trapped air from the chips and had the added benefit of heating the plant up, thus preventing the temperature from lagging behind the set point at the start of the cook when the heat input required was greatest.

2) Liquor loading and pressurisation.

The prepared liquor was loaded into the cooking liquor accumulator and the vessel pressurised with nitrogen to 4 Barg. The laboratory digester was loaded first by opening the vent valve and the liquor loading valve. Once the digester was full, the vent valve on the satellite digester plant was opened and the automatic isolation valve manually opened. When liquor loading was complete, the vent valve on the satellite digester plant was closed and the liquor circulation pumps on both plants were started. (Note that the liquor loading valve was left open).

At this point, all of the gas pockets tended to accumulate in the main digester. To purge this, the vent valve on the digester was opened until the digester was completely full of liquor.

3) Cooking.

Once the liquor load was complete, the heating cycle could be started. For the first 15 to 20 minutes of the cook, the liquor loading valve was left open and the whole plant was pressurised to 5 Barg using nitrogen pressure from the cooking liquor accumulator. Once the liquor loading valve was closed, the pressure rose rapidly and was controlled at ± 10.4 Barg for 90 minutes. After 90 minutes, side relief of approximately 1.5 litres was performed. At this point the pressure dropped

rapidly and eventually stabilised at the vapour pressure of SO₂, once a near equilibrium condition could be attained. The pressure was then allowed to rise to 10.4 Barg where it was controlled for the rest of the cook.

A typical temperature profile used in the experimental cooks can be found in Table 4.2.

TABLE 4.2		
<u>Typical Experimental Temperature Profile</u>		
Time (min)	From (°C)	To (°C)
45	T_{start}	85
45	85	110
60	110	126
60	126	T_{max}

The estimated time at maximum temperature required to achieve a pulp viscosity of approximately 120 cp can be found in Table 4.3. The isolation of the first mini digester was based on these estimates. Subsequent mini digesters were isolated and quenched at 15-minute intervals. This procedure resulted in most pulp viscosities falling in the range of interest, namely 120 to 20 cp SNIA.

TABLE 4.3	
<u>Cook Times at Maximum Temperature</u>	
Maximum Temperature	Time at Maximum Temperature*1 (Minutes)
130	210
140	120
145	90
150	30
*1 Time to isolation of first mini digester	

4) Digester Isolation.

Once the inlet and outlet of a mini digester had been isolated, the vent valve to the SO₂ absorption column was opened and the pressure dropped to atmospheric pressure. (The absorption column proved quite capable of handling gas emissions even at the fastest depressurisation rates). The time for depressurisation was of the order of 1 minute. Once the local pressure gauge indicated 0.5 Barg, the quench water was opened and left to run for about 5 minutes in order to completely displace the liquor and cool the pulp and the digester. Once the digester was cool enough to handle, the quench feed and vent valves were shut, the digester was opened and the pulp sample was removed.

The isolation of the last mini digester required that the entire plant be shut down, which involved the following sequence of operations:

- a) The temperature control was switched off.
- b) Circulation pumps on both plants were stopped.
- c) The last mini digester was then isolated and quenched in order to insure an accurate cook time.
- d) Vent valves on both plants were opened and the automatic isolation valve between the two was manually opened. Depressurising the combination of the two plants took 15 to 20 minutes.
- e) Once a pressure of 0.5 Barg was reached, the liquor was discharged into the spent liquor accumulator where it could cool and eventually be put to drain. Once the liquor discharge was complete, the main digester vent valve and the quench water valve were opened and the circulation pumps on both units started in order to wash and cool both plants. This took up to 30 minutes depending on the maximum temperature of the cook. (Circulation on the satellite plant was routed through the first digester to be isolated).

5) Liquor and Pulp Sampling.

a) Liquor Samples:

The first liquor sample could only be taken at side relief as the removal of any liquor prior to this caused the hydraulic pressure in the digesters to be lost.

An additional restriction on liquor sampling was that no more than 3.5 litres could be removed in total without the risk of exposing the chips in the main laboratory digester. Unfortunately, the high cooling capacity required by the liquor

sampling unit resulted in the unit having a large capacity, and thus each sample taken required that a volume of at least 500ml be removed.

As a result of the above restrictions, the quantity of side relief taken was kept to a minimum to allow as many liquor samples as possible to be taken during the rest of the cook. The minimum amount of side relief which could be taken was found to be 1.5 litres, as this was just sufficient to prevent liquor carryover during pressure control after side relief. The number of subsequent liquor samples which could be taken was thus restricted to six (including side relief and load liquor).

b) Pulp Samples:

Pulp samples required some preparation before they could be analysed. This involved disintegrating the sample (± 150 grammes) in 10 litres of water with a standard pulp disintegrator for 10 minutes. Three pulp pads were then made by pouring 500ml of the slurry onto a 150mm diameter vacuum filter and washing with methanol. These pulp pads were then dried at 60°C for approximately four hours and were then used as follows:- one for viscosity analysis, one for K number analysis and one spare.

The remaining pulp slurry was then made into a 300mm pulp pad and air-dried at 60°C for about 12 hours (no methanol wash). A chlorine dioxide extraction was then performed on a 20 gram sample

of this air-dried raw pulp, and the resultant extracted pulp was used for the S₁₈ hemicellulose analysis.

Now that the characteristics of the experimental equipment and method have been explained, the results obtained can be presented in context and the required models can then be developed. This work is presented in the following chapter.

CHAPTER 5

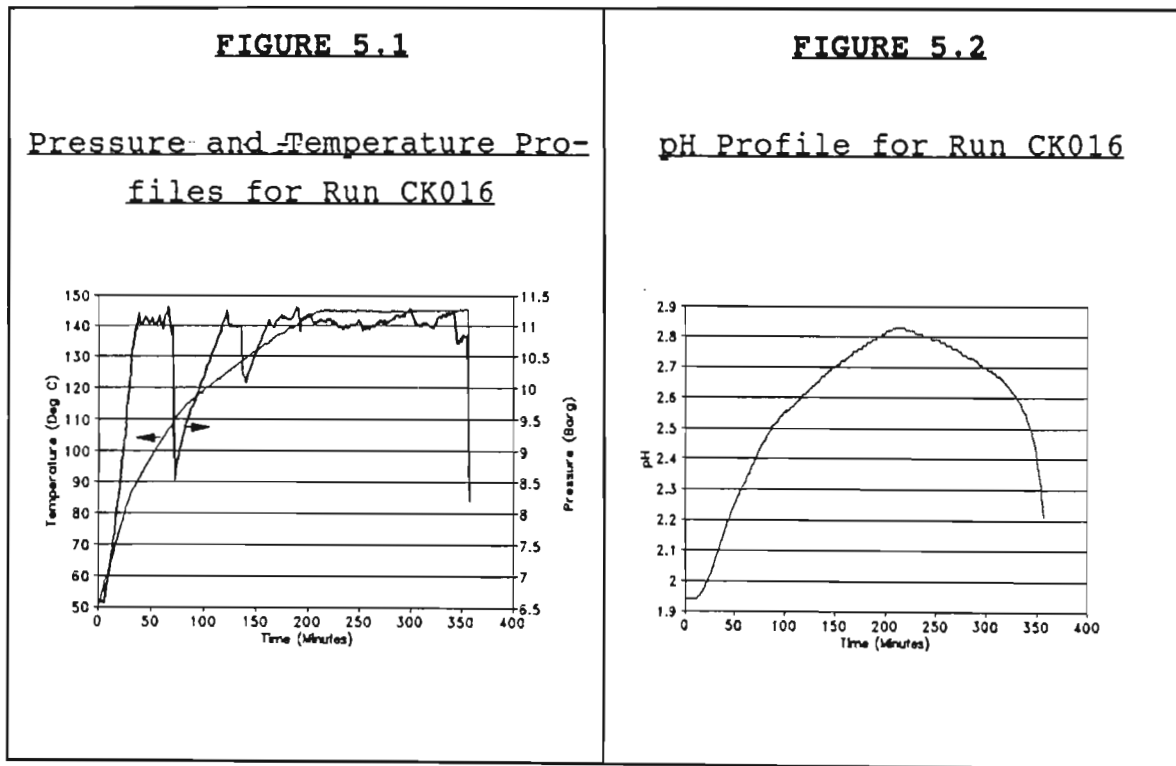
EXPERIMENTAL RESULTS AND KINETIC ANALYSES

5.1 Typical Set of Results.

Each experimental run produced a large quantity of data; the detailed data for all the experimental runs performed can be found in Appendix 5. A sample set from a typical run has been included here in Table 5.1.

TABLE 5.1						
<u>Typical Set of Results From an Experimental Run</u>						
COOK NUMBER		CK016		MAXIMUM TEMPERATURE		145°C
WOOD LOAD		7.0 Kg		LIQUOR LOAD		46 litre
WOOD MOISTURE		34 %		TOTAL COOK TIME		6h15
<u>Liquor Sample Analysis</u>			<u>Pulp Sample Analysis</u>			
Elapsed Time	Total SO ₂	Combined SO ₂	Elapsed Time	Pulp Viscosity	K Number	S ₁₈
LOAD	7.36 %	1.26 %	5h00	124.7	4.90	5.78
0h00	6.73 %	1.24 %	5h15	91.7	4.08	5.86
1h30	6.41 %	1.16 %	5h30	73.3	3.62	5.44
2h00	6.34 %	1.13 %	5h45	63.0	2.98	5.17
2h35	6.19 %	1.05 %	6h00	54.0	2.77	5.25
3h30	5.92 %	0.82 %	6h15	43.9	2.31	5.13
4h30	5.40 %	0.46 %				

Graphs of the temperature, pressure and pH data collected during the run have been included as Figures 5.1 and 5.2. The characteristics and trends observed from these sets of data are discussed in the following section.



A series of experimental runs were performed at maximum temperatures ranging from 130°C to 150°C to gather data for the purpose of determining the kinetic parameters of the various reactions. A summary of this data set has been included in Table 5.2.

TABLE 5.2

Series of Experimental Runs Performed to
Provide Data for Kinetic Analyses

Cook Number	Maximum Temperature °C	Total Cook Time (Mins)
16	144.9	375
17	130.3	495
18	139.7	405
19	149.9	315
20	145.0	360
21	140.0	405
22	149.8	330
23	135.9	450
24	135.8	450

5.2 Discussion of Results.

5.2.1 Pressure.

From the pressure profile it can be seen that the pressure control tended to be slightly erratic, but the degree of variability experienced during the run was not sufficient to exert any significant influence on the measured pH value. In general, the pH value proved to be insensitive to small changes in pressure and only exhibited a marked change with substantial changes in pressure, such as those experienced at the end of the run.

The drop in pressure at the end of the hydraulic pressurisation phase, caused by the removal of side relief liquor, can be clearly seen from the graph of the pressure profile above (Figure 5.1).

5.2.2 Temperature.

Three temperature profiles were recorded during each experimental run, namely the inlet to and outlet from the six mini digesters, and the temperature of the mini digester scheduled to be isolated next. Temperature control on the satellite digester plant proved to be very accurate with the inlet and outlet temperatures deviating at most by 0.4°C.

Despite complete insulation of all the liquor lines, heat losses in the liquor transfer lines to and from the satellite digester plant still occurred. This resulted in the temperature of the main laboratory digester running slightly higher than those in the satellite digesters. This deviation increased with increasing maximum temperature and ranged from $\Delta T \approx 0^\circ\text{C}$ at 130°C to $\Delta T \approx 4^\circ\text{C}$ at 150°C. Even the inclusion of heaters on the liquor lines did not greatly improve this situation. Consequently, accurate temperature control on the main laboratory digester was forfeited in favour of that on the satellite digester plant. The only possible effect that this temperature deviation could have had was on the production of acidic by-products, as the bulk of the wood load ($\pm 74\%$) was in the main laboratory digester.

5.2.3 pH Value.

The pH profiles for each of the experimental runs exhibited the trends expected. This included the rise in pH value (drop in acidity) during the rise to maximum temperature, caused by

the decrease in SO₂ solubility and the decrease in the degree of dissociation of the sulphurous acid. Once the maximum temperature had been reached, a distinct inflection point was evident and the pH value started to decrease due to the formation of acid by-products. As was expected, the rate at which the pH value decreased during this phase was strongly dependent on the maximum temperature. If the extremes were considered, ie. 130°C and 150°C, then the nature of the pH value decrease while at maximum temperature could be seen to be distinctly different. The drop in pH value for a 130°C run was a slow almost linear decrease whereas the higher temperature runs were characterised by more rapid pH value decreases until a point was reached where the pH value dropped extremely rapidly. This was most probably a result of the sulphurous acid equilibrium reversing when the concentration of [HSO₃⁻] became very small (as mentioned in Chapter 3 Section 3.1).

The range of pH values measured during cooking was in close agreement with measurements taken by Ingruber³⁵. He reported pH values at the start of the experimental run in the region of 1.8 to 2.4, maximum pH values during the run of 2.7 to 3.1 and pH values at the end of the run between 2.4 and 2.9, using a calcium-based liquor on spruce. A sample set of profiles reported by Ingruber has been included as Figures 5.3 and 5.4 for reasons of comparison.

FIGURE 5.3

Typical Pressure and Temperature Profiles for Cook Reported by Ingruber³⁵.

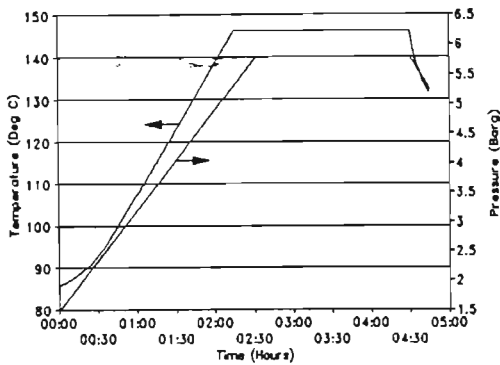
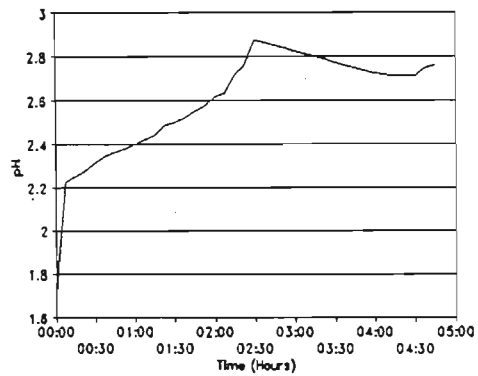


FIGURE 5.4

Typical pH Profile for Cook Reported by Ingruber³⁵.



When comparing the pH profiles reported by Ingruber and those measured in this study, it is important to note that Ingruber's cooks were characterised by a 90 minute depressurisation phase during which the pH value rose due to the loss of SO₂. During this period, reactions continued - albeit at an ever decreasing rate. In addition to this, at the end of most of the cooks performed by Ingruber there was a small but measurable concentration of combined SO₂, in contrast to most of the experimental runs performed in this study where combined SO₂ concentration became zero during the run (all measured using the Palmrose method). These are the most probable reasons why the rapid drop in pH value towards the end of the runs observed in this study were not apparent in Ingruber's cooks³⁵.

A progressive upward drift in the pH value was observed from cook to cook. This drift (which was also observed by Ingruber³⁵) most probably resulted from the glass electrode aging,

indicating that this problem is still a factor despite the improvements made in the manufacture of pH probes. A drift of approximately 0.21 pH units was observed over a period of 10 experimental runs. Two methods were attempted in an effort to prevent or limit this drift - cleaning the probe with hydrochloric acid and water flushing it between runs; however, neither were successful.

Subsequent re-calibration of the probe indicated that the drift in readings resulted mostly from the upward displacement of the reading and not from a variation in the span of measurement. Constant re-calibration of the probe, apart from being impractical, reduces the reliability and repeatability of the measurement. The instrument settings were thus left constant and the readings were corrected by calculating the pH value during the initial phases of the run (before significant quantities of acid by-products have formed), using the relationships given in Chapter 3 (Section 3.2). The details of these calculations are presented in Section 5.3.

5.2.4 Liquor Analysis.

The analysis of the load liquor as indicated in Table 5.1 was performed on a sample of the cooking liquor before being loaded into the cooking liquor accumulator. The sample taken at the start of the run, however, was withdrawn just before the liquor loading valve was closed, ie. about 10 minutes into the run. This method provided a homogeneous liquor sample which characterised the liquor at the start of the run and avoided a negative effect on the hydraulic pressurisation of the plant.

The fairly large drop in total SO₂ observed between the load liquor and the liquor at the start of the run was the result of free SO₂ being lost during loading. This loss of free SO₂

was unavoidable and was caused by SO₂ gas flashing off as the liquor was loaded into the digesters, which were hot after pre-steaming the chips. The amount of free SO₂ lost at this point varied from run to run. In addition to this, a slight drop in concentration was expected as a result of liquor dilution with condensate remaining in the digester, due to incomplete draining of the plant after steaming. The drop in combined SO₂ observed between these two samples was therefore more likely to be the result of liquor dilution.

5.2.5 Pulp Sample Analysis.

Viscosity and K number analyses of pulp samples were found to be accurate and reliable, and exhibited the expected trends with both steadily decreasing during the run. A common problem experienced with the viscosity measurement was the interference of lignin, especially if the sample contained an appreciable percentage of lignin. The net effect of the error caused by a high lignin content was a low viscosity measurement. As the cook progressed and the lignin content dropped, the viscosity would increase until sufficient lignin had been removed. (There was no reference in the literature as to what the lignin content should be reduced to in order to ensure an accurate viscosity measurement.)

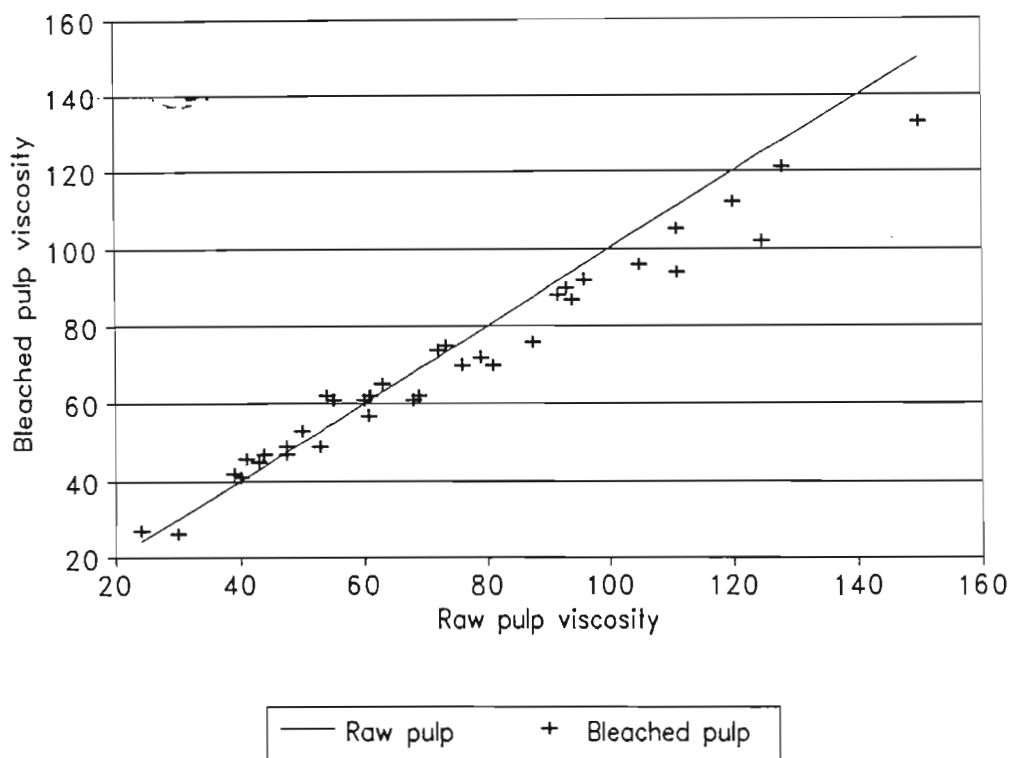
The influence of residual lignin on viscosity measurement was investigated during the initial scoping study. This was done by performing shorter than usual cooks to ensure a high residual lignin content. The raw pulp viscosities were then measured. Samples of the pulp were then bleached to remove the lignin and the viscosity of the bleached samples measured. The bleaching procedure chosen was a mild chlorine dioxide bleach, as this has the least tendency of all the bleaching procedures to attack the carbohydrate fraction especially if the pH value

is in the acid region³. Since a slight degradation of the cellulose was unavoidable during bleaching, the viscosity of the bleached samples was lower than the raw pulp measurement. However, trends could still be identified. In addition to this, the method of viscosity determination on bleached pulp required a slightly greater mass of pulp sample to be used. When the residual lignin content was very small (as in very low viscosity samples) and the bleaching process had been closely controlled, this led to the apparently anomalous result of higher bleached pulp viscosities than raw pulp viscosities.

A graph comparing raw pulp viscosity with bleached pulp viscosity has been included as Figure 5.5. From this graph it can be seen that as long as the raw pulp viscosities were less than 100 cp SNIA, the effect of residual lignin could be ignored and a reasonably accurate viscosity measurement could be obtained from a raw pulp sample. Despite the interference of lignin on the viscosity measurement of raw pulp, it was still found to be more repeatable than measurements on bleached pulp. This was due to the fact that the extent of cellulose degradation caused by bleaching was found to vary from sample to sample and thus introduced larger errors than those caused by the lignin in the raw pulp. As a result, all DP values were estimated from raw pulp viscosity measurements.

FIGURE 5.5

Comparison of Viscosity Measurements on Raw pulp and Bleached Pulp (cp SNIA).



S₁₈ measurements were found to be erratic and often did not even follow the correct trend. As mentioned above, the bleaching process resulted in an attack on the carbohydrate fraction and this was a definite source of error. In addition to this, subsequent investigation into the S₁₈ analytical procedure has indicated that it is extremely sensitive to the dissolved CO₂ concentration present in the NaOH⁴⁴. (Precautions have since been taken at SAPPi SAICCOR to eliminate these inaccuracies.) The effects of this source of error are discussed in Section 5.5.2.

5.2.6 General.

As mentioned in Chapter 4, the lowest liquor-to-wood ratio that could be achieved in this equipment was of the order of 10:1. Varying the liquor-to-wood ratio proved to be a problem in that it could be only further increased. Higher liquor-to-wood ratios resulted in less combined SO₂ being consumed by the wood and this led to serious scaling problems. The liquor-to-wood ratio was therefore always kept as low as possible.

The effect of chip size on pulp characteristics was also investigated by cooking samples of a specific range of sizes in separate compartments within the main digester. The rest of the wood load was made up of unscreened chips. The pulp characteristics of the various samples have been included in Table 5.3.

<u>TABLE 5.3</u>					
<u>Effect of Chip Size on Pulp Characteristics</u>					
Size Fraction (mm)		Viscosity	DP	K Number	% lignin
From	To	cp	Value		
7	12	31.8	941	2.48	2.09
13	18	31.0	933	1.99	1.51
19	25	30.2	925	2.20	1.75
Mixed Sizes		31.3	936	1.85	1.36

The viscosity of the pulp showed a distinct trend towards lower viscosities for the larger chip sizes, with a variation of 1.8 cp between the largest and smallest size fractions.

The viscosity of the pulp produced from the unscreened chips was very close to that of the 13 to 18 mm range. This was to be expected as the majority of unscreened wood chips fell in this range ($\pm 90\%$). This variation in viscosity (1.8 cp) between the extremes in chip sizes was thus not significant in the context of this study.

The K number (lignin content) showed no clear trend, with the mixed chip size sample yielding the lowest K number. As in the case of viscosity, the K number of the pulp produced from the unscreened chips was closest to that of the 13 to 18 mm range. It would therefore appear from these results that K number is fairly dependent on chip size; however, the relationship appears to be complex and indicates the possibility that there exists an optimum chip size for achieving maximum delignification. A rigorous definition of this relationship will require more research directed specifically at these aspects.

While the acidity of the cooking liquor could be measured directly, the concentration of bisulphite had to be calculated using the charge balances and equilibrium correlations developed in Chapter 3. These calculations are covered in section 5.3.

5.3 Calculation of Bisulphite and Strong Acid Concentrations.

5.3.1 Direct Calculation Using Raw Data.

The concentrations of HSO_3^- and SA^- were calculated from the measured variables, viz. temperature, $[\text{H}^+]$, total SO_2 and combined SO_2 , using the following procedure:

- i) Calculate K_{SO_2} using either the values given by Rydholm et al³ or the correlation reported by Schön & Wannholt²⁸ (cf Section 3.2).
- ii) The $[HSO_3^-]$ concentration was calculated from the following expression, which was obtained by solving equation 3-9 to obtain an expression for $[HSO_3^-]$ in terms of total SO_2 , $[H^+]$ and K_{SO_2} :-

$$[HSO_3^-] = \frac{K_{SO_2} \cdot [SO_2^{tot}]}{(K_{SO_2} + [H^+])} \quad (5-1)$$

- iii) The $[SA^-]$ concentration was calculated by solving equation 3-1 to obtain the following expression:-

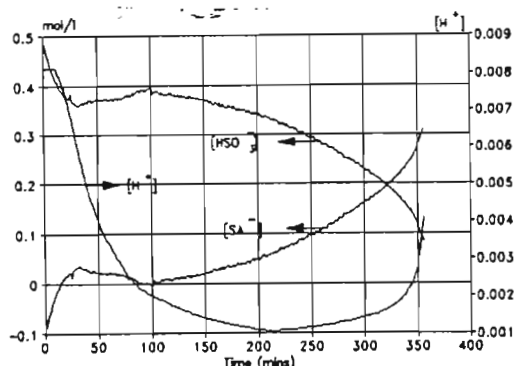
$$[SA^-] = [H^+] + 2 \cdot [\text{Initial Combined } SO_2] - [HSO_3^-] \quad (5-2)$$

Sample sets of profiles of $[H^+]$, $[HSO_3^-]$ and $[SA^-]$ have been included as Figures 5.6A and 5.6B. The profiles of $[HSO_3^-]$ and $[SA^-]$ shown in Figure 5.6A were calculated using Rydholm's³ values for K_{SO_2} , while those shown in Figure 5.6B were calculated using the correlation given by Schön & Wannholt²⁸.

FIGURE 5.6

Sample Profiles of $[H^+]$, $[HSO_3^-]$ and $[SA^-]$ during an Experimental Run.

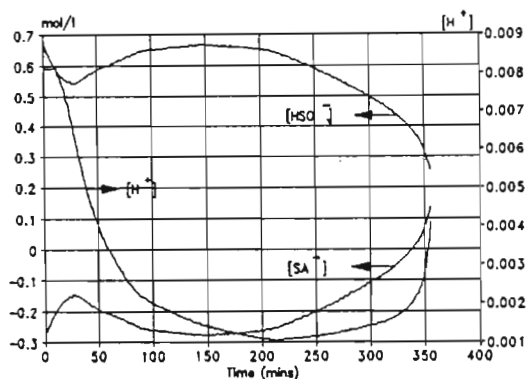
FIGURE 5.6A



Calculations based on values of K_{SO_2} Reported by Rydholm³

Note:- Calculated values of $[SA^-]$ in expected range after hydraulic pressurisation phase.

FIGURE 5.6B



Calculations Based on Schön & Wannholt's' Correlation for K_{SO_2} ²⁸

Note:- Calculated values of $[SA^-]$ negative for most of the cook.

The following can be observed from the profiles shown in Figures 5.6:

- i) The calculated concentration profiles of HSO_3^- and SA^- (which is partially dependent on $[HSO_3^-]$) show a distinct deviation from the expected profiles during the hydraulic pressurisation phase at the start of the run. This deviation was the result of the extreme non-equilibrium conditions prevailing during this stage.
- ii) From the $[SA^-]$ concentration profiles it can be seen that the calculations based on K_{SO_2} as given by Rydholm³ yielded far better results here than the correlation reported by Schön & Wannholt²⁸. The $[SA^-]$ should start off at zero and gradually increase only once the

delignification reactions start becoming significant. Figure 5.6A, excluding the deviations during the hydraulic pressurisation phase, closely follows the expected trend in $[SA^-]$ concentration.

The values of K_{SO_2} as given by Rydholm clearly yielded better results here than the correlation reported by Schön & Wannholt. A probable explanation for this is that while both groups used direct potentiometric measurements, their methods of calibration differed. The results reported by Rydholm, and confirmed by Ingruber³², were based on direct potentiometric measurements, where the calomel reference electrode was at the same temperature and pressure as the measuring electrode. In addition to this, both Rydholm and Ingruber appear to have calibrated at only one set temperature. In contrast to this, Schön & Wannholt used an instrument in which the standard calomel electrode was maintained at $\pm 23^\circ C$ and connected to the solution being measured by a salt bridge. They also re-calibrated the instrument for each temperature at which a measurement was made.

Since the nature of the instrument and the calibration techniques used in this study were identical to those used by Rydholm and Ingruber, the values for K_{SO_2} as reported by Rydholm were therefore used for all subsequent calculations.

5.3.2 Calibration and Calculation of Corrected Profiles

As mentioned in Section 5.2.3, the pH values were found to be prone to a constant upward drift. In order to obtain directly comparable sets of data for each experimental run, the pH profiles of each run were re-calibrated by calculating the pH value at a specific point in time, using the charge balance

and equilibrium correlations presented in Chapter 3 (cf. Section 3.2). All measured pH profiles were then adjusted by adding a correction factor equal to the difference between the calculated and measured pH values at that point in time. This method was found to produce reliable repeatable results even when the actual pH value had drifted by up to 0.21 units.

The rationale behind this 'on line' calibration technique was based on the following aspects of pH measurement:

1. A pH value is obtained by measuring the electrode potential developed across the measuring and reference electrodes and is based on the relationship given in Equation 5-3:

$$E_{el} = E_0 - S(pH_a - pH_i) \quad (5-3)$$

where:-

- E_{el} - electrode potential
- E_0 - zero potential
- S - slope (mV per pH unit)
- pH_i - pH value of internal buffer
- pH_a - pH value of measured solution

From the above it can be seen that the pH measurement depends on a reversible interaction between the sensor and the measuring solution. A change in the slope (S in equation 5-3) or a shift in the zero point (E_0 in equation 5-3) are both phenomena associated with either a reaction with the measuring solution or the aging of the electrode.

A shift in the zero point can be directly allowed for if the pH of the measuring solution is known or can be calculated, as in this case. In fact, the use of the actual measuring solution for calibration eliminates a number of complicating factors related to pH probe

calibration, for example differing temperature curves between the buffer solutions and the measuring solution are no longer a problem.

A shift in the mV-to-pH slope can be corrected if the pH is known or can be calculated at two points. In practice, this was extremely difficult to achieve on a repeatable basis. Some of the complications were as follows:-

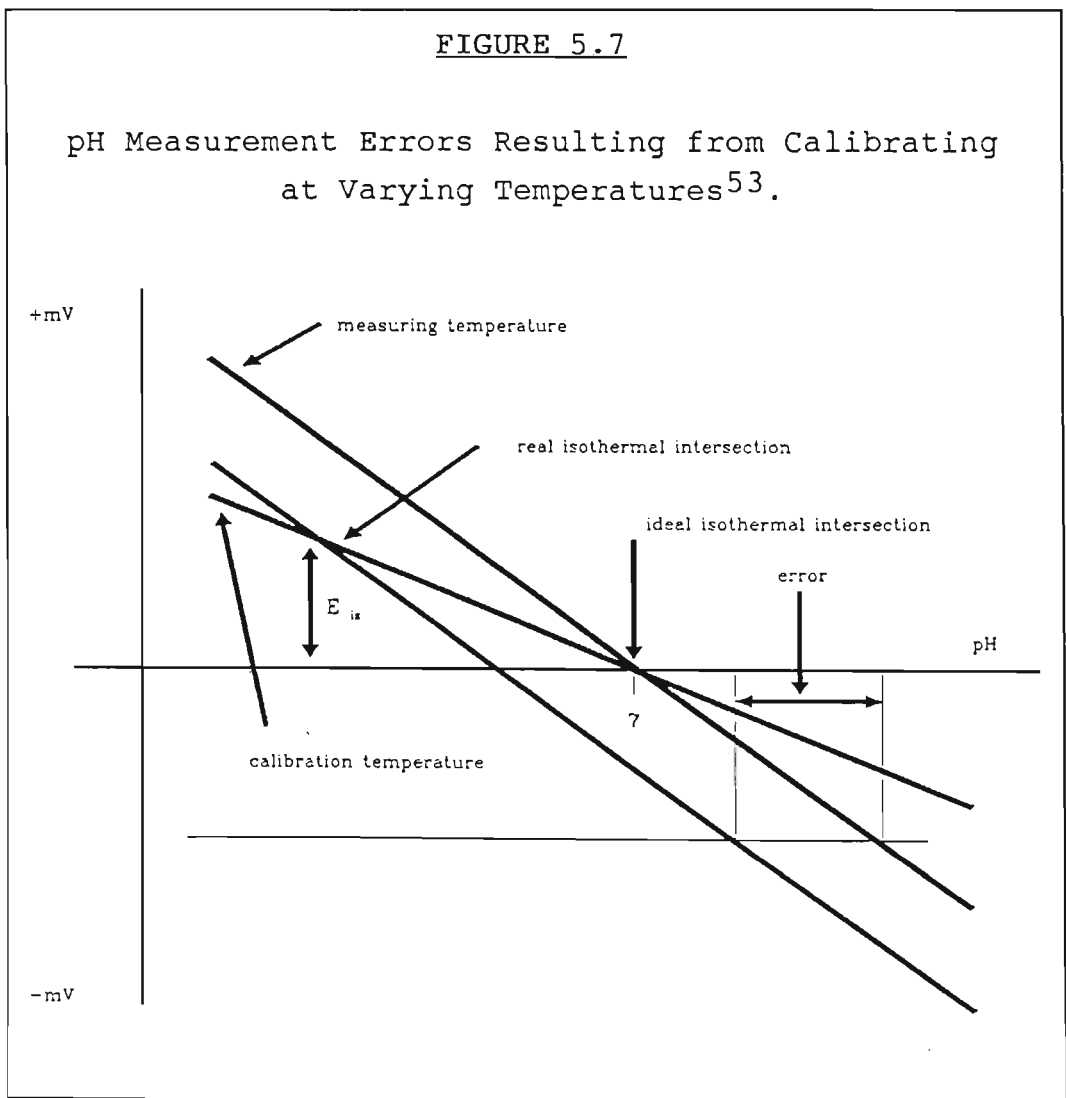
- i) Only one point during a cook cycle could be found where this could be achieved (discussed later).
- ii) The two points would of necessity be at widely differing temperatures and this was extremely undesirable (see point 2 below).
- iii) The pH range over which these measurements were made was small; consequently, small errors in the calculation of the pH may have led to substantial errors in calibration

For the above reasons no attempts were made to correct for shifts in the mV-to-pH slope. In addition to this, acceptable results were obtained by correcting only for zero point shift.

2. A fixed point during the cook must be selected to ensure that this correction is always performed at the same temperature. This is important for the accuracy of the calibration since the temperature influences both the various individual potentials relating to the electrode and the ion activity.

Although the instrument used included automatic temperature compensation, it is important to realise that

there will always be a calibration error incurred if calibrations are carried out at different temperatures and the isothermal intersection (E_{is}) characteristic of the electrode does not correspond to 0 mV. Despite the fact that a tremendous amount of effort⁵³ has gone into trying to produce probes with isothermal points as close to 0 mV as possible, in practice this point very rarely occurs at 0 mV. The nature of the error incurred by calibrating at different temperatures is graphically illustrated in Figure 5.7.



Calculation of the hydrogen ion concentration required first that the bisulphite ion concentration ($[HSO_3^-]$) be calculated. This was calculated using Equation 3-9:

$$[HSO_3^-] = [SO_2^{com}] - \frac{1}{2}K_{SO_2} + \left\{ \frac{(2[SO_2^{com}] - K_{SO_2})^2}{4} + K_{SO_2}[SO_2^{tot}] \right\}^{\frac{1}{2}} \quad (3-9)$$

where:-

$[SO_2^{tot}]$:- total SO_2 concentration

$[SO_2^{com}]$ - available combined SO_2 concentration

which, in turn was calculated as follows:-

$$[SO_2^{com}] = [\text{Initial combined } SO_2] - \frac{1}{2}[SA^-] \quad (3-3)$$

The hydrogen ion concentration (and hence pH value) were then calculated using equation 3-10, viz:

$$[H^+] = K_{SO_2} * \left\{ \frac{[SO_2^{tot}] - [HSO_3^-]}{[HSO_3^-]} \right\} \quad (3-10)$$

The selection of the point at which the pH correction is best effected depends on the calculation of $[HSO_3^-]$, as this calculation is heavily dependent on the concentration of initial combined SO_2 . Due to the interference of the hydraulic pressurisation phase on these calculations (illustrated in Figures 5.6A and B), the most stable starting point for the calculations had to be carefully selected. Use of the following three measurements as initial combined SO_2 were investigated:

i) The combined SO_2 of the load liquor:-

This proved to be unsuitable because the dilution of the liquor by wood moisture and trapped water in the units proved impossible to predict.

ii) The combined SO₂ of the liquor at the start of the run:-
The manner in which liquor was loaded resulted in a hydraulic pressure of between 4 and 6 Barg even before the run was started, and so the use of this measurement produced erratic results.

iii) The combined SO₂ of the liquor ±20 minutes after side relief:-

By this time (±120 mins at 125°C), very little delignification had taken place although some of the base had already combined with lignin in the solid phase. Thus insignificant quantities of the strong acid by-products had formed and it was safe to assume that $[SA^-] \approx 0$. In addition to this, since the system had stabilised after the hydraulic pressurisation phase, the equilibrium expressions could be used. This measurement, despite the assumptions, proved to be the most stable starting point for calculations and was thus used as the initial combined SO₂.

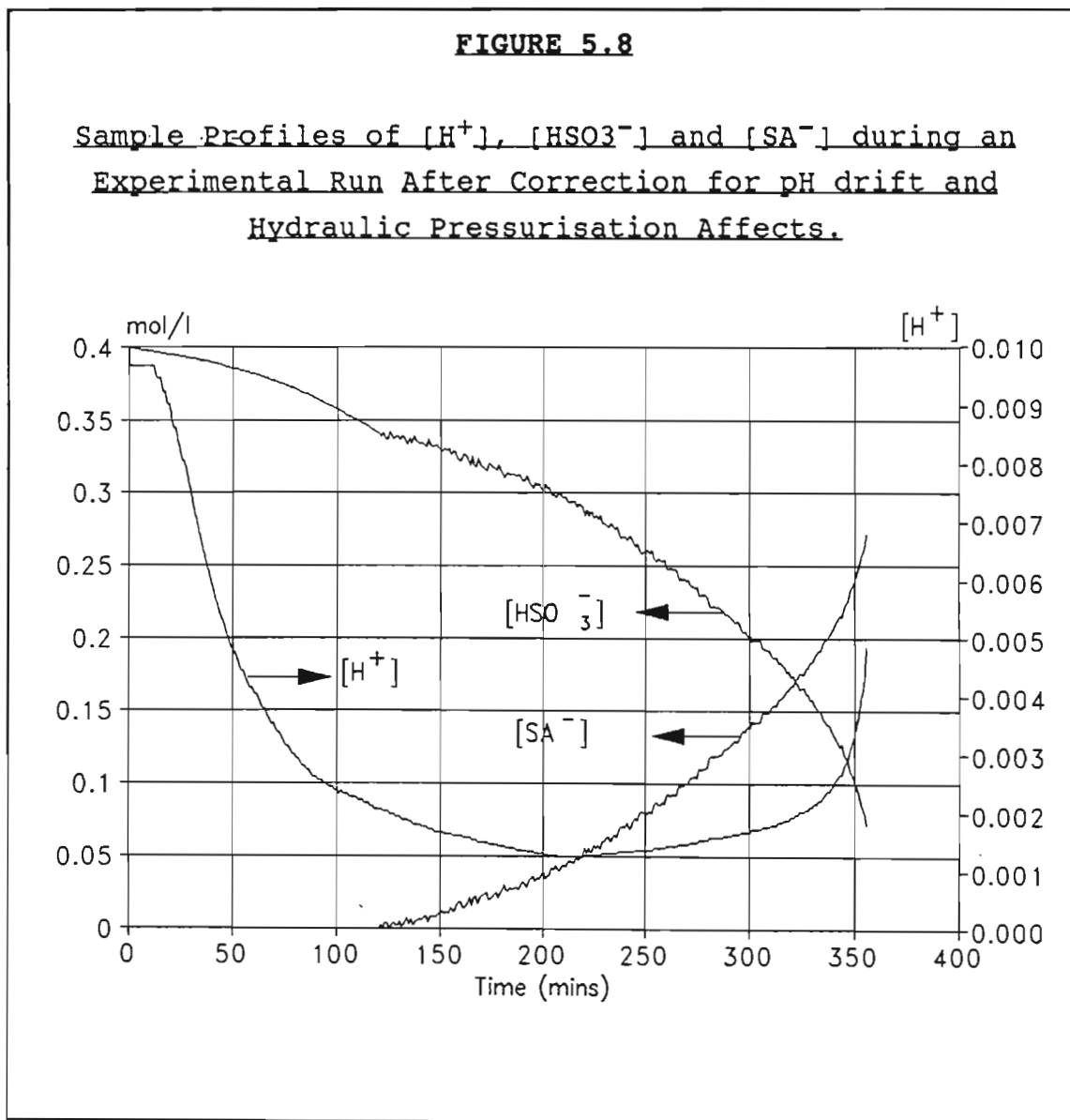
In this case the charge balance given in equation 3-1 was also used to calculate $[H^+]$ as follows:

$$[H^+] = [HSO_3^-] - 2[\text{Initial combined } SO_2] \quad (5-4)$$

The concentration profiles of HSO_3^- and SA^- during the hydraulic pressurisation phase were calculated by a simple interpolation between the measured concentrations of combined SO₂ at the start of the run and the concentration after side relief, and by assuming $[SA^-]=0$ for $t < 120$ min.

Sample sets of profiles of $[H^+]$, $[HSO_3^-]$ and $[SA^-]$ calculated on the basis described above have been included as Figure 5.8, ie. after re-calibration of the pH readings and calculation of $[HSO_3^-]$ during the hydraulic pressurisation phase based on measured combined SO₂. The concentrations of HSO_3^- and SA^-

for the rest of the experimental run were then calculated using the expressions presented in section 5.3.1 (ie using equations 5-1 and 5-2). A spreadsheet illustrating these calculations has been included as Appendix 6.



Having established a repeatable procedure for calculating the various chemical concentration profiles during a run, the kinetic fits were then performed.

5.4 Kinetic Analysis of the Cellulose Hydrolysis Reaction.

5.4.1 Kinetic Analysis.

The kinetics of cellulose degradation by the acid hydrolysis reaction were determined using the concept of Degradation Increase (DI) developed in Section 2.4. The kinetic expression for cellulose degradation thus became:

$$DI = A_c e^{\left(-\frac{E_c}{RT}\right)} \int_{t=t_0}^{t=t_f} [H^+] dt \quad (5-5)$$

where:-

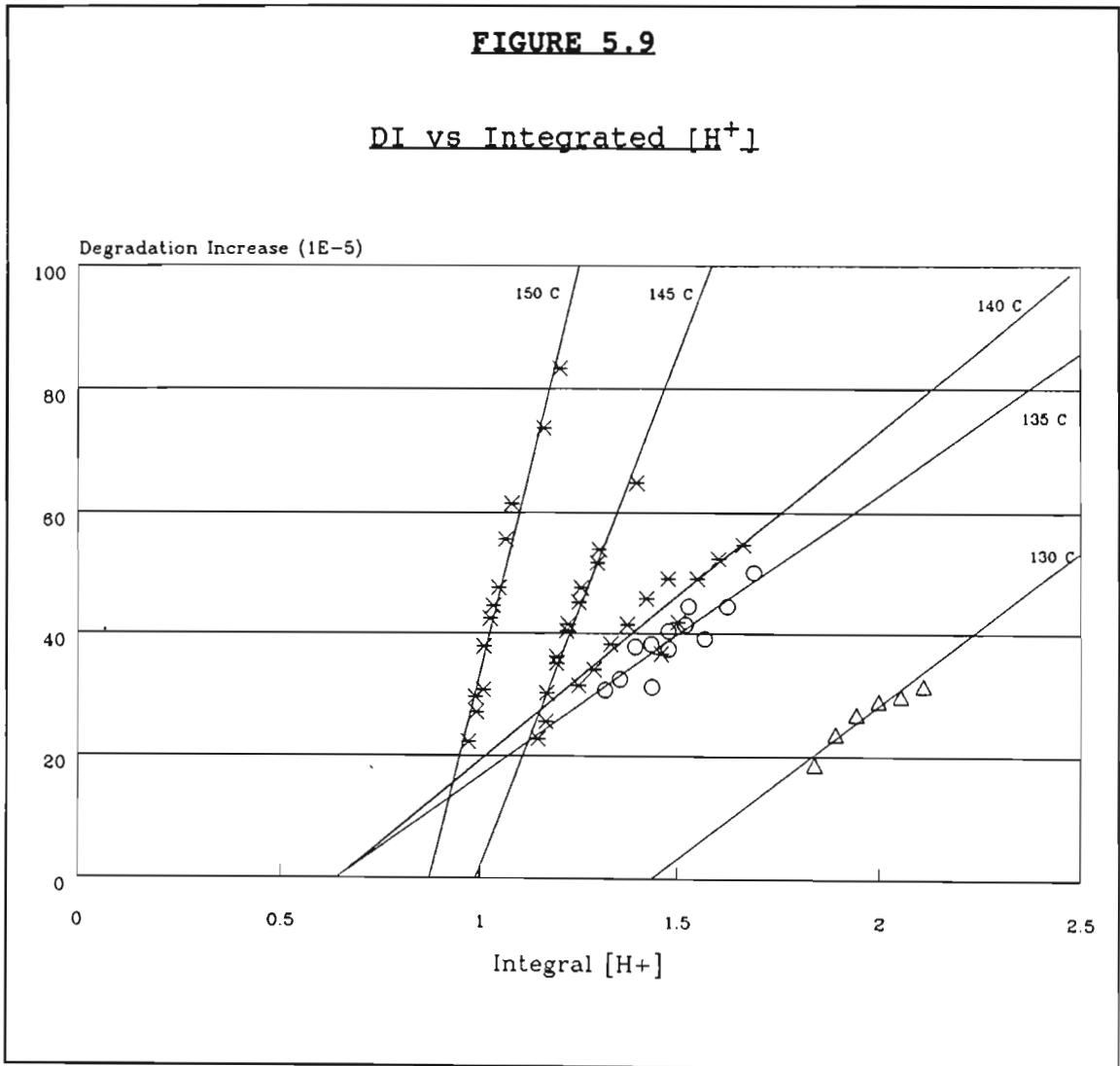
- i) $k_c = A_c e^{\left(-\frac{E_c}{RT}\right)}$
- ii) $DI = \frac{1}{DP_f} - \frac{1}{DP_0}$
- iii) $DP = 285.4 * \mu^{0.345}$
 $\mu = \text{SNIA viscosity in cp}$

The kinetic fit for cellulose degradation was then performed as follows:

- 1) Measured pulp viscosities were converted to a DP value using the correlation given as (iii) above.
- 2) The degradation increase (DI) for each sample was then calculated. The calculation of DI here required that a value for DP_0 be chosen as a reference point. One way this could be done would be to use the first sample in each run as DP_0 . This however was undesirable as it resulted in reducing the number of points available for determining a kinetic fit. The use of assumed values for DP_0 were tested ($2000 < DP_0 < 4000^3$); however, this value was found to have no affect on the determination of the kinetics of the reaction. (It is important to note at

this point, however, that the value of DP_0 used for modelling purposes is vitally important since it is used to calculate the final DP value and hence the viscosity.)

- 3) For each experimental run, the constant k_c relating to the maximum temperature of the run was determined from the slope of a plot of DI against the integrated hydrogen ion concentration. A summary of these curves has been included in Figure 5.9.

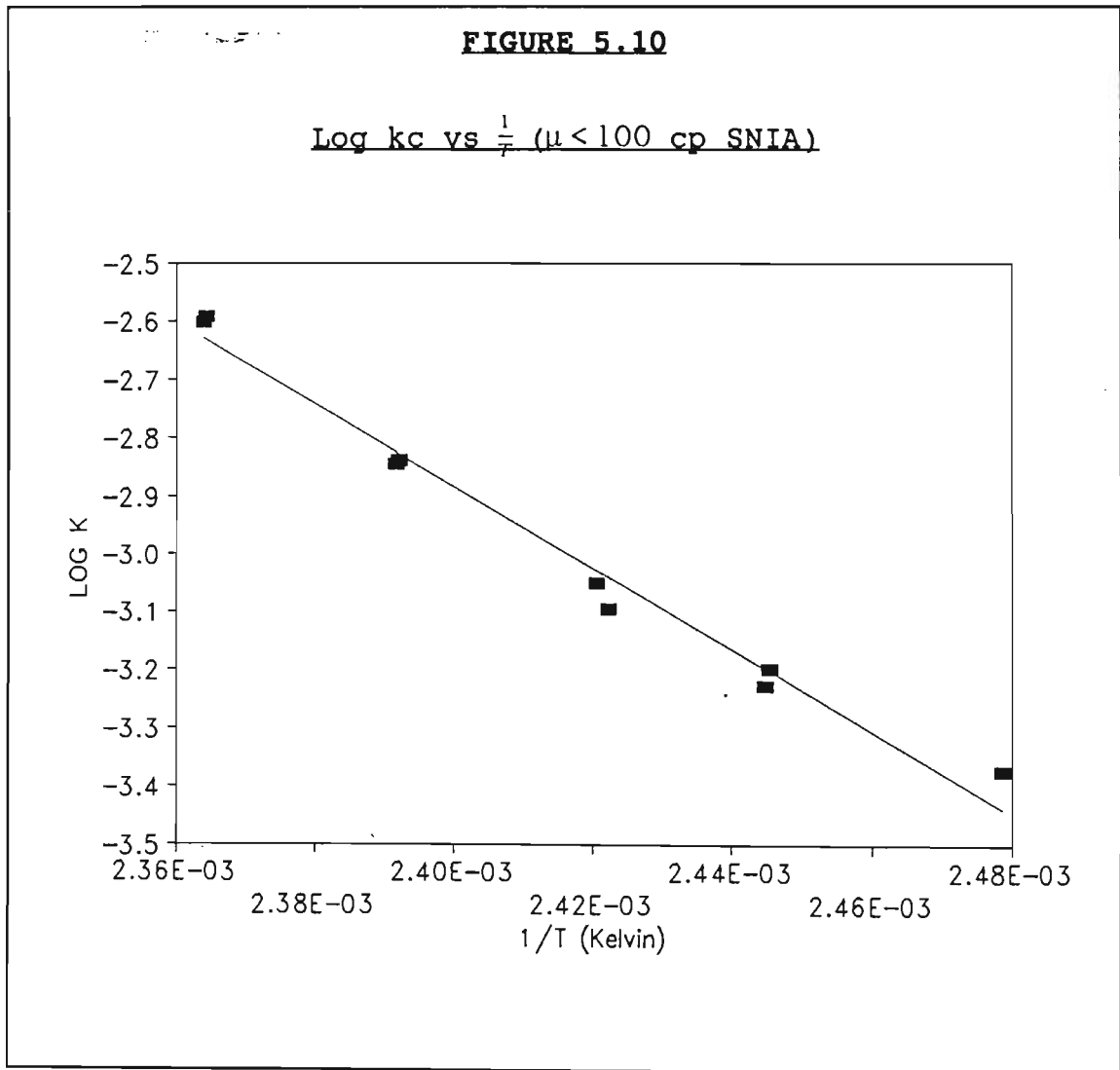


- 4) The values of the pre-exponential constant A_c and the activation energy E_c were then determined from a plot of the values of $\log k_c$ against $\frac{1}{T}$ in the following manner:-

$$E_c = 2.303 * 1.987 * \text{slope}$$

$$A_c = 10^{\text{Y intercept}}$$

A graph of this plot can be found in Figure 5.10.



The results of this kinetic analysis were as follows:-

$$E_c = 33\,867 \text{ cal/gmol}$$

$$A_c = 7.68 \times 10^{14}$$

$$R^2 = 0.981 \text{ ('Goodness of Fit')}$$

5.4.2 Comparison of Results with Other Studies.

The activation energy for acid hydrolysis of cellulose determined from this work is very similar to those reported by other researchers despite the fact that they used various acids, different sources of cellulose to those used here, and different methods of analysing for the extent of reaction. Other values reported in the literature have been included in Table 5.4 for the purpose of comparison.

TABLE 5.4			
<u>Activation Energies for Acid Hydrolysis of Cellulose</u> <u>Reported in Literature</u>			
Source of Cellulose	Type of Acid	Temperature Range °C	E_c kcal/gmol
Douglas-fir ⁴⁵	Dilute sulphuric	170-190	33
Cellobiose ⁴⁶	Not Specified	60	34
Cellulose ⁴⁷	Dilute Acids	Unspecified	40-44
Coniferous woods ⁴⁸	Not Specified	94-250	29.5
Cotton linters ³	81% Phosphoric	40	32
Sulphite Pulp ³	81% Phosphoric	40	34
Cotton Linters ⁴⁹	1 to 7% Hydrochloric	146-187	36
Hemlock chips ³⁴	Acid Bisulphite	125-155	35

The range in activation energies reported in the literature most probably arises from the different methods of analysis used to determine the extent of the hydrolysis reaction, eg. viscometric, chromatographic, gravimetric, etc. From Table 5.4 it can be seen that all except two studies report the activation energy of the cellulose hydrolysis reaction as falling between 32 and 36 kcal/gmol. Consequently, the value of 33.9 kcal/gmol determined from this study is in agreement with other studies.

5.4.3 Modelling of the Cellulose Hydrolysis Reaction

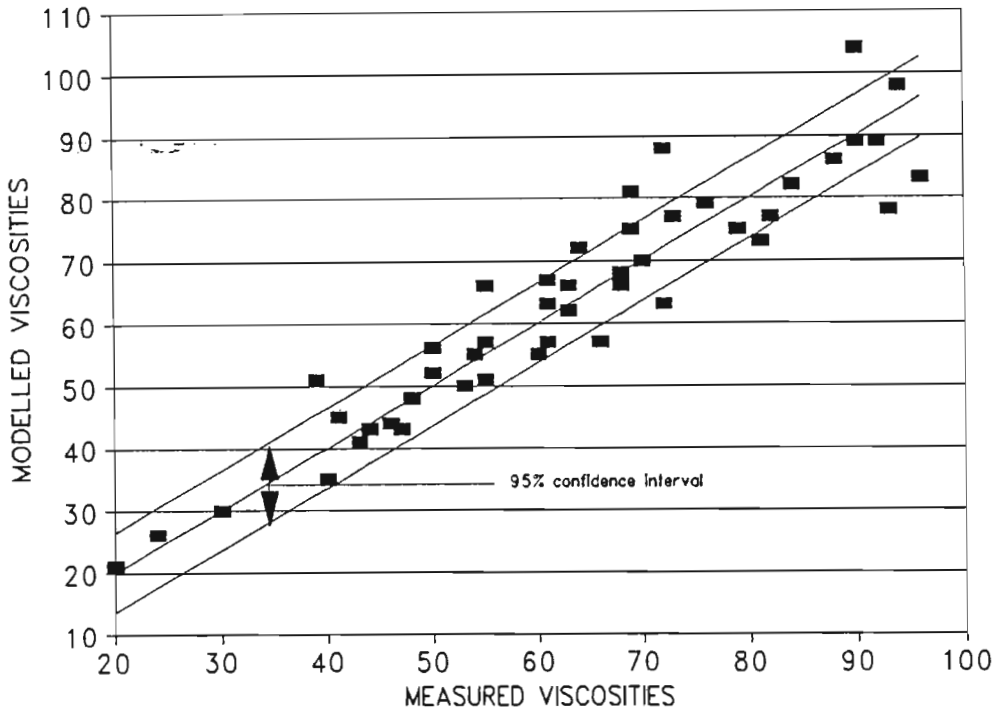
Although the use of an assumed DP_0 exerts no influence on the determination of the kinetic parameters, it is obviously essential for modelling purposes. The value of DP_0 required for the purpose of modelling the reaction can be determined by extrapolating back to $t=0$ for each run using the kinetics of the reaction as determined above. This analysis was performed on each set of results and the average DP_0 determined from each experimental run can be found in Table 5.5. The average value for DP_0 calculated in this manner was of the order of 2150. This value is by no means an accurate indication of the native DP value of the cellulose in situ (estimates of the native DP value of cellulose available in the literature vary from 1000 to greater than 10 000^{3,4}, the reason being that the estimates are entirely dependent on the methods of isolation and analysis). However, it serves the purpose of providing an effective starting point for the model.

TABLE 5.5	
<u>Estimation of DP₀</u>	
Cook Number	Average DP ₀
16	2136
17	2333
18	2223
19	1967
20	2044
21	2173
22	2013
23	2262
24	2137
Average	2143

The kinetic expression developed above can be used to calculate the extent of the cellulose degradation reaction at any time during the cooking process. Using the estimate of DP₀ obtained above as the starting point (ie. at t=0) will then enable the average DP value of the pulp to be determined and hence the viscosity calculated at any point during the cook. This predicted viscosity will, however, only be accurate if it is less than 100 cp (as explained above in Section 5.2.5). A comparison of the actual and calculated viscosities can be found in Figure 5.11. A statistical analysis of the resulting residuals indicated that the model is capable of predicting viscosities within ±6.5 cp on a 95% confidence interval, which translates to a coefficient of variation of 10.3% (based on an average viscosity of 55 cp SNIA).

FIGURE 5.11

Comparison of Actual and Calculated Viscosities



Now that the kinetics of the most important reaction have been determined, namely the cellulose hydrolysis reaction, those of the secondary reactions can be analysed. The importance of the delignification reaction arises mainly from the fact that the residual lignin in the pulp must be removed in the bleaching process. The kinetics of the delignification reaction were determined in the following section.

5.5 Kinetic Analysis of Other Reactions.

5.5.1 Delignification Reaction.

i) Kinetic Analysis.

The kinetics of the delignification reaction were determined using the kinetic expression given in section 2.5.3 and the correlation for converting from the K number to percent lignin on pulp. These expressions are as follows:

$$r_l = A_l e^{\left(-\frac{E_l}{RT}\right)} [L]^{\alpha} [H^+]^{\alpha} [HSO_3^-]^{\beta} \quad (2-7)$$

where:-

- i) $k_l = A_l e^{\left(-\frac{E_l}{RT}\right)}$
- ii) % lignin on pulp = $0.055 * K^{1.47}$ (2-8)
K = Pulp K number
- iii) First order kinetics with respect to $[HSO_3^-]$ and $[H^+]$ were assumed initially, ie. $\alpha = \beta = 1$ in equation 2-7 (cf Section 2.5.3).

The kinetic fit for the rate of delignification was then performed as follows:

- i) Measured pulp K numbers were converted to percent lignin on pulp using the correlation given as (ii) above.
- ii) The concentration profiles of H^+ and HSO_3^- were then calculated using the procedure presented in section 5.3.2, and thus the value of the integral:-

$$\int_{t-t_0}^{t-t_1} [H^+][HSO_3^-] dt$$

could be determined at any point during the run.

- iii) Assuming a value of $[L]_0 = 25.7\%^{42}$ as a starting point, the extent of reaction for each of the six samples taken during the run could be calculated.
- iv) Kinetic fits assuming zero, first and second order kinetics with respect to percent lignin on pulp (ie. $\alpha = 0, 1 \& 2$ were performed as follows:-
- a) Zero order ($\alpha = 0$ in equation 2-7)
 For each experimental run at constant maximum temperature, k_i was determined from the slope of a plot of $[L]_0 - [L]_t$ against the integrated product of $[H^+]$ and $[HSO_3^-]$.
- b) First order ($\alpha = 1$ in equation 2-7)
 For each experimental run at constant maximum temperature, k_i was determined from the slope of a plot of $\ln\left(\frac{[L]_0}{[L]_t}\right)$ against the integrated product of $[H^+]$ and $[HSO_3^-]$.
- b) Second order ($\alpha = 2$ in equation 2-7)
 For each experimental run at constant maximum temperature, k_i was determined from the slope of a plot of $\frac{1}{[L]_0} - \frac{1}{[L]_t}$ against the integrated product of $[H^+]$ and $[HSO_3^-]$.
- v) The values of the pre-exponential constant A_i and the activation energy E_i for each kinetic model (ie. zero, first and second order with respect to percent lignin on pulp) were then determined from a plot of the values of $\log k_i$ against $\frac{1}{T}$ in the following manner:-

$$E_i = 2.303 * 1.987 * \text{slope}$$

$$A_i = 10^Y \text{ intercept}$$

The results of these kinetic fits are summarised in Table 5.6.

TABLE 5.6			
<u>Summary of Results for Kinetic Fits on the Delignification Reaction</u>			
Parameter Description	Reaction order with respect to lignin on pulp (α)		
	ZERO	FIRST	SECOND
Average correlation coefficient (R^2) for determination of k_i	0.890	0.947	0.955
Activation Energy, E_i (cal/gmol)	31002	30475	32704
Pre-exponential Factor, A_i	$2.3 \cdot 10^{18}$	$3.3 \cdot 10^{17}$	$1.5 \cdot 10^{18}$
Correlation coefficient (R^2) for k_i vs $\frac{1}{T}$	0.788	0.905	0.958

From the results presented in Table 5.7, it can be seen that second order kinetics with respect to the residual lignin content on pulp provided the best fit. The high correlation coefficient ($R^2=0.958$) for this fit indicated that the assumption of first order kinetics with respect to $[H^+]$ and $[HSO_3^-]$ is acceptable and that the analysis required no further sophistication.

ii) Comparison of Results with Other Studies.

In contrast to the production of dissolving pulp (dealt with in this study) where the cellulose hydrolysis reaction is

of primary importance, the delignification reaction is of primary importance in the production of paper grade pulps. Since 95% of the world's pulp production is associated with paper grades, it is understandable that far more research has been performed on the delignification reaction than on the cellulose hydrolysis reaction. Essentially the delignification reaction is identical in both processes with the exception that the final degree of delignification is much greater in dissolving pulp grade cooks.

The apparent differences between the results from earlier work and more recent studies can be ascribed to the development of more precise theories and technology. This progression can be observed particularly when comparing the activation energies reported by the various studies. Activation energies reported by earlier studies^{12,20,25} ranged from 16 to 23 kcal while those from more recent studies ranged from 24 to 37 kcal^{21,22}. All these studies used the same form of kinetic expression and found similar orders of reactions with respect to the various chemical concentrations. The apparent discrepancies between the earlier and later studies may be due to the use of different expressions for the concentrations of H^+ and HSO_3^- ; this is discussed in greater detail in (a) below. The wide range in values reported by the later studies appears to be a result of the empirical nature of the kinetic model used, which leaves the order of reaction with respect to lignin open to interpretation; this is discussed in greater detail in (b) below.

a) Concentrations of H^+ and HSO_3^- :-

Prior to the development of the sulphur dioxide protolysis correlation needed to solve the charge balances to obtain values for the concentrations of H^+ and HSO_3^- in the cooking liquor (cf Section 3.2), these concentrations were estimated as being proportional to the partial

pressure of SO_2 (P_{SO_2}). While the partial pressure of SO_2 has been found to approximate the product $[\text{H}^+][\text{HSO}_3^-]^1$, it does not include the effects of temperature on the protolysis constant of sulphur dioxide. If these temperature effects are ignored, the value obtained for the activation energy is considerably reduced. This was shown by Hagberg & Schön²¹ where the omission of the temperature effects on the SO_2 protolysis constant dropped the activation energy from 24 kcal to 17 kcal.

- b) Effect of reaction order with respect to lignin content:-
As mentioned in section 2.5.3, the kinetic model used for the delignification rate is essentially empirical - thus the orders of reaction with respect to $[\text{H}^+]$, $[\text{HSO}_3^-]$ and lignin are open to interpretation and are usually taken to be the values at which the statistical fit is best. In addition to this complication, the delignification reaction rate has long been known to vary considerably with the extent of the reaction^{25,50,51} (cf. section 2.5.2); thus the values of all the kinetic parameters (activation energy and orders of reaction) become dependent on the extent of delignification over which the study was performed.

The three most recent studies (including this one) were performed over very different ranges of extent of reaction. The ranges covered can be found in Table 5.7 and the kinetic parameters determined from these studies have been included in Table 5.8.

TABLE 5.7Extent of Delignification Covered by Various Studies

Study	Range of K Numbers		Approximate Range of %lignin on pulp	
	From	To	From	To
Hagberg et al ²¹	±3	±60	±0.3	±22
Sloan ²²	7.3	37.6	±1.0	±11
This study	2.1	6.5	0.2	0.9

TABLE 5.8Kinetic Parameters for the Delignification Reaction

Parameter	Hagberg et al ²¹		Sloan ²²		This Study	
	[L]≥5.3%	[L]<5.3%	α = 1	α = 2	α = 1	α = 2
A_i	5.6×10^{13}	1.2×10^{13}	3.1×10^{15}	4.3×10^{20}	3.3×10^{17}	1.5×10^{18}
E_i	24400		26800	36900	30500	32700
α	0.648	1.578	1	2	1	2
α	0.792		1	1	1	1
β	0.740		1	1	1	1
R^2	Not Available		0.960	0.956	0.905	0.958

Note:-

- i) Units of energy - calories
- ii) Units of time - minutes
- iii) Concentration - $\frac{\text{kmol}}{\text{m}^3}$
- iv) Temperature - Kelvin
- v) Lignin content [L] - percent lignin on pulp

The results of these three studies demonstrated the variations of the reaction rate with the extent of delignification. This is indicated by the shift in the

order of reaction with respect to residual lignin from first order at high concentrations to second order at low concentrations. This shift in reaction order is clearly shown by Hagberg & Schöön's²¹ work as their study covered a wide range of extent of reaction. This apparent shift in reaction order with respect to residual lignin content was also reported by Goldfinger²⁵.

This trend is also apparent in the other two studies where the correlation coefficients from Sloan's²² work for first and second order with respect to residual lignin are extremely close. The range of delignification covered by Sloan excluded very high residual lignin concentrations but still spanned the transition point as reported by Hagberg & Schöön²¹. In contrast to this, only very low residual lignin concentrations were covered in this study and the results indicated that second order kinetics with respect to residual lignin content provided the best fit in this region.

The shift in lignin reactivity is thought to be caused by the following factors⁵¹:

- Lignin consists of a heterogeneous mixture of compounds which exhibit different reactivities (cf. Section 2.5.2).
- The accessibility and composition of lignin in various parts of the fibre varies.

An extensive study into the 'regional reactivity' of lignin in wood fibres (known as Topochemistry) under the influence of acid sulphite pulping was conducted by Proctor et al⁵¹. Their findings indicated that lignin is removed preferentially from the cell wall at the start of the cooking process. At a later stage the lignin in

the middle lamella begins to dissolve, with the lignin in the secondary wall being removed last. The conclusions drawn from this work were that these different reaction rates were most likely caused by variations in the lignin structure and composition and that diffusional aspects have a very minor influence.

An important difference between the three studies was the difference in methods used to determine the kinetic parameters. Hagberg & Schöön used an iterative error minimisation technique, while the parameters in the other two studies were determined using the integral method of analysis for batch reactors. While both methods yielded good fits, the iterative procedure resulted in non-integer orders of reaction, both less than one, with respect to $[H^+]$ and $[HSO_3^-]$ (α and β). In addition to this, the order of reaction with respect to residual lignin (while spanning a similar range in all three studies), was reported by Hagberg & Schöön as being slightly lower than those found in the other two studies. The lower activation energy reported by Hagberg & Schöön, compared to the other two studies, is thus most likely due to the cumulative affect of the lower reaction orders reported by them. These differences emphasise the empirical nature of the model and indicate a degree of interdependence between the activation energy and the orders of reaction.

5.5.2 Hemicellulose Hydrolysis Reaction.

i) Kinetic Analysis.

The kinetics of the hemicellulose hydrolysis reaction were determined using the kinetic expression given in section 2.6.3. These expressions are as follows:

$$r_h = A_h e^{\left(-\frac{E_h}{RT}\right)} [H]^a [H^+]^a \quad (2-9)$$

where:

- i) $k_h = A_h e^{\left(-\frac{E_h}{RT}\right)}$
- ii) First order kinetics with respect to $[H^+]$ were assumed initially ie. $\alpha = 1$ in equation 2-9 (cf Section 2.6.3).

The kinetic fit for the rate of hemicellulose hydrolysis was then performed as follows:

- i) Measured pulp K numbers were converted to percent lignin on pulp using the correlation given as equation 2-8:-

$$\% \text{ lignin on pulp} = 0.055 * K^{1.47} \quad (2-8)$$

- ii) From the concentration profile of H^+ , the value of the integral:-

$$\int_{t=t_0}^{t=t_f} [H^+] dt$$

could be determined at any point during the run.

- iii) Assuming a value of $[H]_0 = 26.6\%^{42}$ as a starting point, the extent of reaction for each of the six samples taken during the run could be calculated.
- iv) Kinetic fits assuming zero, first and second order kinetics with respect to percent lignin on pulp (ie. $\alpha = 0, 1 \& 2$) were performed as follows:-

- a) Zero order ($\alpha = 0$ in equation 2-9)

For each experimental run at constant maximum temperature, k_h was determined from the slope of a plot of $[H]_0 - [H]_f$ against the integrated product of $[H^+]$.

b) First order ($a = 1$ in equation 2-9)

For each experimental run at constant maximum temperature, k_h was determined from the slope of a plot of $\ln\left(\frac{[H]_0}{[H]_t}\right)$ against the integrated product of $[H^+]$.

b) Second order ($a = 2$ in equation 2-7)

For each experimental run at constant maximum temperature, k_h was determined from the slope of a plot of $\frac{1}{[H]_0} - \frac{1}{[H]_t}$ against the integrated product of $[H^+]$.

v) The values of the pre-exponential constant A_h and the activation energy E_h for each kinetic model, (ie. zero, first and second order with respect to percent hemi-cellulose on pulp) can then be determined from a plot of the values of $\log k_h$ against $\frac{1}{T}$ in the following manner:-

$$E_h = 2.303 * 1.987 * \text{slope}$$

$$A_h = 10^{\text{Y intercept}}$$

The results of these kinetic fits are summarised in Table 5.9.

TABLE 5.9

Summary of Results for Kinetic Fits
on the Hemicellulose Hydrolysis Reaction

Parameter Description	Reaction order with respect to hemicellulose in pulp (α)		
	ZERO	FIRST	SECOND
Average correlation coefficient (R^2) for determination of k_a	0.702	0.700	0.698
Activation Energy, E_a (cal/gmol)	16300	16600	17000
Pre-exponential Factor, A_a	1.3×10^9	3.7×10^8	9.8×10^7
Correlation coefficient (R^2) for k_a vs $\frac{1}{T}$	0.610	0.616	0.604

From the results presented in Table 5.9, it can be seen that all of the correlations are weak with the zero, first and second order models all yielding similar correlation coefficients. This contradicts the results reported from other studies^{21,26}. Problems with the S₁₈ analysis (used to estimate the residual hemicellulose content) were identified early on in the study due to the erratic nature of the results, with increases in S₁₈ values during the experimental run occasionally being reported. These same problems were experienced simultaneously with the routine quality control analyses being performed at the factory. An intensive investigation has indicated that part of the problem was being caused by CO₂ contamination of the 18% caustic being used for the analysis.

Additional problems associated with the chlorine dioxide bleaching process were experienced, in which an attack on the carbohydrate content of the pulp was apparent. Although this phenomenon contradicts expected behaviour of the ClO₂ bleaching process³, it has been identified as a problem area

in more recent work⁵². The development of a repeatable ClO₂ bleaching process which does not attack the carbohydrate fraction of the pulp is on-going.

ii) Results from Other Studies.

The kinetic parameters for the hemicellulose hydrolysis reaction reported by other researchers can be found in Table 5.10. As can be seen from these results, the activation energies are similar to those for the cellulose hydrolysis reaction. This is not surprising as the compounds are all carbohydrates and thus have closely related structures and reactions.

The most striking difference between the findings of the two studies is the order of reaction with respect to residual hemicellulose content. This difference was thought to have been a result of the different methods used in the two studies for analysing the residual hemicellulose content²⁶. Hagberg & Schön²¹ used an indirect technique in which the hemicellulose content was calculated as the difference between the pulp yield and the sum of the lignin and the acid resistant carbohydrate fraction of the original wood. This method was not used in the more recent study, as it was felt that this was more a measure of the cellulose content corresponding to the average crystalline segment (ie. that corresponding to the limit DP value of 100 to 200 - cf. Section 2.4.2) than an accurate measure of the retained hemicellulose²⁶. The more recent study²⁶ used the S₁₈ value as a measure of the residual hemicellulose; however, no mention is made as to how the residual lignin interference with this method was avoided.

TABLE 5.10Kinetic Parameters for the Hemicellulose Hydrolysis
Reaction Reported in Literature

Parameter	Hagberg et al ²¹	Sloan ²⁶
A_h	7.6×10^{12}	6.3×10^{11}
E_h	27880	24800
α	0.707	1
α	2.542	1

Note:

- i) Units of energy -calories
- ii) Units of time -minutes
- iii) Concentration $\frac{\text{kmol}}{\text{m}^3}$
- iv) Temperature -Kelvin
- v) Hemicellulose [H] -percent hemicellulose in pulp

As can be seen from the parameters presented in Table 5.10, both of these studies found the order of reaction with respect to percent hemicellulose on pulp to be in the region of one. Comparing these results with the parameters obtained from this study, for the first order reaction with respect to percent hemicellulose on pulp, highlights the discrepancies between the values of the activation energy. This study found the activation energy to be significantly lower (16600) compared to the other studies (± 25000 ²⁶ and 28000 ²¹). Since the hemicellulose reaction is very similar to the cellulose reaction (both acid hydrolysis), the higher activation energies are credible. The anomalous results for this reaction obtained from this study probably resulted from the difficulties with the analytical procedures mentioned earlier.

5.6 Chapter Summary.

In order to consolidate the findings of the experimental work, it is appropriate at this stage to summarise some of the more important findings:

i) pH Measurement.

The measurement of the pH value of cooking liquor during a cook was found to be possible although measurements were subject to an apparent zero drift. This problem was solved by performing a calibration correction on the reading as follows:

- a. 20 minutes after the completion of side relief, a liquor sample was taken and analysed to determine the concentrations of total and combined SO_2 ($[\text{SO}_2^{\text{tot}}]$ and $[\text{SO}_2^{\text{com}}]$) respectively.
- b. From these concentrations and the temperature, the bisulphite concentration could be calculated:-

$$[\text{HSO}_3^-] = [\text{SO}_2^{\text{com}}] - \frac{1}{2}K_{\text{SO}_2} + \left\{ \frac{(2[\text{SO}_2^{\text{com}}] - K_{\text{SO}_2})^2 + K_{\text{SO}_2}[\text{SO}_2^{\text{tot}}]}{4} \right\}^{\frac{1}{2}} \quad (3-8)$$

- c. Assuming the concentration of strong acid anions at this point to be zero (ie. $\text{SO}_2^{\text{com}} = [\text{initial combined } \text{SO}_2]$), then the $[\text{H}^+]$ and hence the pH could be calculated using:-

$$[\text{H}^+]_{\text{calc}} = [\text{HSO}_3^-] - 2[\text{Initial combined } \text{SO}_2] \quad (5-6)$$

and

$$\text{pH}_{\text{calc}} = -\log[\text{H}^+]_{\text{calc}} \quad (5-7)$$

From this the zero point correction could be determined:-

$$\text{pH}_{\text{corr}} = \text{pH}_{\text{calc}} - \text{pH}_{\text{meas}} \quad (5-8)$$

This factor was then used to correct for the shift in the zero point:-

$$pH_{act} = pH_{meas} + pH_{corr} \quad (5-9)$$

where:-

- pH_{calc} - calculated pH value
- pH_{meas} - measured pH value
- pH_{corr} - Zero point correction factor
- pH_{act} - corrected pH value

ii) Cellulose kinetics.

The rate of cellulose degradation was found to be accurately represented ($R^2 = 0.98$) by the following kinetic expression:

$$DI = A_c e^{\left(-\frac{E_c}{RT}\right)} \int_{t=t_0}^{t=t_f} [H^+] dt \quad (5-5)$$

and the parameter values:-

$$E_c = 33\,867 \text{ cal/gmol}$$

$$A_c = 7.68 \times 10^{14}$$

where the degradation increase was characterised by:-

$$DI = \frac{1}{DP_f} - \frac{1}{DP_0} \quad (2-1)$$

For modelling purposes the best estimate of the value of DP_0 , which was used as the starting point in order to calculate the final DP value (DP_f) relating to the extent of the reaction (ie. a specific value of DI), was found to be 2143.

The final viscosity, in centipoise SNIA, could then be calculated from the final DP value using the following correlation (derived from equation 2-4):-

$$\mu = \left(\frac{DP_f}{285.4} \right)^{2.899} \quad (5-10)$$

ii) Kinetic analysis of other reactions.

a) Delignification.

The rate of delignification towards the end of the cooking process was found to be accurately represented ($R^2 = 0.96$) by the following kinetic expression:

$$r_l = A_l e^{\left(-\frac{E_l}{RT} \right)} [L]^2 [H^+] [HSO_3^-] \quad (5-11)$$

and the parameter values:-

$$E_l = 32\,704 \text{ cal/gmol}$$

$$A_l = 1.5 \times 10^{18}$$

Although this kinetic expression accurately represents the reaction rate toward the end of the cook (ie. where lignin percent on pulp is < 1% or K number < 6.5), it is evident from the literature^{21,22,25} that this reaction rate will not apply throughout the cooking process.

b) Hemicellulose dissolution.

Due to a combination of factors, the kinetics of the hemicellulose dissolution reaction could not be accurately determined with the best results, relating to a first order reaction with respect to residual hemicellulose, only achieving a 'goodness of fit' of the order of $R^2 = 0.62$. The kinetic expression obtained was as follows:

$$r_h = A_h e^{\left(-\frac{E_h}{RT}\right)} [H][H^+] \quad (5-12)$$

and the parameter values:-

$$E_h = 16\,600 \text{ cal/gmol}$$

$$A_h = 3.7 \cdot 10^8$$

Now that the correlations and techniques for measuring the pH of cooking liquor throughout the cooking process have been developed and a kinetic model representing the cellulose degradation rate obtained, it is possible to use a combination of these correlations in order to develop a complete cooking model capable of controlling a cook to a final target DP value in a fixed cooking time.

CHAPTER 6

DIGESTER COOKING MODEL DEVELOPMENT

6.1 Model Selection.

As mentioned in Chapter 1, the primary quality control parameter associated with a dissolving pulp cook is the final pulp viscosity or DP value. Due to the batch nature of the cooking process, however, it is equally important that a cook is performed in a fixed time in order to facilitate sequencing of the digesters and a smooth interface with the rest of the factory, which operates on a continuous basis. In addition to these two constraints, it is important that a model of this nature is as simple and robust as possible in order to facilitate its implementation in an industrial situation.

Two basic approaches are available for developing a model of this nature, which are as follows:

6.1.1 Direct use of the Kinetic Model.

This would involve using the kinetic model directly to determine the extent of reaction at any point in time, and then manipulating cooking conditions in order to achieve the desired target DP value by the end of the cook. This approach, without the inclusion of any form of predictive capability, is not really feasible since it would require continuous manipulation of either the temperature or the pH value in order to vary the rate of reaction. Both parameters would be difficult to control on this basis for the following reasons:

- i) Temperature control would be difficult because the rate of cellulose degradation increases rapidly towards the end of the cook as a result of the decreasing pH value.

This would mean that the temperature would have to be decreased in order to reduce the reaction rate towards the end of the cook. It would therefore require some method of decreasing temperature in a controlled fashion and this is not feasible on the existing equipment.

- ii) The pH value by virtue of its nature is difficult to control accurately, especially in the extremely acid or alkali regions. Taking into consideration the magnitude of a digester load of liquor (± 150 to 180 m^3) emphasises the magnitude of this problem.

If the pH value is controlled only by manipulating pressure, the reaction rate could only be reduced towards the end of the cook unless some way of adding SO_2 were included. In addition to this, it was apparent from this study that pH value sensitivity to pressure variations is not great. It can thus be seen that this is an undesirable means of control.

The only other manner in which the pH could be manipulated would be to add mineral acids or alkalis as required. The physical difficulty of achieving this and the quantities of chemicals required immediately excludes this as an option.

6.1.2 Development of a Predictive Model.

This system would utilise some method of predicting the future cooking conditions required to achieve the target DP value in the specified time. This could be as simple as a 'target model' correlation which estimates the final cooking temperature required based on conditions at some point during the cook, or as sophisticated as an extended non-linear Kalman filter model which dynamically updates its estimate of the required cooking temperature as more data becomes available. These two models are discussed below:

i) Target Model Approach.

This system would have a similar format to the 'target S Factor' model. However, there would be a number of significant differences between the two, namely:-

- The correlation would have a sound mechanistic basis and therefore many of the errors involved in the 'S Factor' system would be excluded.
- The actual extent of reaction at the end of the cook would be available from the kinetic model, thus any form of parameter updating would have a sound theoretical basis.
- Additional data would be available for inclusion in the model, eg. the pH value. This could be used to include factors affecting the cooking rate previously not allowed for in the 'S Factor' model.

A model of this nature would be easily implemented in the industrial environment by virtue of the fact that it is simple and in many ways similar to the existing system.

ii) Extended Non-Linear Kalman Filter Model,^{55,56}.

This form of model consists of two main aspects, namely:

- A dynamic model of the process which in this case would consist of the kinetic model obtained for the cellulose degradation reaction (equation 5-5).
- A measurement system model which consists of the relationships between the measured values and the state variables, as well as a noise model.

Using the initial conditions, the best available estimate of the state variables and estimates of the standard deviations of the measurement parameters the state estimates, which in this case would include the degradation increase (DI), are propagated into the future.

Using this data in conjunction with a cost function of the form:-

$$J = \alpha ||DI_{pred} - DI_{tgt}|| + \beta ||t_{pred} - t_{tgt}||$$

the cooking temperature for which the cost function is a minimum can be found.

As can be seen, this type of model is complex and calculation intensive, with the majority of the calculations involving manipulation of matrices as well as iterative optimisation calculations. The computing power required to run this model in real time for a number of digesters would exceed that available in a modern Distributed Control System (DCS), and consequently a high-powered supervisory system would be required.

When deciding which of these two approaches is best, the level of sophistication required must be considered. From the kinetic analysis of the cellulose hydrolysis reaction (cf. Chapter 5 Section 5.4.3), it can be seen that the standard error in the prediction of viscosity is of the order of 6.5 cp SNIA. Thus if the simple 'target model' correlation is able to achieve this sort of accuracy, there will be no real gain in implementing a more sophisticated model. From a practical point of view it can also be seen that in terms of implementing the model in an industrial situation, there are distinct advantages associated with the 'target model' approach because it is relatively simple and similar to the existing strategy. In contrast to this, the Kalman filter model is complex and would require sophisticated computer equipment and maintenance by highly trained personnel. In view of this, the capabilities of a 'target model' correlation were investigated.

6.2 Model Requirements.

As mentioned earlier, the primary function of the cooking model must be to control a cook in such a manner as to achieve a target DP value within a set cooking time.

A cook control philosophy involving the use of a 'target model' would require the following components:

- i) An accurate kinetic model for the reaction.
- ii) A 'target model' expression which must be able to predict the cooking conditions required to achieve the target DP value in the allotted time, based on measurements taken at some point during the early phases of the cook.
- iii) Some form of statistical feedback which must be capable of dynamically updating the model. This aspect of the model as a whole is vitally important since the model must be capable of adapting to variable characteristics, eg. it is suspected that the original DP value (DP_0) of cellulose is not constant and may vary with age, region of origin or even from sub-species to sub-species. Thus as various batches of timber pass through the process, it would be an advantage if this type of variation could be allowed for.

With this structure as a basis a target model is developed and evaluated in the following two sections.

6.3 Model Development.

6.3.1 Kinetic Model.

The kinetic model for cellulose hydrolysis (equation 5-5) developed in Chapter 5 Section 5.4 plays a pivotal role in the cooking model because it provides an accurate estimate of

the cellulose DP at the end of the cook. This not only enables meaningful feedback for updating the target model but also excludes the possibility of out-of-specification cooks occurring. This is an extremely important factor since, in the industrial situation, cooks are frequently ended purely on pulp appearance due to upset plant conditions. The 'S Factor' model can often not be relied on to provide an indication of when the cook should be stopped since the actual cooking conditions are beyond its region of applicability. In these cases, cooks are ended without regard for the fixed cooking time and scheduling is sacrificed for quality. These situations occasionally result in a 'burnt cook' or a 'raw cook', both of which are devastating for the remainder of the process.

Since the accuracy of the kinetic model is totally dependant on the measurement system, the procedures for measuring, checking and correcting the pH value (cf. Chapter 5 Section 5.3.2) form an integral part of the kinetic model.

6.3.2 Target Model.

Before a target model correlation could be developed, the basic control strategy had to be decided on. It can be seen from Section 6.1 that the most practical option available at this stage is to use a set temperature profile and manipulate the final cooking temperature (T_{max}) in order to achieve the desired target DP value (DP_{tgt}) within the set time (t_{tgt}). The target model correlation thus had to be structured in such a manner that, from data available during the early stages of the cook, it could predict the final cooking temperature.

At this point it is necessary to define more clearly what is meant by the 'early stages' of the cook. From the control strategy selected it can be seen that the model must be capable

of estimating the final cooking temperature before the ramp up to this temperature commences. The temperature ramps traditionally used on the plant (for the calcium-based cooks) can be found in Table 6.1. Using this temperature profile as a guideline, the target model must be structured to ensure that the estimation of the final cooking temperature is available before 126°C (190 minutes into the cook).

TABLE 6.1		
<u>Plant Temperature Profile</u>		
Time (min)	From (°C)	To (°C)
60	T_{start}	85
55	85	110
75	110	126
185	126	T_{max}
35	Time at T_{max}	
$135^{\circ}C < T_{max} < 148^{\circ}C$		

From the results of the kinetic study it is apparent that all those parameters which influence the pH profile of a cook should be considered for inclusion in the target model correlation. From the experimental work conducted in this study it was clear that the following parameters have a direct effect on the pH profile of a cook:

1. Liquor concentrations (total and combined SO_2).
2. Temperature.
3. Pressure.

4. Liquor-to-wood ratio.
5. Wood characteristics (eg. varying total lignin content, varying combinations of lignin components, and varying initial DP values for cellulose).

The selection of key parameters were based on the following analyses of their relative importance:

1) Liquor Concentration.

The total and combined SO_2 contents of the cooking liquor have a fundamental influence on the pH value throughout the cook. The concentration of both components must be considered, although either the free or the total SO_2 concentrations can be used interchangeably due to their common relationship with the combined SO_2 concentration (cf. Chapter 3 Table 3.1). In this case, the total SO_2 concentration was selected as it was immediately available from the experimental results and avoided an unnecessary additional calculation.

The most important points during the cook for the liquor concentration are at the start of the cook and at side relief. As mentioned previously (cf. Chapter 5 Section 5.2.4), the liquor analysis at side relief is the most representative of the effective liquor strength during the cook. Since a liquor analysis ($[\text{SO}_2^{\text{tot}}]$ and $[\text{SO}_2^{\text{com}}]$) is required 20 minutes after side relief for the purposes of checking the pH value measurement, these values could also be used directly in the target model.

2) Temperature.

Since the ramp to the final cooking temperature is set, the only temperature of importance is the final cooking temperature (T_{\max}). In fact it is this temperature which the model must be able to forecast.

3) Pressure.

The pressure is really a composite function of the liquor strength and the temperature as well as the extent of reaction; consequently there is no point during the cook at which the system pressure provides any unique additional data. As a result of this, no pressure term was considered necessary.

4) Liquor-to-Wood Ratio and Wood Characteristics.

These aspects have an extremely powerful influence on the cooking rate since they have a direct effect on the formation and concentration of the strong acid anions, due to the following reasons:-

- a) The dilution of the strong acid anions is directly dictated by the liquor-to-wood ratio (on a bone-dry basis) and this is obviously influenced by the moisture content of the wood.
- b) The rate of formation of the strong acid anions is also a function of the lignin composition of the wood and this tends to be variable, especially for hardwood species⁵⁴.

Although the importance of these parameters is easily identified, they are the most difficult to allow for in the model since:-

- a) Physically measuring the liquor-to-wood ratio for each cook would require extensive additional instrumentation in order to measure the quantity of liquor loaded and the moisture content of the wood load. In addition to this, reliable measurement of the moisture content of wood is yet to be achieved although various instruments are currently being evaluated.
- b) Characterisation of the nature and content of the lignin for individual wood loads is impractical.

Since both of these aspects have a direct impact on the pH value of the liquor, it was felt that the variations from cook to cook could be adequately characterised by the single variable $\frac{\Delta[H^+]}{\Delta T}$ during a selected period of the cook. The use of this parameter during the period before side relief is inadvisable, however, since conditions are unstable due to the hydraulic pressurisation which has an unpredictable affect on the pH value. In addition to this due to the relatively low temperatures at this stage (less than 110°C), the rate of strong acid formation is relatively slow. The period during which this parameter would be most useful is thus from 20 minutes after the completion of side relief to 126°C - the point where the ramp to the final cooking temperature begins.

Using the parameters selected above, a target model of the form shown in Equation 6-1 resulted:

$$T_{\max} = f\left(DI_{tgt}, t_{tgt}, [SO_2^{tot}], [SO_2^{com}], \frac{\Delta[H^+]}{-\Delta T}\right) \quad (6-1)$$

where:-

- T_{\max} - Maximum cooking temperature required to achieve target DP value in fixed cook time.

- DI_{igt} - Extent of reaction required to achieve the target DP value.
- t_{igt} - Target cooking time (minutes).
- SO_2^{tot} - Total SO_2 concentration 20 minutes after side relief.
- SO_2^{com} - Combined SO_2 concentration 20 minutes after side relief.
- $\frac{\Delta[H^+]}{\Delta T}$ - Rate of change in $[H^+]$ from 20 minutes after side relief to the point when the temperature reaches $126^\circ C$.

A stepwise multi-linear regression using the maximum cooking temperature (T_{max}) as the dependant variable was used as a starting point. The results of this regression can be found in Table 6.2.

TABLE 6.2**Regression Results for Linear Target Model**

R squared - 'Goodness of fit'	0.958
R squared corrected for degrees of freedom	0.951
Standard Error in T _{max} estimate (°C)	1.12

Values for Coefficients of Independent Variables

Constant	Time	DI	SO ₂ ^{com}	SO ₂ ^{tot}	$\frac{\Delta[H^+]}{\Delta T}$
[A]	[B]	[D]	[E]	[F]	[G]
147	-0.0842	21010	21.996	-1.643	2367

These results indicate that a strong correlation exists. The contribution of each parameter is as follows:

(i) Time.

Contribution : This has the strongest contribution with an absolute 't-value' (ratio of coefficient with its standard error) of 17.6.

Component effect : An analysis of the residuals with respect to time indicated that the use of a power of time (eg. the square) should be investigated.

Functionality : This is correct in that the longer the cooking time, the lower the temperature required.

Data Range :

Maximum = 150 °C

Minimum = 135 °C

(ii) DI Value - Extent of Reaction.

Contribution : This has the second strongest contribution with an absolute 't-value' of 7.4.

Component effect : An analysis of the residuals with respect to DI indicated a linear dependence.

Functionality : This is correct in that the greater the extent of reaction (greater DI), the higher the temperature required.

Data Range :

Maximum : $DI = 3.09 \times 10^4$ or Viscosity = 79 cp (SNIA)

Minimum : $DI = 6.16 \times 10^4$ or Viscosity = 30 cp (SNIA)

(iii) Combined SO_2 -(SO_2^{com})

Contribution : This has the third strongest contribution with an absolute 't-value' of 5.4.

Component effect : An analysis of the residuals with respect to SO_2^{com} indicated a linear dependence.

Functionality : This is correct in that the greater the SO_2^{com} , the higher the temperature required to achieve a target DI.

Data Range :

Maximum : $SO_2^{com} = 0.99\%$

(during this specific period of the cook since the increase in temperature causes a net increase in the pH value).

Data Range :

$$\text{Maximum : } \left(\frac{\Delta[H^+]}{\Delta T} \right) = 0.00188$$

$$\text{Minimum : } \left(\frac{\Delta[H^+]}{\Delta T} \right) = 0.00221$$

Although the contribution of the rate of change of acidity is the smallest, it must be seen in the context of the range of liquor-to-wood ratios available from the data. As mentioned previously (cf. Chapter 4 and Chapter 5 Section 5.2.6), only very high liquor-to-wood ratios could be achieved with the equipment available and, in addition to this, varying the ratio also proved to be a problem (Min 0.94 l/100g, Max 1.08 l/100g). Under these conditions the net effect of the strong acids is reduced because of the high dilution factor; in addition to this, the small range available is not conducive to an effective statistical fit.

The importance of this parameter is likely to become far more evident on the plant where liquor-to-wood ratios are of the order of 0.2 l/100g. Furthermore, the variation of the liquor-to-wood ratio is large mainly as a result of the wide variations in wood moisture (depending on the ratio of fresh chips to chips reclaimed from the storage piles being used). Under these conditions the relative contribution of this parameter is expected to become significant.

A second stepwise regression was performed, this time including the square of the cooking time as an additional parameter. The inclusion of this parameter further improved the model, as can be seen from the summary of the regression results included in Table 6.3.

TABLE 6.3					
<u>Regression Results for Target Model</u>					
R squared - 'Goodness of fit'					0.974
R squared corrected for degrees of freedom					0.968
Standard Error in T _{max} estimate (°C)					0.91
Constant value from regression [A]					186
<u>Values for Coefficients of Independent Variables</u>					
Time	Time ²	DI	SO ₂ ^{com}	SO ₂ ^{tot}	$\frac{\Delta[H^+]}{\Delta T}$
[B]	[C]	[D]	[E]	[F]	[G]
-0.2748	0.000265	22028	19.81	-2.07	2130
<u>Absolute 't-values' for Coefficients of Independent Variables</u>					
Time	Time ²	DI	SO ₂ ^{com}	SO ₂ ^{tot}	$\frac{\Delta[H^+]}{\Delta T}$
5.71	3.97	9.55	5.95	4.66	1.78

An analysis of the contribution of each variable indicated that these were now all linear. The functionality of the coefficients remained the same as in the previous model. The significance of the parameters altered slightly with the t-value of time reducing as part of the dependence shifts to the time squared parameter. The largest single contribution is now made by the DI term. The significance of $\frac{\Delta[H^+]}{\Delta T}$ increased marginally. However, in comparison with the other parameters, its contribution is still weak - most probably due to the reasons elaborated above. The model thus has the following form:

$$T_{\max} = 186 + 22028 \cdot DI_{t_{gt}} - 0.2748 \cdot t_{t_{gt}} + 2.65 \cdot 10^{-4} \cdot t_{t_{gt}}^2 - 2.07 \cdot [SO_2^{tot}] + 19.81 \cdot [SO_2^{com}] + 2130 \cdot \frac{\Delta[H^+]}{\Delta T} \quad (6-2)$$

Apart from the standard error in the prediction of the maximum cooking temperature, the standard errors in the cooking time and the DI (extent of reaction which translates directly to viscosity) are of importance. Using the model obtained above, arranged in a form where the cooking times (or DI values) are calculated given the other data, the predicted values from the model could be compared to the actual values for the cooking time and viscosity (calculated from the DI value). The standard errors associated with these parameters can be found in Table 6.4.

TABLE 6.4

Standard Error in Cook Time and Viscosity

PARAMETER	UNITS	STANDARD ERROR
Viscosity	cp (SNIA)	5.79
Total-cook time	Minutes	10.01

As can be seen from these results, the standard error in the prediction of viscosity is slightly less from this empirical model than from the actual kinetic model (standard error of 6.5 cp). The main reason for this is the limited range of viscosities used to obtain the empirical model; only data sets with viscosities of between 30 and 80 cp (SNIA) were used, whereas the kinetic model was determined using all the data which had a range of viscosities from 18 to 150 cp (SNIA). If the full data set is used to determine the empirical model, then the standard error in the prediction of viscosities increases to 12.76 cp (SNIA).

From the above results it can be seen that the target model in this form is sufficiently accurate to be used as a means of 'feed-forward' control for a cook. The variations in cooking rate and conditions resulting from aspects which are not included in this model will then be handled by the kinetic model which will be able to accurately predict the end of a cook.

It is important at this point to emphasise the fact that, contrary to the kinetic model, the empirical model presented here is **not** directly transferable to a full-scale digester. Although the general form of the model will still apply, the

coefficients will have to be re-defined using actual data from the plant. This is a direct result of the empirical nature of the model. This phenomenon has been observed frequently in the past when the 'S Factor' model, with coefficients determined from laboratory work, has been tested on full-scale digesters and found to yield vastly different results.

One of the most important aspects of a model of this nature is that some facility must be included to keep the model up-to-date. This is best achieved by some form of statistical feedback which constantly adjusts the model using results achieved in the past. The general form of the statistical feedback required by the model presented here is developed in the next section.

6.3.3 Statistical Feedback and Parameter Updating.

While the actual kinetics of the cellulose degradation will not change over a period of time, there are a number of aspects which could result in a drift in the accuracy of the cooking model as a whole. These aspects can be broadly classified into two categories:

(i) Global Effects.

In general, the effects of variations in most of the wood characteristics (such as moisture content and lignin content and characteristics) will be accounted for by the kinetic model, as these aspects will affect the pH. The accuracy of the model on all the digesters will be affected, however, by a change in the native DP value (DP_0) of the wood, since the kinetic model is based on a value of $DP_0 = 2143$ which was the average value obtained from data gathered for this study.

(ii) Factors affecting individual digesters.

As mentioned in Chapter 5, pH probes are prone to gradual aging. The condition of the probes on each digester will have to be monitored and they will have to be re-calibrated using the methods described (cf. Section 5.3.2), on an individual basis.

In addition to pH electrode aging, digesters (by virtue of the fact that they are individual units) tend to behave slightly differently from each other. The contributions of these differences are likely to come from a number of sources, some of which may include differences in: liquor distribution, heat losses, instrument positioning and calibration, etc. The best manner in which to allow for these differences is to adjust one or more of the parameters in the model on a digester by digester basis, using the results from previous cooks on each digester as a guide.

Taking into consideration all of the aspects mentioned above, the following strategies for incorporating statistical feedback into the model were devised.

i) Global Model Updates.

At the end of a cook, the actual viscosity achieved can be used to calculate the extent of reaction achieved by the cook (DI_{act}). In addition to this, from the data collected during the cook and the kinetic model, the extent of reaction as predicted by the kinetic model (DI_{kin}) is also known. Any consistent deviation between these two values indicates a shift in the native DP value of the raw timber. This will have an effect on the results from all cooks and consequently the value of DP_0 must be updated globally. Due to the fact

that errors from a number of sources will cause deviations between these two values, the global value of DP_0 cannot be updated based on the results of each individual cook. The value of DP_0 could thus be updated after a certain number of cooks, using a filtered average from all digesters.

At this point, it is important to note that the end of a cook is defined as the point when the period at T_{max} is complete. At this stage the steam to the digester is shut, circulation is stopped, the circulation line through the heat exchanger is isolated and high pressure gas release is started (pressure ramp from 10 Barg to ± 4 Barg). From this point on, no accurate temperature or pH values can thus be measured. The high pressure release is controlled along a linear ramp over a period of ± 25 minutes. When the pressure reaches 4 Barg, the low pressure gas release (during which the pressure is reduced to 0.5 Barg) is started. This is not controlled along a ramp and times vary from 20 to 40 minutes for calcium digesters and from 35 to 75 minutes for magnesium digesters. When the pressure reaches 0.5 Barg, the digester is discharged.

During the gas release phase, the pH of the cooking liquor climbs rapidly and thus the reaction rates also slow down; however, cellulose will still undergo some additional degradation. This additional drop in the cellulose DP cannot be controlled. If, however, this additional amount of degradation is considered to be constant, then the correction of the DP_0 value will automatically correct the model and so variations in the degree of degradation during this period will be constantly corrected. For this reason calcium and magnesium based cooks must be treated separately, ie. separate global DP_0 values must be used.

The contribution to the average value of DP_0 from individual cooks can be calculated using the values of DI_{kin} and the resultant viscosity (μ_{act}) as follows:

$$DP_{act} = 285.4 * \mu_{act}^{0.345} \quad (6-3)$$

$$DP_0 = \frac{1}{\left\{ \frac{1}{DP_{act}} - DI_{kin} \right\}} \quad (6-4)$$

A filtered average of these individual values can then be used as the value of DP_0 in the model.

ii) Statistical Feedback for Individual Digesters.

a) pH Calibration Correction.

In order to offset the drift in pH measurement resulting from the gradual aging of an electrode, the pH calibration must be checked for every cook using the liquor strength analysis from a sample taken at least 20 minutes after the completion of side relief, as described in Section 5.3.2.

Using the liquor analysis from each individual cook to adjust the the pH calibration may introduce an error because the liquor strength analysis is itself subject to error. The best solution is to use a filtered result from, say, the last 5 cooks. This aspect of the model makes the following positive contributions:-

- (i) This cross-check will all but eliminate the negative effects of a bad liquor analysis - in fact the analyst can be warned immediately of a suspect liquor strength measurement.

- (ii) The aging and calibration of the pH instrument is constantly monitored and checked. This will greatly assist in trouble-shooting and planned maintenance, as a threshold for electrode aging can be set beyond which the unit must be replaced.

In view of the importance of the pH measurement, it would be necessary to have two pH probes per digester so that their readings can be compared. This will immediately indicate a fault on any one of the electrodes, and will also provide a fixed pH reference point (continuity in measurement) when one of the probes is replaced.

b) Viscosity Offset Correction.

As mentioned above, digesters tend to behave slightly differently from each other. Since these differences are likely to be dynamic, some allowance must be made in the model to continuously correct for them. This could be achieved by adjusting either:-

- (i) The constant in the T_{\max} expression (equation 6-2).
- (ii) The coefficient for the DI value (extent of reaction) in the T_{\max} expression (equation 6-2).

These adjustments would relate to individual digesters, ie. the coefficient would have a unique value for each digester. Adjusting the coefficient for DI ($[G]$ in Table 6.3) is the most direct approach since this is the parameter around which the model centres. The value of this coefficient will have to be carefully monitored, however, as any significant variation may require that the model be updated by a statistical regression to update all the parameters.

The corrected value of [G] (the coefficient for DI) for a specific digester can be determined from the results of individual cooks on the following basis:

From the actual viscosity achieved at the end of a cook, the extent of reaction achieved by the cook (DI_{act}) can be calculated. Since the value of DP_0 is statistically updated on a global basis, the deviation between the actual extent of reaction achieved by a cook, DI_{act} , and the desired extent of reaction, DI_{tgt} , relates to errors arising from the differences between individual digesters. The updated coefficient of DI can thus be calculated using equation 6-5:

$$[G]_{NEW} = \frac{1}{DI_{act}} \left\{ T_{max} - [A] - [B] * t_{gt} - [C] * [SO_2^{act}] - [D] * [SO_2^{tgt}] - [E] * \frac{\Delta[H']}{\Delta T} \right\} \quad (6-5)$$

where [A] through [E] refer to the coefficients of the target model as given in Table 6.3.

In order to eliminate the effects of significant errors relating to individual cooks, this parameter would be best adjusted if a filtered value using results from a number of previous cooks were used. The exact nature of the filter and the number of previous results would have to be determined from plant data.

6.4 Summary.

In summary, the implementation of the cooking model on the plant would consist of the following aspects:

- (i) The target total cook time t_{tgt} and target viscosity must be specified. From the target viscosity μ_{tgt} the 'degradation increase' DI_{tgt} required to achieve it can be calculated as follows (cf Section 5.4.1):-

$$DP_f = 285.4 * \mu_{tgt}^{0.345} \quad (2-4)$$

and

$$DI = \frac{1}{DP_f} - \frac{1}{DP_0} \quad (2-1)$$

where the value of the constant DP_0 should be set at 2143 based on this study (cf Section 5.4.3); however, this value must be verified using data from the plant.

- (ii) A digester must be charged with wood chips and cooking liquor, and the cook initiated in the usual fashion.
- (iii) A liquor sample must be taken 20 minutes after the completion of side relief (2hr 15 min after the start of the cook if the profile given in Table 6.1 is followed), and this is analysed for total and combined SO_2 using the Palmrose method.
- (iv) The pH value is then calculated using the following set of calculations (cf Section 5.3.2):-

$$[HSO_3^-] = [SO_2^{com}] - \frac{1}{2}K_{SO_2} + \left\{ \frac{(2[SO_2^{com}] - K_{SO_2})^2 + K_{SO_2}[SO_2^{tot}]}{4} \right\}^{\frac{1}{2}} \quad (3-9)$$

$$[H^+] = [HSO_3^-] - 2[SO_2^{com}] \quad (5-4)$$

and

$$pH_{calc} = -\text{Log}_{10}[H^+] \quad (5-7)$$

where the values used for K_{SO_2}
are those given by Rydholm³.

and from the Palmrose test:-

$[SO_2^{tot}] =$ Total SO_2 concentration

$[SO_2^{com}] =$ combined SO_2 concentration

- (v) The pH value is then corrected using the following set of calculations (cf Section 5.3.2):

$$pH_{err} = pH_{meas} - pH_{calc} \quad (6-6)$$

If this value is significantly different from the previous values, it should be ignored and a repeat liquor analysis performed if possible.

$$pH_{corr} = pH_{meas} - \text{Avg } pH_{err} \quad (6-7)$$

where Avg pH_{err} is the average of the five previous values for that specific digester.

Once this value exceeds the maximum allowable deviation (0.2 pH units should be used initially and the optimum value determined using actual plant data), the pH electrode must be replaced.

- (vi) The extent of the reaction can be followed throughout the cook using the corrected pH value and the kinetic expression for the cellulose degradation reaction (cf Section 5.4.1):

$$[H^+] = 10^{-pH_{corr}} \quad (6-8)$$

$$DI = A_c e^{\left(-\frac{E_c}{RT}\right)} \int_{t=t_0}^{t=t_f} [H^+] dt \quad (5-5)$$

If for any reason cooking conditions vary from the norm (for example, if the temperature profile cannot be maintained accurately), then the target viscosity can still be obtained by terminating the cook when the target 'degradation increase' is achieved.

- (vii) When the cook temperature reaches 126°C just prior to the final temperature ramp to T_{max} (which starts at $T = 126^\circ\text{C}$), the value for $\frac{\Delta[H^+]}{\Delta T}$ can be calculated using the pH values measured during the cook. The target model can then be used to calculate the target value for T_{max} (cf Section 6.3.2):

$$T_{max} = 186 + 22028 * DI_{igt} - 0.2748 * t_{igt} + 2.65 * 10^{-4} * t_{igt}^2 - 2.07 * [SO_2^{tot}] + 19.81 * [SO_2^{com}] + 2130 * \frac{\Delta[H^+]}{\Delta T} \quad (6-2)$$

- (viii) As the cook approaches the target cook time, t_{igt} , the actual degradation increase, calculated using the pH values measured during the cook (see point vi), can be used to calculate the current viscosity value. If the difference between this and the target value is less than ± 6 cp, then the cook can be stopped on time. If the two values differ by more than this amount, a decision as to whether the cook time should be altered to achieve

the target viscosity can be made. Altering the cook time should be avoided at all costs as this affects the scheduling of the other digesters, which not only has a detrimental affect on quality but also causes delays and subsequent loss of production.

- (ix) A pulp sample from the discharged cook must be taken and the viscosity value measured and fed back to the control system. From this value the model parameters can then be updated as follows:

a) Global DP₀ Update:

The contribution to the average value of DP₀ from individual cooks can be calculated using the values of DI_{kin} and the resultant viscosity (μ_{act}) as follows:-

$$DP_{act} = 285.4 * \mu_{act}^{0.345} \quad (6-3)$$

$$DP_0 = \frac{1}{\left\{ \frac{1}{DP_{act}} - DI_{kin} \right\}} \quad (6-4)$$

A filtered average of these individual values can then be used as the global value of DP₀ in the model.

b) Viscosity Offset Correction:

From the actual viscosity achieved at the end of a cook, the actual extent of reaction achieved by the cook (DI_{act}) can be calculated. Since the value of DP₀ is statistically updated on a global basis, the deviation between the actual extent of reaction achieved by a cook, DI_{act}, and the desired extent of reaction DI_{tgt}, relates to errors arising from the differences between individual digesters. The updated coefficient of DI can thus be calculated using equation 6-5:-

$$[C]_{new} = \frac{1}{DT_{act}} \left\{ T_{max} - [A] - [B] * t_{igt} - [C] * [SO_2^{tot}] - [D] * [SO_2^{com}] - [E] * \frac{\Delta[H^+]}{\Delta T} \right\} \quad (6-5)$$

where [A] through [E] refer to the coefficients of the target model as given in Table 6.3.

In summary, the target cooking model presented in this chapter should be capable of predicting the maximum cooking temperature required to achieve a target viscosity at a set cook time within 1°C. This accuracy will not only reduce viscosity variations but will also improve digester scheduling. In addition to this, the cooking model incorporates the following desirable features:

- (i) The progress of the cook is constantly monitored by a kinetic model with a sound mechanistic basis; thus any variations in cook conditions, such as a deviation from the temperature profile, will still enable the cook to be terminated at the point when the target viscosity has been achieved.
- (ii) The cooking conditions are monitored by a continuous 'on line' pH reading; thus errors arising from bad liquor sampling and analyses are avoided as these will be detected at the point when the actual and theoretical pH values are cross-checked.
- (iii) The usual undesirable aspects associated with pH measurements, such as any drifts in calibration, are also addressed by checking and correcting the drift over a period of time by using the liquor analyses. This will enable a probe to be replaced when the electrode has aged excessively. In addition to this the comparison of readings from two probes will enable pH electrode damage to be detected and provide continuity of measurement when a probe has to be changed.

- (iv) The model is constantly corrected on a global basis as well as on individual digesters for varying characteristics in the wood and varying cooking conditions not specifically addressed in the cooking models.
- (v) Consistent variations over a period of time in the length of gas releases and the additional extent of cellulose degradation which occurs during this phase are constantly corrected and accounted for.

Now that a mechanistically based kinetic expression for the cellulose degradation reaction has been determined, and this has been incorporated into a cooking model, the significance of these results with respect to the plant must be identified. Furthermore, the work required to implement this model in practice must also be determined.

CHAPTER 7

CONCLUSIONS AND RECOMMENDATIONS

7.1 Conclusions.

In order to summarise the findings of this project and to put their significance into context, it is best to refer back to the original objectives as stated in Chapter 1 and to identify how these have been achieved.

7.1.1 Experimental Equipment.

The experimental equipment available at the time consisted of a single 30-litre laboratory digester. This unit was considered as being unsuitable for collecting the kind of data required to develop kinetic expressions, due to the fact that multiple pulp samples could not be obtained during a single cook.

As a result of this, a new experimental laboratory digester plant was designed and constructed specifically to meet the requirements of this project. This unit consisted of six 2-litre digesters through which liquor from the main laboratory digester (the existing 30-litre unit) could be circulated. These 'mini digesters' thus enabled six individual pulp samples to be obtained during a single cook. In addition to this, the new unit included comprehensive instrumentation for the measurements of the cooking liquor temperature, pressure, pH value and circulation rate, all of which were logged on a computer during the cook.

7.1.2 Development of Kinetic Expressions.

Using the data obtained from the six pulp samples taken from each cook, the liquor samples and the data logged during the cook, the kinetics of the primary reactions were investigated.

i) Cellulose Hydrolysis Reaction.

The kinetics of cellulose degradation by the acid hydrolysis reaction were determined using the concept of Degradation Increase (DI) developed in Section 2.4. The kinetic expression for cellulose degradation thus became:

$$DI = A_c e^{\left(-\frac{E_c}{RT}\right)} \int_{t=t_0}^{t=t_f} [H^+] dt \quad (5-5)$$

where:-

$$k_c = A_c e^{\left(-\frac{E_c}{RT}\right)}$$

$$DI = \frac{1}{DP_f} - \frac{1}{DP_0}$$

$$DP = 285.4 * \mu^{0.345}$$

μ = SNIA viscosity in cp

The results of the kinetic analysis were as follows:

$$E_c = 33\ 867 \text{ cal/gmol}$$

$$A_c = 7.68 \times 10^{14}$$

In order to relate the 'extent of reaction' or Degradation Increase (DI) at any point during a cook to a viscosity value, a fixed starting point for the DP value must be used. An average value for this set of data was determined by extrapolating the kinetic expression back to the start of the cook. This value was found to be in the region of 2143

and this was consequently used as the starting point for calculating predicted viscosities from the kinetic model. A statistical analysis of the difference between the actual and predicted viscosities indicated that the model is capable of predicting viscosities within ± 6.5 cp on a 95% confidence interval, which translates to a coefficient of variation of 10.3% (based on an average viscosity of 55 cp).

The activation energy for the acid hydrolysis of cellulose determined from this work is very similar to those reported by other researchers despite the fact that they used various acids, different sources of cellulose to those used here and different methods of analysing for the extent of reaction. The value for the activation energy reported in the literature ranges from 29.5 to 44 kcal/gmol with the vast majority falling between 32 and 36 kcal/gmol; consequently the value of 33.9 kcal/gmol determined from this study is in agreement with other studies. In addition to this, although the value determined for DP_0 can in no way be considered an accurate indication of the native DP value of the cellulose in situ, it is well within the range from 1000 to greater than 10 000^{3,4} reported in the literature.

The development of this mechanistically based kinetic expression for the cellulose degradation reaction is of fundamental importance to the operation of the digesters at SAPPi SAICCOR. For the first time the root causes behind previously unexplained variations in viscosities from the digesters can be determined, since the actual mechanism of the reaction is now known and the impact of the various parameters on the reaction rate can be isolated and identified. The empirical nature of the current cooking model prevents this type of analysis. In addition to this, the range of conditions over which the kinetic expression applies is not restricted by virtue of its mechanistic basis.

ii) Analysis of Other Reactions.

a) Delignification Reaction.

The kinetics of the delignification reaction were found to be best described by a first order rate with respect to $[H^+]$ and $[HSO_3^-]$, and second order with respect to residual lignin on pulp. The kinetic expression for the delignification reaction was thus found to be as follows:

$$r_l = A_l e^{\left(-\frac{E_l}{RT}\right)} [L]^2 [H^+] [HSO_3^-] \quad (5-11)$$

where:-

$$k_l = A_l e^{\left(-\frac{E_l}{RT}\right)}$$

$$\% \text{ lignin on pulp} = 0.055 * K^{1.47} \quad (2-8)$$

K = Pulp K number

The results of the kinetic analysis were as follows:

$$E_l = 32\,704 \text{ cal/gmol}$$

$$A_l = 1.5 \times 10^{18}$$

$$R^2 = 0.958$$

Comparing the results from this study with those available from the literature emphasised the widely varying values reported for the activation energy and the order of reaction with respect to residual lignin ($[L]$), $[H^+]$ and $[HSO_3^-]$. The wide discrepancy in the values reported for the activation energy between the earlier and more recent work is thought to be a result of the different methods used in estimating the concentrations of $[H^+]$ and $[HSO_3^-]$ in the cooking liquor. The values for the activation energy

reported in the most recent study (Sloan²²) ranged from 27 to 37 kcal and are in the same range as those determined from this study, viz. 30.5 to 32.7 kcal.

Comparison of the results available from the literature with respect to order of reaction indicate that the kinetics of the reaction vary with the extent of delignification. This occurs in the form of a shift in the order of reaction with respect to residual lignin from first order at high concentrations to second order at low concentrations. Only very low residual lignin concentrations were covered in this study and the results indicated that second order kinetics with respect to residual lignin content provide the best fit in this region.

The shift in lignin reactivity is thought to be caused by the following factors⁵¹:

- Lignin consists of a heterogeneous mixture of compounds which exhibit different reactivities (cf Section 2.5.2).
- The accessibility and composition of lignin in various parts of the fibre varies.

It is apparent from the results of this and other studies that a single kinetic expression cannot be used to accurately model the delignification reaction throughout the cook, particularly if extremely low residual lignin values will be attained (K number < 20). These results are of particular importance in terms of the existing cooking model used at SAPPI SAICCOR, since they illustrate the inaccuracies associated with using a model based on the delignification reaction (such as the 'S Factor Model') to control final viscosities.

b) Hemicellulose Hydrolysis Reaction.

The form of the kinetic expression investigated for the hemicellulose hydrolysis reaction was as follows:

$$r_h = A_h e^{\left(-\frac{E_h}{RT}\right)} [H][H^+] \quad (5-12)$$

where:-

$$k_h = A_h e^{\left(-\frac{E_h}{RT}\right)}$$

The analysis of the hemicellulose hydrolysis reaction kinetics produced inconclusive results for the zero, first and second order models with respect to residual hemicellulose, which yielded very low correlation coefficients ($R^2 < 0.62$). The fact that the activation energy determined from this study ($E_h \approx 16500$ kcal) is significantly less than that reported in other studies ($24000 < E_h < 28000$ kcal) emphasises the inaccuracy of the kinetic model determined here.

The problems associated with the determination of this kinetic model were traced to the analytical procedures used to estimate the residual hemicellulose content of the pulp. The chlorine dioxide bleaching process used to prepare the pulp for analysis exhibited varying degrees of attack on the carbohydrate fraction. In addition to this the S₁₈ analysis, used to estimate the residual hemicellulose content, proved to be inaccurate; it is suspected that this was a result of CO₂ contamination of the 18% caustic being used for the analysis. The inaccuracies associated with the S₁₈ analysis had not been detected earlier because the analysis had previously only been used to estimate the

hemicellulose content of bleached pulp. In this study, small differences in S_{18} values between unbleached pulp samples were being investigated.

The main benefit obtained from these results was that they highlighted the inaccuracy of the S_{18} analytical method. Since the S_{18} value is one of the parameters closely monitored by customers, the accuracy of the procedure had to be improved. A subsequent investigation at the factory was performed to achieve this.

Due to the fact that the parameter of primary importance during cooking is the cellulose DP value, it can be seen that no direct control can be exercised over the final residual hemicellulose content at the end of a cook. This parameter is of interest, however, as the residual hemicellulose content (S_{18} value) of the final pulp (bleached pulp) is restricted to a maximum value. A knowledge of the reaction kinetics governing the hemicellulose hydrolysis reaction would thus be useful in that it would permit the removal of hemicellulose to be optimised throughout the process. The bulk of the hemicellulose is removed during the cooking process and the alkali bleaching stage, therefore any increase in hemicellulose dissolution during cooking will reduce the load on the alkali extraction phase.

As can be seen, the kinetic expression for hemicellulose hydrolysis is very similar to that found to apply to the cellulose hydrolysis reaction. The main difference between the two is the dependence of the hemicellulose hydrolysis rate on the residual hemicellulose content of the pulp as reported by Hagberg & Schöön²¹ and Sloan²⁶. As a result of this difference, as well as the difference between the value of the activation energies for the two reactions,

it can be seen that a long-low temperature cook and a shorter high-temperature cook can be used to achieve the same final viscosity. However, the final residual hemicellulose content of the resultant pulp from these two cooks will differ because of the differences between the reaction kinetics.

In order to determine the most beneficial cooking conditions for the removal of hemicellulose, the residual hemicellulose content on pulp was simulated using data from actual experimental cooks and the kinetic parameters as reported in the literature. A simple Runge-Kutta 4 algorithm was used. The parameters reported by Hagberg & Schön²¹ were found to produce the most realistic estimates of the hemicellulose content at the end of a cook. The reason for this trend is most likely a result of the rate of hemicellulose hydrolysis varying during the cook in a similar fashion to that for lignin. Since the work performed by Sloan²⁶ concentrated on conditions toward the end of the cook while that done by Hagberg & Schön²¹ covered the entire cook, the kinetic model reported by the latter is best suited to simulating the residual hemicellulose content from the start of a cook. The results from this simulation can be found in Table 7.1

TABLE 7.1**Hemicellulose Variation with Temperature for a
Constant Viscosity Value of 55 cp (SNIA)**

<u>Tmax (°C)</u>	<u>Cook Time (Mins)</u>	<u>%Hemicellulose on Wood</u>	<u>%Hemicellulose on Pulp*1</u>
135	456	5.61	±14.0
140	382	5.86	±14.7
145	345	5.96	±14.9
150	330	6.03	±15.0

*1 This value should be similar to the S₁₈ value.

As can be seen from the results presented in Table 7.1, hemicellulose removal, for a specific cellulose DP (or viscosity), is favoured by lower maximum cooking temperatures and longer cooks. Unfortunately this is impractical unless there is surplus capacity in the digester plant, which is not the case at the SAPPI SAICCOR plant. This finding is of importance as it highlights the fact that improvements in hemicellulose removal can only be achieved by addressing the operation of the alkali extraction process (unless surplus digester capacity is installed).

7.1.3 Local and Global Significance.

In terms of the process operation at SAPPI SAICCOR, these findings offer the potential of greatly improving the process control of the Digester plant which would result in reduced viscosity variability. Furthermore, the risk of producing out-of-specification product as a result of disturbances in

plant operation will be all but eliminated, since the range of conditions over which the kinetic model applies is much greater than the existing model.

The benefits resulting from reduced pulp variability would be especially evident in the bleaching plants, where chemical dosage rates have to be varied as characteristics of the incoming pulp changes in an attempt to produce a final product which falls within specifications. The large variations in the pulp being fed to the Bleaching plants frequently results in over- or under-corrections in the bleaching chemical dosage rates, which therefore results in the production of out-of-specification product. Reduced variability in the characteristics of the pulp being fed to the bleaching plants will thus not only reduce the amount of 'out-of-specification' product produced but will also result in the more efficient use of bleaching chemicals and consequently reduce the running costs.

The international market for dissolving pulp is extremely competitive and the price of pulp has always been a key issue. However, the quality aspect has recently become extremely important as well, to the point where higher prices are willingly paid for pulp with consistent characteristics. A number of key issues have formed the driving force behind this trend. Some of the more important are:

- i. With the advent of international standards such as ISO 90002, the awareness of quality and 'conformance to requirements' has increased dramatically.
- ii. The level of automation and sophistication in process control is steadily increasing and this inevitably results in improved standards of quality control.

- iii. Technological advancements in downstream users as well as the development of new uses for pulp products frequently result in reduced tolerance of variations in characteristics and thus tighter specifications.
- iv. The situation has become exacerbated by the recent slump in world pulp markets.

In view of this scenario, the implementation of any system which can improve quality control and reduce product variability can no longer be ignored.

7.2 Recommendations.

In view of the extremely strong correlations obtained from the experimental data for the cellulose degradation kinetic expression and the empirical digester cooking model, the implementation of these models should definitely be investigated on the plant. The most effective way of implementing them would be in a phased manner. This would enable the early identification of potential problems and ensure a smooth transition from one control algorithm to another. Due to the fact that the parameters for the kinetics of only the calcium-based process have been determined from this study, the implementation of the models should be investigated initially on the calcium-based digesters.

7.2.1 Verification of the Kinetics for the Cellulose Hydrolysis Reaction.

The first stage in the implementation should be to check the applicability of the kinetics established for the cellulose hydrolysis expression to conditions on the plant digesters. This will be accomplished best by attaching the satellite mini

digester equipment to a specific digester in the plant, and performing a number of cooks in a similar fashion to those performed in the laboratory.

The advantages associated with this procedure are that the satellite digester plant enables direct pulp samples to be taken at varying times during the cook. The data from these samples will enable the kinetics of the reaction to be isolated, while eliminating the influence of 'distorting' factors such as temperature and pressure profiles through the digester, variable hydrolysis during gas release, and factors peculiar to individual digesters. This procedure will enable data to be gathered rapidly for the purpose of cross-checking the kinetic parameters. As mentioned previously, the mechanistic basis of the kinetic expression developed in this study should ensure that the expression is directly applicable to conditions on the plant. If any variations do occur, they will be identified at this stage and will allow any adaptations to the model to be made before continuing implementation.

7.2.2 Adaptation to Plant Conditions.

Once the kinetic expression has been verified for plant conditions, sufficient data must be collected to enable the 'target model' to be developed for the plant. This will require the collection of on-line data from various digesters using computerised logging. During this data collection phase, data relating to actual digester conditions will have to be gathered. This data must include the following:

- i. Temperatures on the circulation line before and after the heat exchanger.
- ii. Dome pressure of the digester.
- iii. Two liquor pH measurements from the circulation line.

- iv. Liquor strength analysis 20 minutes after the completion of side relief.
- v. Viscosity value of the final pulp sample from the cook.

This data set will have to be gathered for a number of cooks before the target model can be determined with any degree of accuracy. Care will have to be exercised during this phase of data collection to monitor trends associated with possible drifts in the value of the initial degree of polymerisation (DP_0).

During this stage, the increase in the extent of the cellulose hydrolysis reaction (increase in DI) during gas releases must be determined to establish whether this is constant enough from cook to cook, to be accounted for in the adjustment of the DP_0 value affected by statistical feedback. This can be done using the satellite digester system whereby one of the mini digesters can be isolated immediately after the onset of the high-pressure gas release phase. A second mini digester can then be isolated once the high-pressure gas release phase is complete and the low-pressure gas release is commenced, and a third unit can be isolated just prior to the commencement of the pulp discharge.

7.2.3 Model Implementation.

In order to check the integrity of the new model thoroughly and to tune the parameters which are updated using statistical feedback, it must be operated in parallel with the existing process control algorithm. As soon as it becomes apparent that the new model is operating in a stable fashion, the control of one digester at a time can be switched over to the new algorithm. The 'S Factor' system could continue to run in

parallel with the new model as a manual back-up in the event of problems being experienced with both pH probes simultaneously.

Once the new cooking control system has been successfully implemented on the calcium-based digesters, the process will have to be repeated for the magnesium-based cooking process. This process should duplicate the initial runs performed in the laboratory, since it is only here that cooking parameters (such as temperature and cook time) can be manipulated to give data over a wide enough range to enable an accurate kinetic model to be determined.

7.2.4 Long Term Developments.

With the advent of increasingly powerful process control computers, it will not be in the too distant future before these machines will be capable of routinely handling the calculation load associated with 'expert system' algorithms such as the extended Kalman Filter. When these systems become available, it is possible that the implementation of such an algorithm could further improve digester control; however, the best basis for such a system to be formed would be by the correlations developed here. The added advantages offered by algorithms like the Kalman filter derive from their highly structured and powerful predictive capabilities.

The necessity of further increasing the sophistication of the digester control algorithm can, however, only be assessed once the capabilities of the system proposed here have been fully determined. Extreme caution has to be exercised when making a decision such as this, since it is conceivable that the accuracy of the control algorithm can be increased beyond the physical capabilities of the actual plant - at which point

further sophistication becomes useless. Placing the algorithm developed here into this context, further investigation of the implementation of the proposed cooking control model can be justified on the basis of two important points:

- i. The proposed model has a sound theoretical basis which definitely offers a more powerful model of the actual process than does the existing model.
- ii. A comparison of the results actually achieved by the existing model on the plant and those achieved by this model indicate the possibility that further improvements in process control can be achieved.

The actual implementation of the complete cooking control model should, however, be based on the results achieved during the verification of the kinetic model on the actual plant.

REFERENCES

- | <u>No.</u> | <u>REFERENCE</u> |
|------------|--|
| 1. | Yorston, F. H. & Liebergott, N., "Correlation of the Rate of Sulphite Pulping with Temperature and Pressure", <u>Pulp and Paper Magazine of Canada</u> , May 1965. |
| 2. | Watson, E., "A Kinetic Model and Simulation Programme for Acid Sulphite Dissolving Pulp Production", Laboratory Project, University of Natal (Durban), May 1988. |
| 3. | Rydholm, S. A., <u>Pulping Processes</u> , Interscience, London, 1965. |
| 4. | Smook, G. A., <u>Handbook for Pulp and Paper Technologists</u> , Joint Textbook Committee of the Paper Industry, 1986. |
| 5. | Clark, J. d'A., <u>Pulp Technology and Treatment for Paper</u> , Miller Freeman Publications Inc., San Francisco, 1978. |
| 6. | Macdonald, R. G. (ed.), <u>Pulp and Paper Manufacture</u> , Vol. I (2nd ed.), McGraw-Hill, 1969. |
| 7. | Clermont, L. P. & Schwartz, H., <u>Pulp and Paper Magazine</u> , 53 , No. 6, 142, 1952. |
| 8. | Matthus, A., <u>Kolloid Z.</u> , 98, 1942. |

9. Matthus, A., J. Prakt. Chemie, 162, 1943.
10. Weston, W. W., Personal Communication, SAPPI SAICCOR, Umkomaas (Natal), 22 March 1988.
11. Corey, A. J. & Maas, O., Can. J. Research, B13, 336, 1936.
12. Yorston, F. H., "Studies in Sulphite Pulping", Dominion Forest Service Bulletin (Ottawa), 97, 1942.
13. Suzuki, T., Tosaka, K. & Hayashi, J., "Rate Determining Steps of Cooking Reactions in Birchwood Digestion with Acid Sulphite Liquors", JAPAN TAPPI, 38, 5, 1984.
14. Conca, R. J., Gray, J. P. & Sloan, T. H., "Process for Controlling Intrinsic Viscosity of Sulphite Pulp", U.S. Patent No. 4,086,129, April 25, 1978.
15. Libby, C. E. (ed.), Pulp and Paper Science and Technology, Vol. I, McGraw-Hill, 1962.
16. Adler, E. in Treiber (ed.), Der Chemie der Pflanzenzellwand, Springer Berlin, 1957; Papier, 15, 604, 1961; TAPPI, 40, 294, 1957.
17. Adler, C. E. & Lindgren, B. O., Svensk Papperstid., 55, 563, 1952.
18. Hibbert, H. et al, Journal of the American Chemical Society, 62, 1412, 1940; 63, 3031, 1941.

19. Björkman, A., Svensk Papperstid., 59, 477, 1956.
20. Rydholm, S. & Lagergren, S., Svensk Papperstid., 62, 103, 1959.
21. Hagberg, B. & Schöön, N., Svensk Papperstid., 76, 15, 1973.
22. Sloan, T. H., "Activation Energy for Delignification in Acid Sulphite Pulping", Unpublished Work for ITT Rayonier Inc., November 4, 1982.
23. Fischer, K. & Schmidt, I., Conference Proceedings: 1989 Symposium on Wood and Pulping Chemistry, 1989.
24. Schöön, N., Svensk Papperstid., 85, 18, 1982.
25. Goldfinger, G., Paper Trade Journal, 112, No. 24, 1941.
26. Sloan, T. H., "Activation Energy for Hemicellulose Dissolution Sulphite Pulping", Unpublished Work for ITT Rayonier, Inc., December 29, 1982.
27. Hagberg, B. & Schöön, N., Svensk Papperstid., 77, 15, 1974.
28. Schöön, N. & Wannholt, L., Svensk Papperstid., 72, 13, 1969.
29. Beazley, W. B., Campbell, W. B. & Maas, O., "The Physical Properties of Sulphite Liquors", Dominion Forest Service Bulletin (Ottawa), 93, 1938.

30. Kauffman, Z., Dissertation, ETH, Zurich, 1951.
31. Rydholm, S., Svensk Papperstid., 57, 427, 1954.
32. Ingruber, O. V., Svensk Papperstid., 65, No. 11, 1962.
33. Hagberg, B. & Schöön, N., Svensk Papperstid., 77, No. 4, 1974.
34. Sloan, T. H., "Acid Hydrolysis of Cellulose in Sulphite Pulping", Unpublished Work for ITT Rayonier, Inc., 1982.
35. Ingruber, O. V., TAPPI, 41, No. 12, 1958.
36. Rydholm, S., Svensk Papperstid., 58, No. 8, 1955.
37. Ingruber, O. V., Pulp and Paper Magazine of Canada, 60, 1959.
38. Ingruber, O. V. & Allard, G. A., TAPPI, 50, No. 12, 1967.
39. Conca, R. J., Gray, J. P. & Sloan, T. H., "Process for Controlling Intrinsic Viscosity of Sulphite Pulp", Canadian Patent No. 1,080,910, July 8, 1980.
40. Weightman, D. A., "Cook Viscosity Control by Liquor pH/Refractive Index Measurement", SAPPI SAICCOR Report No. 320, September 1977.

41. Marr, S. Y. & Bondy, W. B., "Application of Viscosity Prediction Model in Sulphite Pulping", CPPA/TAPPI International Sulphite Conference, Quebec, 1986.
42. Birkett, M. D., Personal Communication, SAPPI Research & Development, 5 October 1989.
43. Earnshaw, J. L., "Welding - Stainless Steel Piping at New Extensions", Internal Memo, SAPPI SAICCOR, 13 May, 1980.
44. Simpson, D. A., Personal Communication, SAPPI SAICCOR, March 1990.
45. Saeman, J. F., *Ind. and Eng. Chem.*, **37**, 1945.
46. Moelwyn-Hughes, E. A., "The Kinetics of Reactions in Solutions", Oxford University Press, London, 1947.
47. Wise, L. E. & John, E. C., Wood Chemistry, Reinhold, York, PA., 1952.
48. Stanem, A. J., Wood and Cellulose Science, Roland Press, New York, 1964.
49. Sarkanen, K. V. & Lai, Y-Z., Cellulose Chemistry and Technology, **1**, 1967.
50. Wilder, H. D. & Harris, S. T., TAPPI, **45**, 1962.
51. Proctor, A. R., Yean, W. Q. & Goring, D. A., *Pulp and Paper Magazine of Canada*, **68**, 1967.

52. Weightman, D. A., "Viscosity Drop Across the Chlorine Dioxide Stage", SAPPI SAICCOR Report No. 373, 7 November 1978.
53. Meier, P., Lohrum, A. & Gareiss, J., "Practice and Theory of pH Measurement", Ingold Messtechnik AG, Urdorf, Switzerland, 1989.
54. Sarkanen, K. V., Hou-Min Chang & Allan, G. G., "Species Variation in Lignins, III. Hardwood Lignins", TAPPI, Vol. 50, December 1967.
55. Bozic, S. M., Digital and Kalman Filtering, Edward Arnold Publishers, London, 1979.
56. Eitelberg, E., Optimal Estimation for Engineers, NOYB Press, Durban (South Africa), 1991.
57. Ingruber, O. V., The Ind. Chem., 32, 1956.

APPENDIX 1

SECTION A : VISCOSITY

1) Method

- 1.1 1.035 gm of raw pulp (or 1.050 gm of bleached pulp [to give 1 gm bone dry) is weighed out into an amber glass bottle.
- 1.2 15 ml of 1M (N/1) NaOH is added and the bottle shaken vigorously to thoroughly wet the pulp.
- 1.3 85 ml of cuprammonium solution is then added. The solution is stirred using a mechanical stirrer for 3 minutes to dissolve the pulp.
- 1.4 When the pulp has dissolved, the bottle is placed into the 20°C thermostat bath for ten minutes to allow the solution to reach temperature equilibrium.
- 1.5 The solution is then sucked up into the Ostwald-type viscometer, and the time for the solution to flow out between two marks on the viscometer is timed with a stopwatch.

2) Calculation

Viscosity (SNIA) = Viscometer Coefficient x time in seconds.

3) Sources of Error.

- 3.1 The pulp must be weighed out quickly to avoid moisture uptake.
- 3.2 The temperature of the thermostat baths must be controlled at 20°C.

3.3 If discrepancies occur between results obtained in the Central Laboratory and one of the other Departments, then the viscosity of the weighed out standard pulp is determined by both laboratories to indicate which one is in error.

4) Basis

The SNIA viscosity method has been based on method T 206-05-63 of TAPPI Test Methods, Vol 1. The conversion between results obtained from these two methods accepted by clients of SAPPI SAICCOR is as follows:

$$\mu \text{ (SNIA)} \approx 1.56 * \mu \text{ (TAPPI)}$$

SECTION B : PERMANGANATE NUMBER (K No.)

1) Method

- 1.1 Pulp must be clean and free of knots and shives.
- 1.2 A 2 gm pulp pad is made and washed with methylated spirits, and then dried thoroughly in a 105°C oven for more than 10 mins.
- 1.3 1.053 gm of raw pulp or 1.050 gm of bleached pulp is weighed out into a 600 ml beaker.
- 1.4 180 ml of distilled water and 20 ml of 10% sulphuric acid is added. The mixture is then stirred vigorously.
- 1.5 With the beaker on a magnetic stirrer, 25 ml of 0.02M (N/10) KMnO_4 is added.
- 1.6 After exactly 3 minutes, 25 ml of 0.1076M (N/10) ferrous ammonium sulphate (Mohrs salt) is added, followed by 10 drops of N - phenyl anthranilic acid indicator.
- 1.7 The excess is back titrated with 0.02M (N/10) potassium permanganate to a purple end point.
- 1.8 A blank is also carried out, as above, except no pulp is added.

2) Calculation.

$$(\text{ml } \text{KMnO}_4 - \text{ml blank}) \times 0.355 = \text{K No.}$$

3) Basis

This is based on methods UM 251 and UM 201 from TAPPI Useful Methods.

SECTION C : ALKALI SOLUBILITY OF PULP (S₁₈)

The solubility gives an indication of the amount of short chain and hemicellulose present in the pulp. Too much will mean the final rayon strength will be low as it does not polymerise completely in the viscose process. Conversely, too many long chain alpha-cellulose molecules will block the spinarets in the rayon spinning process.

1) Method

- 1.1 100 ml of 18% NaOH is pipetted into a wide-mouthed glass bottle. This is cooled for 30 minutes in a 20°C water bath.
- 1.2 1.6 gm of the pulp sample is weighed out and placed in the bottle. A second amount of 10 gm is weighed out for moisture determination, and left in a 125°C oven for 1.5 hours.
- 1.3 After 2 minutes, the bottle is placed under a stirrer for 4 minutes at 1700rpm (approximately), so that while air is not stirred into the mixture, there is complete disintegration after 3 minutes. If necessary, the disintegration can be extended slightly. It may be necessary to tilt the bottle slightly to ensure that all the pulp is brought through the stirrer.
- 1.4 The bottle is then removed, stoppered and replaced in the water bath.
- 1.5 60 minutes after adding the pulp to the NaOH, the sample is filtered through a dry G3 filter funnel.
- 1.6 The initial 10 ml or so should be discarded, and thereafter 10 ml of the filtrate is pipetted out and transferred to a 1-litre conical flask.

- 1.7 10 ml of 0.067M (0.4N) potassium dichromate and 30 ml of concentrated sulphuric acid are added. After 10 minutes, 250 ml of distilled water is added and the solution is replaced in the waterbath for 30 minutes.
- 1.8 10 ml of 10% KI solution is added and after 5 minutes, the solution is titrated with 0.1M (N/10) sodium thio-sulphate.
- 1.9 Colour change is from brown - green - light blue. Starch is added when solution is yellow.
- 1.10 A blank (without pulp) is carried out at the same time by pipetting 10 ml of the 18% sodium hydroxide into a conical flask and proceeding with the method from there.

2) Calculation

A is the sample titre ml

B is the blank titre ml.

G = bone-dry weight of pulp.

$$\text{Alkali solubility} = \left\{ \frac{(B - A) * 0.685}{G} \right\} \%$$

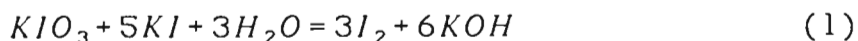
3) Basis

This is based on method T 235 m-60 of TAPPI Test Methods, Vol 1.

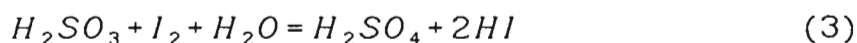
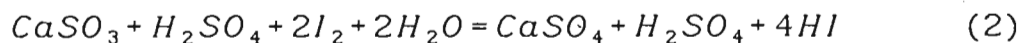
SECTION D : PALMROSE METHOD

1) Discussion

When potassium iodate is added to potassium iodide solution, iodine is liberated which will immediately react with any SO₂ present:



The SO₂ is present in both the combined form as calcium bisulphite Ca(HSO₃)₂ (alternatively CaSO₃ + H₂SO₄), and as free SO₂ dissolved in water, ie. sulphurous acid H₂SO₃. They react with iodine as follows:



No iodine is available to form a colour with the starch until sufficient iodate has been added to consume the total SO₂ content. In equation (2) the gain in acidity from consuming 2I₂ is the 4HI generated, which exactly balances the 4KOH produced in equation (1). In equation (3) there are four equivalents of acid produced in consuming one I₂, which is two more than 2 KOH produced in equation (1). Thus the resulting acidity can be titrated with sodium hydroxide and directly relate to the free SO₂ that was present.

2) Method

2.1 75 ml of distilled water is added to a conical flask, followed by three drops of methyl red indicator and 10 ml of starch iodide solution.

- 2.2 2 ml of the liquor being tested is carefully pipetted into the flask. The end of the pipette is kept just below the surface of the liquid, whilst transferring the 2 ml, to avoid free SO₂ losses.
- 2.3 The contents of the flask are then titrated with 0.0208M (N/8) KIO₃. Initially, the KIO₃ is added quickly and the flask not swirled until the liquor begins to turn blue. The flask is then gently swirled and the titration continued until a permanent blue colour is obtained. The volume of iodate used is recorded.
- 2.4 One small drop of sodium thiosulphate is added to the solution to decolourise it.
- 2.5 0.125M (N/8) NaOH is added from a Burette until the solution turns yellow, and the volume is noted.

3) Calculation

Total SO₂ : ml 0.0208M KIO₃ x 0.2 = % Total SO₂

Free SO₂ : ml 0.125M NaOH x 0.2 = % Free SO₂

Combined SO₂ : % Total SO₂ - % Free SO₂ = Combined SO₂

CaO : % Combined SO₂ x 0.875 = % CaO

4) Basis

This is based on method T 604 from TAPPI Test Methods, Vol 1.

SECTION E : CHLORINE DIOXIDE BLEACHING

1) Bleach Conditions

ClO₂ Dosage - 1% on pulp
Consistency - 8%
Temperature - 70°C
Time - 3 hours

2) Method

- 2.1 Pipette a 10 ml aliquot of ClO₂ into a flask containing KI, ± 0.5 gm NaHCO₂ and starch indicator.
- 2.2 Titrate with 0.1N Na₂S₂O₃:- Titre A.
- 2.3 After end point, acidify with 3% HCl and again titrate with 0.1N Na₂S₂O₃:- Titre B.
- 2.4 Then % ClO₂ = (B - A) x .0444 as Avg. Cl₂.
This is usually in the region of 1.5%.

3) Calculations

3.1 Weight of Pulp:-

Take 20 gm BD pulp and make up into initially to a ±20% consistency solution.

$$\text{Then wt. solution} = 20 * \frac{100}{20} = 100 \text{ gm.}$$

3.2 Volume ClO₂ solution:

If 1% ClO₂ is to be added to the pulp, then on 20g sample:-

$$20 * \frac{1}{100} = .2 \text{ gm ClO}_2 \text{ required.}$$

If solution is 1.5% ClO₂:-

Then $\frac{2}{1.5} * 100 = 13.4$ ml ClO₂ solution required.

3.3 Volume of water to be added:

If consistency of ClO₂ bleach stage is to be 8%, then 20 gm BD pulp must be diluted to:-

$$20 * \frac{100}{8} = 250 \text{ gm}$$

3.4 To calculate the volume of water needed, subtract from this the volume of ClO₂ to be added and the weight of the wet pulp:-

$$\text{Volume of water needed} = 250 - (100 + 13.4) = 136.6 \text{ ml}$$

Add this volume as hot water when preparing sample.

4) Bleach Procedure

- 4.1 ClO₂ bleaching is carried out in a polythene bag placed in a water bath, with the temperature maintained at 70°C throughout the bleach period.
- 4.2 The sample must be thoroughly mixed, and exclude as much air as possible from the bag before sealing.
- 4.3 The bag containing the sample is then placed in another bag containing lead weights and immersed in the water bath.

5) Washing Bleached Pulp

- 5.1 After bleaching, add a small volume of SO₂ water ($\pm 2.0\%$ free SO₂ in water) to neutralise any ClO₂ residual. (This is not done should it be necessary to measure residual ClO₂ after bleaching.)
- 5.2 On 20 gm BD pulp sample add ± 5.5 ml SO₂ solution.
- 5.3 Dewater the pulp to 20% consistency on a buchner funnel, and wash by displacing the liquor remaining on the pulp with six times its volume of water (on 20 gm sample use approximately 500 ml).

APPENDIX 2

SOLUTION OF CORRELATIONS TO OBTAIN EXPRESSIONS FOR $[HSO_3^-]$ AND $[H^+]$.

The charge balance and equilibrium correlations presented as equations 3-2 to 3-8 can be solved to obtain expressions for $[HSO_3^-]$ and $[H^+]$ in terms of the total and combined SO_2 and either K_{SO_2} or K_P - presented as equations 3-9, 3-10, 3-11 and 3-12. The solutions of these expressions can be found below.

1) EQUATION 3-10

The expression for sulphur dioxide protolysis (equation 3-5) can be solved to obtain an expression for $[H^+]$ in terms of $[HSO_3^-]$, K_{SO_2} and $[SO_2^{tot}]$:

$$[H^+] = K_{SO_2} * \left\{ \frac{[SO_2^{tot}] - [HSO_3^-]}{[HSO_3^-]} \right\} \quad (3-10)$$

2) EQUATION 3-12

The expression for sulphur dioxide solubility (equation 3-6) can be solved to obtain an expression for $[H^+]$ in terms of $[HSO_3^-]$, K_P and P_{SO_2} :

$$[H^+] = \frac{K_P * P_{SO_2}}{[HSO_3^-]} \quad (3-12)$$

3) EQUATION 3-9

Solving the charge balance expression (equation 3-2) for $[HSO_3^-]$:

$$[HSO_3^-] = [H^+] + 2[Ca^{2+}] - [SA^-] \quad (A)$$

Substituting (3-10) for $[H^+]$ in (A):

$$[HSO_3^-]^2 = K_{so_2} * \{[SO_2^{tot}] - [HSO_3^-]\} + [HSO_3^-] * \{2[Ca^{2+}] - [SA^-]\} \quad (B)$$

Re-arranging (B):

$$[HSO_3^-]^2 - [HSO_3^-] * \{2[Ca^{2+}] - [SA^-] - K_{so_2}\} - K_{so_2} * [SO_2^{tot}] = 0 \quad (C)$$

From equation 3-4:

$$[SO_2^{com}] = [Ca^{2+}] - \frac{1}{2}[SA^-] \quad (D)$$

Substituting (D) into (C):

$$[HSO_3^-]^2 - [HSO_3^-] * \{2[SO_2^{com}] - K_{so_2}\} - K_{so_2} * [SO_2^{tot}] = 0 \quad (E)$$

Treating (E) as a quadratic expression and solving for $[HSO_3^-]$ yields:

$$[HSO_3^-] = [SO_2^{com}] - \frac{1}{2}K_{so_2} + \left\{ \frac{(2 * [SO_2^{com}] - K_{so_2})^2 + K_{so_2} * [SO_2^{tot}]}{4} \right\}^{\frac{1}{2}} \quad (3-9)$$

4) EQUATION 3-11

Solving the charge balance expression (equation 3-2) for $[HSO_3^-]$:

$$[HSO_3^-] = [H^+] + 2[Ca^{2+}] - [SA^-] \quad (A)$$

Substituting (3-12) for $[H^+]$ in (A):

$$[HSO_3^-]^2 = K_p P_{so_2} + [HSO_3^-] * \{2[Ca^{2+}] - [SA^-]\} \quad (B)$$

Re-arranging (B):

$$[HSO_3^-]^2 - [HSO_3^-] * \{2[Ca^{2+}] - [SA^-]\} - K_p K_{so_2} = 0 \quad (C)$$

From equation 3-4:

$$2[SO_2^{com}] = 2[Ca^{2+}] - [SA^-] \quad (D)$$

Substituting (D) into (C):

$$[HSO_3^-]^2 - 2[HSO_3^-][SO_2^{com}] - K_p P_{SO_2} = 0 \quad (E)$$

Treating (E) as a quadratic expression and solving for $[HSO_3^-]$ yields:

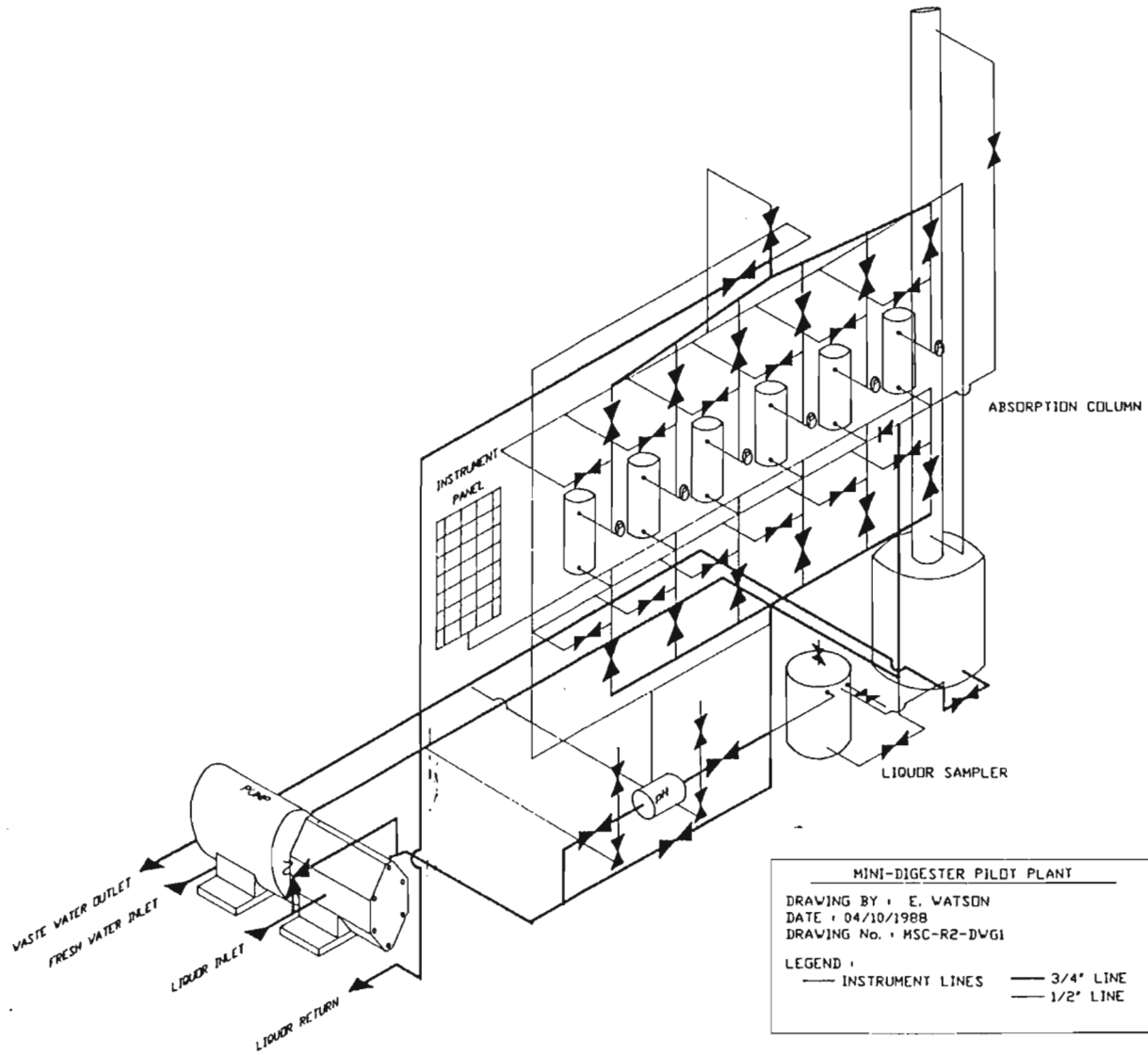
$$[HSO_3^-] = [SO_2^{com}] + \left\{ [SO_2^{com}]^2 + K_p P_{SO_2} \right\}^{\frac{1}{2}} \quad (3-11)$$

APPENDIX 3

MECHANICAL DRAWINGS OF SATELLITE MINI-DIGESTER PLANT

<u>FIGURE</u>	<u>TITLE</u>
A3-1	SATELLITE MINI-DIGESTER PLANT LAYOUT.
A3-2	MINI-DIGESTER CONSTRUCTION.

FIGURE A3-1



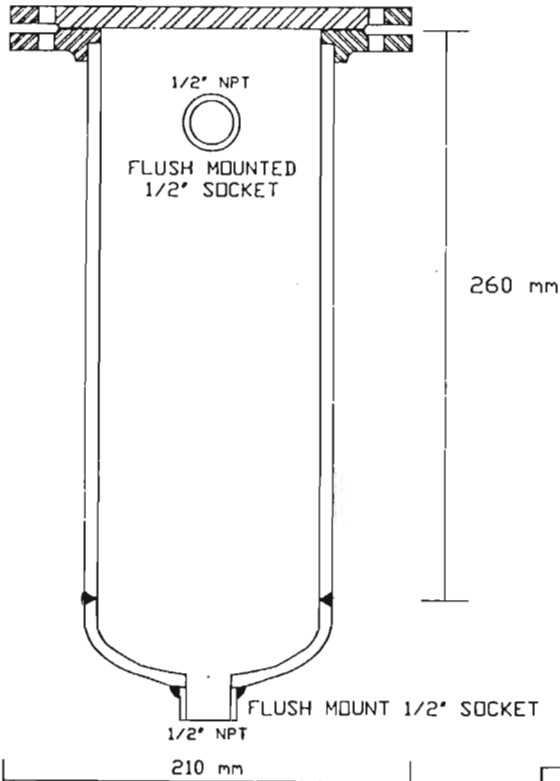
MINI-DIGESTER PILOT PLANT

DRAWING BY : E. WATSON
DATE : 04/10/1988
DRAWING No. : MSC-R2-DWG1

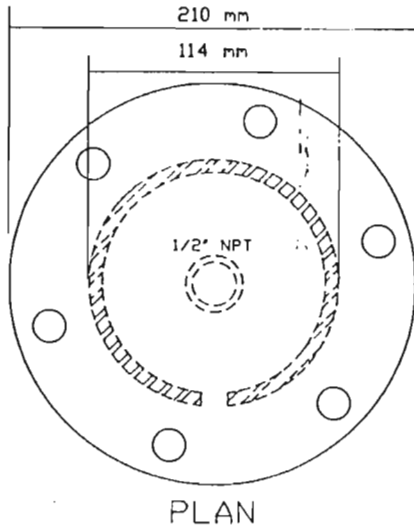
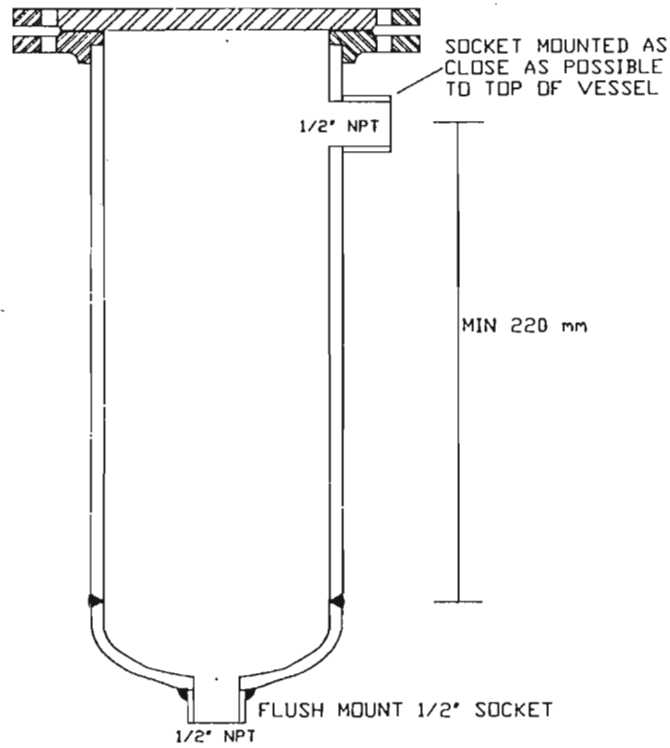
LEGEND :
— INSTRUMENT LINES — 3/4" LINE
— 1/2" LINE

FIGURE A3-2

FRONT ELEVATION



SIDE ELEVATION



DRAWING NAME : MINI-DIGESTER CONSTRUCTION
 DRAWING BY : E.WATSON
 No : MSC-R2-DWG2
 DATE : 25/11/1988
 DESIGN STANDARD : BS 5500

MATERIALS :
 4" NOM. DIAMETER PIPE
 316 STAINLESS STEEL
 SCHEDULE 10
 STANDARD D TABLE FLANGE (NARROW FACE)
 316 STAINLESS STEEL WELD ON RING
 MINIMUM THICKNESS (BS 5500) - 11 mm
 SOCKETS
 316 STAINLESS STEEL 1/2" SOCKETS
 ALL SOCKETS FLUSH MOUNTED
 END CAPS
 316 STAINLESS STEEL
 WALL THICKNESS 3 mm
 MINIMUM THICKNESS (BS 5500) - 1.3 mm

APPENDIX 4

DATA COLLECTION PROGRAMME LISTING

A listing of the Turbo Pascal programme written to collect data from the satellite digester plant can be found below. All signals from the plant instrumentation were re-transmitted as 4-20 mA signals. These were only converted to 0-10 V signals at the PC, since voltage signals are prone to excessive interference if transmitted over extended distances in close proximity to electrical equipment. The 0-10 V signals were then fed to a PC-30 Analogue-to-Digital board installed in a standard IBM compatible computer.

The Turbo Pascal programme collected the data at pre-set time intervals, displayed the current readings on the screen and saved the data onto a floppy disk.

NOTE: Some of the routines provided with the PC-30 card have been incorporated into this programme.

Turbo Pascal Programme Source Listing.

```
{ ***** }
{ * * * * * }
{ * DEMONSTRATION SOFTWARE WRITTEN IN TURBO PASCAL V 3.1 FOR * }
{ * THE PC-30 EXTENSION CARD FOR THE IBM-PC AND COMPATIBLES * }
{ * * * * * }
{ * The baseaddress of the PC-30 card must be selected as 700 * }
{ * (Hex) ! * }
{ * * * * * }
{ ***** }
```

PROGRAM CELLMON;

{SC-}

CONST

 xmax = 639 ;
 Boardaddress = \$700;

TYPE

 Loop = RECORD
 No, ChannelNo : INTEGER;
 Name : STRING[20];
 Units : STRING[5];
 Scale, Offset : REAL;
 END;
 string_type = string[80];
 string_20 = string[20];
 vres_t = record
 AX, BX, CX, DX, BP, SI, DI, DS, ES, Flags: integer;
 end;

VAR

 chmin, chmax, sample, ploty, Sampleno, Yposition, MaxFiles, Count, ElapsedTime, Noise : INTEGER;
 ch : char;
 plot_d : array [0..999] of integer;
 Frequ, s_clk, Lreading : REAL;
 dsave : INTEGER ABSOLUTE Cseg:\$0006;
 done, StoreData, plotx : BOOLEAN;
 v_res : vres_t;
 Loopdata : Loop;
 LoopSet : ARRAY[1..16] OF Loop;
 Infile, Outfile : FILE OF Loop;

```

DataOutFile : TEXT;
LoopReading : ARRAY[1..17] OF REAL;
FileName, StoreFile : String[30];

{*****}
PROCEDURE getkey (VAR key : CHAR);
{THIS PROCEDURE NEEDS THE COMPILER COMMAND $C- IN THE MAIN-PROGRAM !
PROCEDURE getkey returns a character if a key is pressed, else it
returns a null character}
BEGIN
  IF KeyPressed THEN READ (kbd,key)
  ELSE key := chr(0);
END;
{*****}
PROCEDURE PUTS (x,y:INTEGER; str:string_type);
BEGIN
  GOTOXY (x,y);      {string_80 must have been declared of TYPE}
  WRITE(str);        {STRING [80] in the main program}
END;
{*****}
PROCEDURE beep;
BEGIN
  Sound(500);
  Delay(150);
  Nosound;
END; {beep}
{*****}
FUNCTION readreal: REAL;
{Idiot proof routine for entering reals with up to max
significant digits. }
VAR
  J,value,max,K:INTEGER;
  I:REAL;
  strng : string_20;
  cr,OK,point,minus:BOOLEAN;
BEGIN
  strng:='          ';
  cr:=FALSE;
  J:=1;
  max:=8;      {max is the max number of significant digits}
  point:=FALSE;
  minus := FALSE;
  REPEAT
    ok := FALSE;
    REPEAT
      getkey(ch);
      IF ORD(ch) IN [8,13,45,46,48..57] THEN OK:=TRUE
      ELSE IF ORD(ch)<>0 THEN BEEP;
    UNTIL OK ;
    CASE ORD(ch) OF
      45,46,48..57 : BEGIN
        IF (J<max) AND ((NOT(point) AND (ch='.')) OR
          ((NOT minus) AND (ch='-')) OR
          (ord(ch) IN [48..57])) THEN
          BEGIN
            WRITE (ch);
            IF ch='.' THEN
              BEGIN
                point:=TRUE;
                max:=max+1;
              END;
            IF ch = '-' THEN
              BEGIN
                minus := TRUE;
                max:=max+1;
              END;
            strng[J]:=ch;
            J:=J+1;
          END ELSE BEEP;
        END;
      13 : BEGIN
        VAL(strng,I,K);
        cr:=TRUE;

```

```

        readreal := i;
    END;
8 : BEGIN
    IF J>1 THEN
    BEGIN
        IF strng[J-1] = '.' THEN point:=FALSE;
        WRITE (ch);      {one backspace}
        WRITE (' ');    {wipe out old character}
        WRITE (ch);    {one backspace}
        strng[J-1]:=' ';
    END;
    J:=J-1;
    IF J>0 THEN
    BEGIN
        IF strng[J]='.' THEN point:=FALSE;
        strng[J]:=' ';
    END ELSE
    BEGIN
        J:=1;
        BEEP;
    END;
    END;

    END; (* case *)
UNTIL cr;
END; (* readreal *)
{*****}
PROCEDURE get_cl;
{* This procedure gets the system clock frequency.          *}

BEGIN
    CLRScr;
    repeat
        PUTS(20,12,'Enter system clock frequency in MHz :      ');
        PUTS(20,12,'Enter system clock frequency in MHz : ');
        s_clk := readreal;
    until ((s_clk < 25.0) and (s_clk > 4.76));
END;{*get_cl*}
{*****}
FUNCTION readint (max:INTEGER):INTEGER;
{ Idiot proof function for entering positive integers with maximal
  digits. }
VAR
    J,value,K:INTEGER;
    i : REAL;
    strng : string_20;
    cr,OK:BOOLEAN;
BEGIN
    IF max > 5 THEN max := 5;
    strng:=' ';
    cr:=FALSE;
    OK:=FALSE;
    J:=1;
    {max:=5;}
    REPEAT
        ok := FALSE;
        REPEAT
            getkey(ch);
            IF ORD(ch) IN [8,13,48..57] THEN OK:=TRUE
            ELSE IF ORD(ch)<>0 THEN BEEP;
        UNTIL ok;
        CASE ORD(ch) OF
            48..57 : BEGIN
                IF J<max+1 THEN
                BEGIN
                    WRITE (ch);
                    strng[J]:=ch;
                    J:=J+1;
                END ELSE BEEP;
            END;
        13 : BEGIN
            VAL(strng,I,K);
            cr:=TRUE;
            IF i > maxint THEN i := maxint;

```

```

        readint := ROUND (i);
    END;
8 : BEGIN
    IF J>1 THEN
        BEGIN
            WRITE (ch);
            WRITE (' ');
            WRITE (ch);
            string[J-1]:= ' ';
        END;
        J:=J-1;
        IF J<1 THEN
            BEGIN
                J:=1;
                BEEP;
            END;
        END;
    END; (* case *)
UNTIL cr;
END; (* readint *)
{*****}
{ The PROCEDURE CONTINUE displays a message at screen location
xposition, yposition and waits until the space-bar is pressed}
PROCEDURE CONTINUE (XPOSITION,YPOSITION :INTEGER);
    VAR
        ch:char;
    BEGIN
        PUTS(xposition,yposition,'PRESS SPACEBAR TO CONTINUE');
        REPEAT
            getkey(ch);
        UNTIL ch = ' ';
    END;
{*****}

PROCEDURE Enable_IRQx(IRQ : BYTE);

{ Three PROCEDURES to enable/disable the IRQ line number
IRQ and to store the Interrupt Vector of Interrupt service
routine number X in the Interrupt Vector table IVT.}

    VAR
        imr, mask : INTEGER;
    BEGIN
        mask := not ( 1 shl IRQ );
        imr := PORT [$21]; { get Interrupt mask register
                           from 8259 }
        imr := imr and mask; { clear mask bit of IRQ }
        PORT [$21] := imr; { and return to controller }
    END;
{*****}

PROCEDURE Disable_IRQx(IRQ : BYTE);

{ This PROCEDURE disables the IRQ line number x }

    VAR
        imr, mask : INTEGER;
    BEGIN
        mask := ( 1 shl IRQ );
        imr := PORT [$21]; { get Interrupt mask register
                           from 8259 }
        imr := imr or mask; { set mask bit of IRQ }
        PORT [$21] := imr; { and return to controller }
    END;
{*****}

FUNCTION TIMER(mf:REAL) : integer;

```

{ This procedure allows the user to program the on-board 8253 timer to the required interval in order to control the sampling frequency of the PC-30 board. }

```

VAR
  Factor:REAL;
  Count1,Count0, tch:INTEGER;
  LBCOUNT1,LBCount0,HBCount1,HBCount0:BYTE;
BEGIN
  REPEAT
    PUTS (10,5,' ');
    PUTS (10,5,'Channel to sample = ');
    tch := readint (2);
  UNTIL (tch>=0) AND (tch<16);
  timer := tch;
  PUTS(5,10,'ENTER SAMPLING FREQUENCY IN Hz      max = ');
  WRITE(mf:6:0, ' Hz');
  PUTS(43,11,'min = 0.002 Hz');
  REPEAT
    PUTS (11,15,'      Frequency (Hz) = ');
    PUTS (11,15,'      Frequency (Hz) = ');
    Frequ := readreal;
  UNTIL (Frequ>=0.002) AND (Frequ<=mf);
  Factor:=(s_clk * 250000.0)/Frequ;
  Count0 := TRUNC (Factor/32767) + 1;
  IF Count0 <= 1 THEN Count0 := 2;
  Count1 := ROUND(Factor/Count0);
  PUTS (11,18,'Actual sample frequency = ');
  frequ := (s_clk * 250000.0)/(Count0);
  frequ := (frequ / Count1);
  Write (frequ:8:3, ' Hz');
  Puts(5,23,'H I T   S P A C E B A R   T O   S T A R T   S A M P L I N G');
  REPEAT UNTIL KeyPressed;
  LBCount1:= LO(Count1);
  HBCount1:= HI(Count1);
  (* Calculate low byte and high byte values for Counter 0 *)
  LBCount0:=LO(Count0);
  HBCount0:=HI(Count0);
  (* Program Counter 0 - timer control address = $707 *)
  PORT[$707]:=$34;          (* Control word for counter 0 *)
  PORT[$704]:=LBCount0;    (* low byte for counter 0 *)
  PORT[$704]:=HBCount0;    (* high byte for counter 0 *)
  (* Program Counter 1 *)
  PORT[$707]:=$74;          (* Control word for counter 1 *)
  PORT[$705]:=LBCount1;    (* low byte for counter 1 *)
  PORT[$705]:=HBCount1;    (* high byte for counter 1 *)
  (* Program counter 2 *)
  PORT[$707]:=$B4;          (* Controlword counter 2 *)
  PORT[$706]:=$2;          (* low byte counter 2 *)
  PORT[$706]:=$0;          (* high byte counter 2 *)
END; { TIMER }

```

{*****}

```

PROCEDURE NOISEFILTER;
BEGIN
  REPEAT
    PUTS(10,25,' ');
    PUTS(10,15,'NOISE SUPPRESSION OPTION (1 to 5 SAMPLES PER READING)');
    GOTOXY(64,15);
    READLN(NOISE);
  UNTIL NOISE IN [1..5];
  PUTS(10,15,' ');
END;

```

{*****}

```

FUNCTION SampleTime : integer;
VAR
  PATHEX : String[2];
  ch1 : CHAR;
BEGIN
  NOISEFILTER;
  PUTS(1,10,'ENTER SAMPLING FREQUENCY IN SECONDS PER SAMPLE      max = ');
  WRITE('1 per 5 secs');
  PUTS(47,12,'Minimum = 1 per 300 secs (5 min)');
  REPEAT
    PUTS (11,15,' Sample Frequency      = ');

```



```

    PUTS (11,15,' Sample Frequency      = ');
    Freq := readreal;
    UNTIL (Freq>=5) AND (Freq<=300);
    StoreData := FALSE;
    PUTS(1,17,'LOG DATA TO DISK (Y/N).....');
    REPEAT
    READ(ch);
    ch := UPCASE(ch);
    UNTIL ch IN ['Y','N'];
    IF ch = 'Y' THEN
    BEGIN
    DONE := FALSE;
    WHILE NOT DONE DO
    BEGIN
    StoreData := TRUE;
    PUTS(1,17,'ENTER FILE NAME TO WHICH DATA MUST BE WRITTEN.....');
    READ(StoreFile);
    PUTS(1,18,'ENTER DISK DRIVE TO WHICH FILE IS TO BE WRITTEN.....');
    READ(PathEx);
    StoreFile := PATHEX+StoreFile;
    GOTOXY(1,19);
    WRITE('STORE DATA TO ---> ',StoreFile,' (Y/N) ');
    REPEAT
    READ(kbd,ch);
    ch1 := UPCASE(ch);
    UNTIL ch1 IN ['Y','N'];
    IF ch1 = 'Y' THEN
    BEGIN
    ASSIGN(DataOutFile,StoreFile);
    REWRITE(DataOutFile);
    DONE := TRUE;
    END;
    END; {WHILE NOT}
    END;
    IF ch = 'N' THEN
    BEGIN
    StoreData := FALSE;
    END;
    Puts(5,23,'H I T   S P A C E B A R   T O   S T A R T   S A M P L I N G');
    REPEAT UNTIL KeyPressed;
    END; { SAMPLETIME }

```

{*****}

```

FUNCTION ADSAMPLE (channel:INTEGER): INTEGER;
VAR I, J, SINGLESAMPLE, SAMPLESUM :INTEGER;
BEGIN
    SAMPLESUM :=0;
    FOR J := 1 TO NOISE DO
    BEGIN
    PORT [$702] := (channel SHL 4) + 2; { channel selection and }
    {clear software-clock bit }
    PORT [$702] := (channel SHL 4) + 3; {channel selection and }
    {setting of software-clock bit }
    FOR I:=1 TO 10 DO
    BEGIN
    {loop until end of conversion }
    END;
    SINGLESAMPLE :=((PORT[$701] AND $0F) SHL 8) + PORT[$700];
    SAMPLESUM := SAMPLESUM + SINGLESAMPLE;
    END;
    ADSAMPLE := ROUND(SAMPLESUM/NOISE);
    END;

```

{*****}

```

PROCEDURE DISPLAYCHANNELS;
BEGIN

```

```

Yposition := 5;
FOR Count := 1 TO MaxFiles DO
BEGIN
    LoopData := LoopSet[Count];
    Yposition := Yposition + 1;
    GotoXY(2,Yposition);
    Write (count);
    PUTS(8,Yposition,LoopData.Name);
    GotoXY(35,Yposition);
    Sample := ADSample(LoopData.ChannelNo);
    Write (Sample,' ');
    GOTOXY(46,Yposition);
    WRITE (LoopData.Offset:7:2);
    LoopReading[Count + 1] := (Sample-LoopData.Offset)/LoopData.Scale;
    GOTOXY(56,Yposition);
    WRITE (LoopReading[Count + 1]:7:2);
    GOTOXY(67,Yposition);
    WRITE (LoopData.Scale:7:2);
END; {DO}
end;

```

{*****}

PROCEDURE PRINT_CHANNELS;

```

VAR
    Channel,Xposition,Yposition,Count, MaxFiles,Counter :INTEGER;
    Sample : REAL;
BEGIN
    CLRScr;
    NOISEFILTER;
    Count := 0;
    FileName := 'C:\CELLMON\SETUP.DAT';
    ASSIGN (InFile,FileName);
    RESET (InFile);
    MaxFiles := FileSize(InFile);
    WHILE NOT EOF (InFile) DO
        BEGIN
            Count := Count + 1;
            READ (InFile,LoopData);
            LoopSet[Count] := LoopData;
        END;
    CLOSE(InFile);
    PUTS (5,25,'PRESS ANY KEY TO RETURN TO MENU!');
    PUTS (1,2,'      Loop No      Loop Name      Reading ');
    FOR Count := 1 TO MaxFiles DO
        BEGIN
            GotoXY(11,Count+4);
            Write (Count);
        END; {FOR}
    FOR Count := 1 TO MaxFiles DO
        BEGIN
            LoopData := LoopSet[Count];
            Yposition := Count + 4;
            PUTS(25,Yposition,LoopData.Name);
        END; {FOR}
    REPEAT
        FOR Count := 1 TO MaxFiles DO
            BEGIN
                LoopData := LoopSet[Count];
                Yposition := Count + 4;
                Sample := (ADSAMPLE (LoopData.ChannelNo) - LoopData.Offset)/LoopData.Scale;
                GotoXY(55,Yposition);
                Write (Sample:7:2,' ');
            END;
        UNTIL KeyPressed;
    END; {PROCEDURE PRINT_CHANNELS}

```

{*****}

{ Interrupt service routine for the use of hardware interrupts with TURBO PASCAL ; for details see BYTE supplementary 'Inside the IBM PC's' Fall 1986.

Don't forget to enable the respective IRQ line with the PROCEDURE Enable_IRQx (x) , and to set the Interrupt vector table of interrupt 5 with the PROCEDURE Set_IVT (x=5) ; !!!

The following is very important ! : define the following ABSOLUTE VARIABLE in the VAR part of the main program :

```
dsave : INTEGER ABSOLUTE Cseg:$0006;
```

the first executable statement in the main program must save the DS address in the absolute variable dsave in the following way:

```
dsave := Dseg;
```

IT IS NOT ALLOWED that the Interrupt_5_Service_Routine interrupts Turbo Pascal during execution of Turbo Pascal functions and procedures which use the IBM's BIOS, because BIOS is not re-entrant . So don't use WriteLn, Read, Plot etc. after enabling the Interrupt 5, and disable Interrupt 5 before using these Routines.

With the Procedures Enable_IRQx(X) and Disable_IRQx(x) you can enable or disable the Hardware Interrupt line number x.

Before using the Interrupt_5_Service_Routine it is recommended to disable the IBM's internal clock with the statement
Disable_IRQx(0); }

```
PROCEDURE Interrupt_5_Service_Routine;
```

```
  BEGIN
```

```
    INLINE ($1E/      { PUSH DS          }
           $50/      { PUSH AX          }
           $53/      { PUSH BX          }
           $51/      { PUSH CX          }
           $52/      { PUSH DX          }
           $57/      { PUSH DI          }
           $56/      { PUSH SI          }
           $06);     { PUSH ES          }

    INLINE ($8C/$C8/  { MOV AX,CS  restore data segment }
           $8E/$D8/  { MOV DS,AX          }
           $A1/dsave/ { MOV AX,dsave         }
           $8E/$D8); { MOV DS,AX          }
```

```
{-----}
```

```
  Sampleno := Sampleno + 1;
```

```
  Yposition := 5;
```

```
  FOR Count := 1 TO MaxFiles DO
```

```
    BEGIN
```

```
      Yposition := Yposition + 1;
      LoopData := LoopSet[Count];
      GotoXY(2,Yposition);
      Write (sampleno);
      PUTS(8,Yposition,LoopData.Name);
      GotoXY(35,Yposition);
      Sample := ADSample(LoopData.ChannelNo);
      Write (Sample,' ');
      GOTOXY(46,Yposition);
      WRITE (LoopData.Offset:7:2);
      LReading := (Sample-LoopData.Offset)/LoopData.Scale;
      GOTOXY(56,Yposition);
      WRITE (LReading:7:2);
      GOTOXY(67,Yposition);
      WRITE (LoopData.Scale:7:2);
```

```
    END;
```

```
  Yposition := 5;
```

```
  PORT[$702] := $8 + 16; {Try to reset interrupt enable - C3}
```

```
  {the following keypressed check uses the BIOS and is
   therefore performed within the interrupt service
   routine}
```

```
{-----}
```

```
  PORT [$0020] := $20;      { nonspecific EOI to the 8259 PIC }
```

```

        INLINE ($07/          { POP ES          }
                $5E/          { POP SI          }
                $5F/          { POP DI          }
                $5A/          { POP DX          }
                $59/          { POP CX          }
                $5B/          { POP BX          }
                $58/          { POP AX          }
                $1F/          { POP DS          }
                $FB/          { STI             }
                $CF);        { IRET      return from interrupt }
    END; { End of PROCEDURE Interrupt_5_Service_Routine }

```

```
{*****}
```

```

PROCEDURE Set_IVT(entry : INTEGER); { entry corresponds with the
                                     number of the interrupt line
                                     IRQ to enter in IVT}

```

```

VAR
    offset, segment, first_word, second_word : INTEGER;
BEGIN
    offset := OFS(Interrupt_5_Service_Routine) + 7;
    segment := Cseg;
    first_word := (entry + 8) * 4;
    second_word := first_word + 2;
    MEMW[$0000:first_word] := offset;
    MEMW[$0000:second_word] := segment;
END;

```

```
{*****}
```

```
PROCEDURE SAMPLER;
```

```

var
    chtm, I, Time, hours, mins, secs, Starthours, Startmins, Startsecs, hundredths, StartTime, NewTime, LastTime :INTEGER;

```

```
Alldone : boolean;
```

```
BEGIN
```

```

    ClrScr;
    PUTS(5,1,'Interrupt controlled Sampling ');
    Count := 0;
    FileName := 'C:\CELLMON\SETUP.DAT';
    ASSIGN (InFile,FileName);
    RESET (InFile);
    MaxFiles := FileSize(InFile);
    WHILE NOT EOF (InFile) DO
    BEGIN
        Count := Count + 1;
        READ (InFile,LoopData);
        LoopSet[Count] := LoopData;
    END;
    CLOSE(Infile);
    Time := SampleTime;
    IF KeyPressed THEN READ(kbd,ch);
    done := false;
    alldone := false;

```

```
REPEAT
```

```

    clrscr;
    Yposition := 5;
    sampleno := 0;
    CLRSCR;
    PUTS (1,1,'Loop      Loop Name          A/D      Offset      Scaled      Scaling ');
    PUTS (1,2,' No          Reading      Factor      Reading      Factor ');
    PUTS(15,25,'(S) Re-start Sampling ,(E) End Sampling and Data Collection');

```

```
DISPLAYCHANNELS;
```

```
with v_res DO
```

```

    begin
        AX:=$2C00;
        MSDOS (v_res);
        Starthours := hi(CX);
        Startmins := LO(CX);
        Startsecs := HI(DX);
    end;

```

```

    StartTime := (Starthours * 3600) + (Startmins * 60) + Startsecs;
    LastTime := 0;

```

```

REPEAT
  REPEAT
    with v_res DO
      begin
        AX := $2c00;
        MSDOS (v_res);
        hours := hi(CX);
        Mins := LO(CX);
        secs := HI(DX);
      end;
      newtime := ((hours-Starthours)*3600)+((mins-Startmins)*60)+(secs-Startsecs);
      ElapsedTime := TRUNC(newtime/60);
      GOTOXY(1,20);
      WRITE('TIME ',HOURS,':',MINS,':',SECS,' ');
      GOTOXY(30,20);
      WRITE('Elapsed Time-----> ',ElapsedTime,' Minutes ');
      IF newtime >= (LastTime + frequ) THEN
        BEGIN
          Sampleno := sampleno + 1;
          GOTOXY(1,22);
          WRITE('Sample Number --->',Sampleno,' ');
          GOTOXY(30,22);
          WRITE('Sample Frequency ---> ',frequ:7:1,' ');
          DISPLAYCHANNELS;
          IF StoreData = TRUE THEN
            BEGIN
              LoopReading[1] := ElapsedTime;
              FOR Count := 1 TO (MaxFiles + 1) DO
                BEGIN
                  WRITE(DataOutFile,LoopReading[Count]:10:2);
                  END;
                  WRITELN(DataOutFile,'');
                END;
                LastTime := NewTime;
                Yposition := 5;
              END; {IF}
            UNTIL keypressed;
            read(kbd, ch);
            ch := UPCASE(ch);
            if (ch = 'S') OR (ch = 'E') then done := true
            else done := false;
            UNTIL done;
            if ch = 'E' then alldone := true;
          UNTIL alldone;
          IF StoreData = TRUE THEN
            BEGIN
              CLOSE(DataOutFile);
            END;
          END;

```

{*****}

PROCEDURE CalibrateLoop;

```

VAR
  LNo, Count, EditLoop, MaxFiles, Sample, Yposition: INTEGER;
  LName, displaystring : STRING[20];
  LUnits : STRING[5];
  LScale, LReading, LOffset, SScale, SReading, SOffset : REAL;
  ch1, ch2 : CHAR;

```

```

BEGIN
  CLRSCR;
  PUTS(13,1,' LOOP CALIBRATION ROUTINE ');
  NOISEFILTER;
  PUTS(1,3,'Loop No          Name          Units          Scale Factor ');
  Count := 0;
  Yposition := 5;
  FileName := 'C:\CELLMON\SETUP.DAT';
  ASSIGN (InFile,FileName);
  RESET (InFile);
  MaxFiles := FileSize(InFile);
  WHILE NOT EOF (InFile) DO
    BEGIN
      Count := Count + 1;
      READ (InFile,LoopData);
      LoopSet[Count] := LoopData;
      WITH Loopdata DO
        BEGIN
          STR(No,displaystring);
          PUTS(4,Yposition,displaystring);

```

```

        PUTS(15,Yposition,Name);
        PUTS(48,Yposition,Units);
        STR(Scale:6:2,displaystring);
        PUTS(60,Yposition,displaystring);
        Yposition := Yposition + 1;
    END;
END;
CLOSE(Infile);
PUTS(1,25,'ENTER LOOP NUMBER TO BE CALIBRATED.....');
REPEAT
    GOTOXY(41,25);
    write(' ');
    GOTOXY(41,25);
    READ(EditLoop);
UNTIL EditLoop IN [1..MaxFiles];
GOTOXY(1,25);
WRITE('Loop Number ',EditLoop,' to be calibrated (Y/N)');
GOTOXY(43,25);
REPEAT
    READ(kbd,ch);
    ch := UPCASE(ch);
UNTIL ch IN ['Y','N'];
IF ch = 'Y' THEN
    BEGIN
        LoopData := LoopSet[EditLoop];
        LScale := LoopData.Scale;
        LOffset := LoopData.Offsets;
        SScale := LScale;
        SOffset := LOffset;
        Done := False;
        REPEAT
            CLRSCR;
            PUTS (1,1,'Loop      Loop Name          A/D      Offset      Scaled      Scaling');
            PUTS (1,2,' No          Reading      Factor      Reading      Factor');
            REPEAT
                GOTOXY(1,25);
                WRITE('(1) Scaled Reading, (2) Scaling Factor, (3) Offset Factor (4) Exit');
                GOTOXY(79,80);
                GotoXY(2,6);
                Write (EditLoop);
                Sample := ADSAMPLE (LoopData.ChannelNo);
                PUTS(8,6,LoopData.Name);
                GotoXY(35,6);
                Write (Sample,' ');
                GOTOXY(46,6);
                WRITE (SOffset:7:2);
                LReading := (Sample-SOffset)/SScale;
                GOTOXY(56,6);
                WRITE (LReading:7:2);
                GOTOXY(67,6);
                WRITE (SScale:7:2);
                GOTOXY(1,8);
                WRITE('Current settings on file for loop ',EditLoop,'-->');
                GOTOXY(46,8);
                WRITE (LOffset:7:2);
                GOTOXY(67,8);
                WRITE (LScale:7:2);
            UNTIL KeyPressed;
        REPEAT
            READ(kbd,ch);
        UNTIL ch IN ['1','2','3','4'];
        CASE ch OF
            '1' : BEGIN
                PUTS(1,25,'New Scaled Reading (Scaling Factor will be calculated).....');
                REPEAT
                    GOTOXY(61,25);
                    write(' ');
                    GOTOXY(61,25);
                    READ(SReading);
                UNTIL SReading > 0;
                SScale := (Sample - SOffset)/SReading;
                END; {1}
            '2' : BEGIN
                PUTS(1,25,'New Scaling Factor.....');
                REPEAT
                    GOTOXY(61,25);
                    write(' ');
                    GOTOXY(61,25);
                    READ(SScale);
                UNTIL SScale > 0;
                END; {2}
        END;
    END;

```

```

'3' : BEGIN
  PUTS(1,25,'New Loop Offset Factor.....');
  REPEAT
    GOTOXY(61,25);
    write(' ');
    GOTOXY(61,25);
    READ(Soffset);
  UNTIL Soffset > -1;
  END; {3}
'4' : BEGIN
  PUTS(1,25,'(1) Update Loop parameters, (2) Leave Loop Parameters at current settings ');
  REPEAT
    READ(kbd,ch1);
  UNTIL ch1 IN ['1','2'];
  IF ch1 = '1' THEN
    BEGIN
      LoopData.Scale := SScale;
      LoopData.Offset := SOffset;
      ASSIGN(OutFile,FileName);
      RESET(OutFile);
      SEEK(OutFile,EditLoop-1);
      WRITE (OutFile, LoopData);
      Close (OutFile);
    END;
    Done := True;
  END; {4}
  END; {case}
  UNTIL Done = True;
END; {IF}
END; {CalibrateLoop}
{*****}
PROCEDURE EditLoopParams;
VAR
  LNo, LChannelNo, Count, EditLoop, MaxFiles : INTEGER;
  LName : STRING[20];
  LUnits : STRING[5];
  LScale, LReading, LOffset : REAL;
BEGIN
  PUTS(13,1,' LOOP EDITING ROUTINE ');
  Count := 0;
  FileName := 'C:\CELLMON\SETUP.DAT';
  ASSIGN (Infile,FileName);
  RESET (InFile);
  MaxFiles := FileSize(InFile);
  WHILE NOT EOF (InFile) DO
    BEGIN
      Count := Count + 1;
      READ (InFile,LoopData);
      LoopSet[Count] := LoopData;
    END;
  CLOSE(InFile);
  PUTS(1,25,'ENTER LOOP NUMBER TO BE EDITED.....');
  REPEAT
    GOTOXY(41,25);
    write(' ');
    GOTOXY(41,25);
    READ(EditLoop);
  UNTIL EditLoop IN [1..MaxFiles];
  GOTOXY(1,25);
  WRITE('Loop Number ',EditLoop,' to be edited (Y/N) ');
  GOTOXY(43,25);
  REPEAT
    READ(kbd,ch);
    ch := UPCASE(ch);
  UNTIL ch IN ['Y','N'];
  IF ch = 'Y' THEN
    BEGIN
      clrscr;
      Done := False;
      WHILE NOT Done DO
        BEGIN
          LName := '';
          LUnits := '';
          LScale := 0;
          LOffset := -1;
          LoopData := LoopSet[EditLoop];
          LChannelNo := -1;
          GOTOXY(1,3);
          WRITELN('Editing Loop No. = ',EditLoop);

```

```

GOTOXY(1,5);
WRITELN('CURRENT LOOP PARAMETERS :');
GOTOXY(1,7);
WITH LoopData DO
  BEGIN
    WRITE ('      Loop Name.....');
    WRITELN (Name);
    WRITE ('      Loop Units.....');
    WRITELN (Units);
    WRITE ('      Loop Scale Factor.....');
    WRITELN (Scale:6:2);
    WRITE ('      Loop Offset Factor.....');
    WRITELN (Offset:6:2);
    WRITE ('      Loop Channel Number.....');
    WRITELN (ChannelNo);
    WRITELN;
  END;
GOTOXY(1,14);
WRITELN('NEW LOOP PARAMETERS :');
GOTOXY(1,16);
WITH LoopData DO
  BEGIN
    WRITE ('      Loop Name.....');
    WRITELN (Name);
    WRITE ('      Loop Units.....');
    WRITELN (Units);
    WRITE ('      Loop Scale Factor.....');
    WRITELN (Scale:6:2);
    WRITE ('      Loop Offset Factor.....');
    WRITELN (Offset:6:2);
    WRITE ('      Loop Channel Number.....');
    WRITELN (ChannelNo);
    WRITELN;
  END;
GOTOXY(31,16);
READLN(LName);
IF LName <> '' THEN
  BEGIN
    LoopData.Name := LName;
    GOTOXY(31,16);
    WRITELN (LName,'          ');
  END;
GOTOXY(31,17);
READLN(LUnits);
IF LUnits <> '' THEN
  BEGIN
    LoopData.Units := LUnits;
    GOTOXY(31,17);
    WRITELN (LUnits,'          ');
  END;
GOTOXY(31,18);
READLN(Lscale);
IF Lscale <> 0 THEN
  BEGIN
    LoopData.Scale := Lscale;
    GOTOXY (31,18);
    WRITELN (Lscale:6:2,'          ');
  END;
GOTOXY(31,19);
READLN(Loffset);
IF Loffset > -1 THEN
  BEGIN
    LoopData.Offset := Loffset;
    GOTOXY (31,19);
    WRITELN (Loffset:6:2,'          ');
  END;
GOTOXY(31,20);
READLN(LChannelNo);
IF LChannelNo > -1 THEN
  BEGIN
    LoopData.ChannelNo := LChannelNo;
    GOTOXY (31,20);
    WRITELN (LChannelNo,'          ');
  END;
END;

```



```

GOTOXY(1,25);
WRITE(' (R) Renter Loop parameters, (A) Accept and save new parameters ');
GOTOXY(79,80);
REPEAT
  READ(kbd,ch);
  ch := UPCASE(ch);
  UNTIL ch IN ['R','A'];
  IF ch = 'A' THEN Done := True;
END; {WHILE NOT}
ASSIGN(OutFile,FileName);
RESET(OutFile);
SEEK(OutFile,EditLoop-1);
WRITE (OutFile, LoopData);
Close (OutFile);
END; {IF}
END; {EditLoop}

```

```
{*****}
```

```
PROCEDURE DeleteLoop;
```

```
VAR
```

```
Count, DelLoop, MaxFiles : INTEGER;
```

```
BEGIN
```

```
PUTS(13,1,' LOOP DELETION ROUTINE ');
```

```
Count := 0;
```

```
FileName := 'C:\CELLMON\SETUP.DAT';
```

```
ASSIGN (InFile,FileName);
```

```
RESET (InFile);
```

```
MaxFiles := FileSize(InFile);
```

```
WHILE NOT EOF (InFile) DO
```

```
BEGIN
```

```
Count := Count + 1;
```

```
READ (InFile,LoopData);
```

```
LoopSet[Count] := LoopData;
```

```
END;
```

```
CLOSE(InFile);
```

```
PUTS(1,25,'ENTER LOOP NUMBER TO BE DELETED.....');
```

```
REPEAT
```

```
GOTOXY(41,25);
```

```
WRITE(' ');
```

```
GOTOXY(41,25);
```

```
READ(DelLoop);
```

```
UNTIL DelLoop IN [1..MaxFiles];
```

```
GOTOXY(1,25);
```

```
WRITE('Loop Number ',DelLoop,' to be deleted (Y/N)');
```

```
GOTOXY(43,25);
```

```
REPEAT
```

```
READ(ch);
```

```
ch := UPCASE(ch);
```

```
UNTIL ch IN ['Y','N'];
```

```
IF ch = 'Y' THEN
```

```
BEGIN
```

```
FOR Count := DelLoop to MaxFiles - 1 DO
```

```
BEGIN
```

```
LoopSet[Count] := LoopSet[Count + 1];
```

```
END; {FOR}
```

```
ASSIGN(OutFile,FileName);
```

```
REWRITE(OutFile);
```

```
FOR Count := 1 to MaxFiles - 1 DO
```

```
BEGIN
```

```
LoopData := LoopSet[Count];
```

```
LoopData.No := Count;
```

```
LoopSet[Count] := LoopData;
```

```
WRITE (OutFile,LoopSet[Count]);
```

```
END; {FOR}
```

```
CLOSE(OutFile);
```

```
END; {IF}
```

```
END; {DeleteLoop}
```

```
{*****}
```

```
PROCEDURE AddLoop;
```

```

VAR
  LNo, LChannelNo, Count : INTEGER;
  LName : STRING[20];
  LUnits : STRING[5];
  LScale, LOffset : REAL;
BEGIN
  Done := FALSE;
  FileName := 'C:\CELLMON\SETUP.DAT';
  ASSIGN(Outfile,FileName);
  RESET(Outfile);
  WHILE NOT Done DO
  BEGIN
    clrscr;
    PUTS(13,1,'L O O P   A D D I T I O N   R O U T I N E');
    WRITELN;
    WRITELN;
    SEEK(OutFile,FileSize(OutFile));
    Count := FileSize(OutFile) + 1;
    WRITELN('Adding Loop No.....',Count);
    WRITELN;
    LNo := Count;
    LoopData.No := LNo;
    LScale := 0;
    LOffset := -1;
    WRITE('Loop Name.....[                ]');
    GOTOXY(39,5);
    READLN(LName);
    LoopData.Name := LName;
    WRITE('Loop Units.....[                ]');
    GOTOXY(39,6);
    READLN (LUnits);
    LoopData.Units := LUnits;
    WRITE('Loop Scale Factor.....');
    REPEAT
      GOTOXY(39,7);
      WRITE('                ');
      GOTOXY(39,7);
      READLN(LScale);
    UNTIL LScale > 0;
    WRITE('Loop Offset Factor.....');
    REPEAT
      GOTOXY(39,8);
      WRITE('                ');
      GOTOXY(39,8);
      READLN(LOffset);
    UNTIL (LOffset >=0) AND (LOffset < 4096) ;
    WRITE('Loop Channel Number.....');
    REPEAT
      GOTOXY(39,9);
      WRITE('                ');
      GOTOXY(39,9);
      READLN(LChannelNo);
    UNTIL LChannelNo IN [0..15];
    LoopData.Scale := LScale;
    LoopData.Offset := LOffset;
    LoopData.ChannelNo := LChannelNo;
    WRITE (OutFile, LoopData);
    PUTS(3,25,'(A) Add New Loop, (Q) Quit!');
    REPEAT
      READ(kbd,ch);
      ch := UPCASE(ch);
      UNTIL ch IN ['A','Q'];
      CASE ch OF
        'A' : Done := False;
        'Q' : Done := True;
      END; {case}
    END; {WHILE NOT}
    Close (OutFile);
    clrscr;
  END; {AddLoop}
  {*****}
PROCEDURE LoopSetup;
  TYPE
    Selection = (A,E,D,Q);
  VAR
    Xposition, Yposition : INTEGER;
    No_str : STRING[2];
    Scale_str : STRING[6];

```

```

{*****          READ  EXISTING  LOOP  SETUP          *****)
BEGIN
  REPEAT
    CLRSCR;
    PUTS(13,1,'CURRENT LOOP CONFIGURATION');
    PUTS(1,3,'Loop No.          Name          Units          Scale Factor');
    Yposition := 5;
    FileName := 'C:\CELLMON\SETUP.DAT';
    ASSIGN (InFile,FileName);
    RESET (InFile);
    WHILE NOT EOF (InFile) DO
      BEGIN
        READ (InFile,Loopdata) ;
        WITH Loopdata DO
          BEGIN
            STR(No,No_str);
            PUTS(4,Yposition,No_str);
            PUTS(15,Yposition,Name);
            PUTS(48,Yposition,Units);
            STR(Scale:6:2,Scale_str);
            PUTS(60,Yposition,Scale_str);
            Yposition := Yposition + 1;
          END;
        END;
      CLOSE(Infile);
    {***** SELECT OPTION REQUIRED AND EXECUTE RELEVANT PROCEDURE *****)
    PUTS(1,25,'(A) Add New Loop, (E) Edit Existing Loop, (D) Delete Loop, (Q) Quit');
    REPEAT
      READ(kbd,ch);
      Ch := UPCASE(ch);
      UNTIL Ch IN ['A','E','D','Q'];
      CASE Ch OF
        'A' : AddLoop;
        'E' : EditLoopParams;
        'D' : DeleteLoop;
      END; {case}
    UNTIL Ch = 'Q';
    CLRSCR;
  END;
{*****}
(          M A I N    P R O G R A M          )
BEGIN
  PORT[$703] := $92;      {Initialization of A/D PPI}
  { Get_cl;}
  dsave := Dseg;
  REPEAT
    CLRSCR;
    IF KeyPressed THEN READ(kbd,ch);
    PUTS(20,1,'ANALOGUE TO DIGITAL MONITERING PACKAGE');
    PUTS(20,3,'CELLMON Version 1.0');
    PUTS(15,7,'1 = Online Monitoring of Loop Inputs');
    PUTS(15,9,'2 = Interrupt controlled sampling ');
    PUTS(15,11,'3 = Edit Loops');
    PUTS(15,13,'4 = Calibrate Loops');
    PUTS(15,15,'5 = Quit');
    PUTS(15,25,'Your choice = ??');
    REPEAT
      READ(kbd,ch);
    UNTIL ch IN ['1'..'5'];
    CASE ch OF
      '1' : Print_channels;
      '2' : Sampler;
      '3' : LoopSetup;
      '4' : CalibrateLoop;
    END; {case}
  UNTIL ch = '5';
  CLRSCR;
END.

```

APPENDIX 5

EXPERIMENTAL RESULTS.

A-5.1 Experimental Run CK016.

TABLE A5.1						
COOKING CONDITIONS AND RESULTS						
COOK NUMBER	CK016		MAXIMUM TEMPERATURE	145°C		
WOOD LOAD	7.0 Kg		LIQUOR LOAD	46 litre		
WOOD MOISTURE	34 %		TOTAL COOK TIME	6h15		
Liquor Sample Analysis			Pulp Sample Analysis			
Elapsed Time	Total SO ₂	Combined SO ₂	Elapsed Time	Pulp Viscosity	K Number	S ₁₈
LOAD	7.36 %	1.26 %	5h00	124.7	4.90	5.78
0h00	6.73 %	1.24 %	5h15	91.7	4.08	5.86
1h30	6.41 %	1.16 %	5h30	73.3	3.62	5.44
2h00	6.34 %	1.13 %	5h45	63.0	2.98	5.17
2h35	6.19 %	1.05 %	6h00	54.0	2.77	5.25
3h30	5.92 %	0.82 %	6h15	43.9	2.31	5.13
4h30	5.40%	0.46 %				

TABLE A5.2**COOK DATA FOR CK016**

TIME (mins)	TEMPERATURE °C	PRESSURE (kPa)	MEASURED pH	TIME (mins)	TEMPERATURE °C	PRESSURE (kPa)	MEASURED pH
20	50.9	659	2.09	210	140.6	1126	2.94
30	62.7	706	2.09	220	143.1	1119	2.96
40	74.0	845	2.13	230	144.5	1105	2.98
50	85.4	1026	2.21	240	145.3	1112	2.97
60	92.0	1100	2.31	250	144.5	1097	2.96
70	98.0	1110	2.40	260	144.7	1099	2.95
80	103.6	1096	2.47	270	144.7	1107	2.94
90	108.6	1101	2.54	280	144.7	1095	2.92
100	113.3	928	2.61	290	144.7	1109	2.91
110	116.7	975	2.66	300	144.4	1109	2.89
120	119.2	1020	2.70	210	144.5	1113	2.87
130	121.9	1066	2.73	320	144.7	1122	2.85
140	124.4	1115	2.76	330	144.7	1098	2.82
150	127.0	1100	2.79	340	145.0	1099	2.79
160	129.3	1008	2.82	350	144.8	1112	2.75
170	132.0	1055	2.85	360	145.1	1120	2.68
180	134.0	1100	2.87	370	144.9	1075	2.55
190	136.8	1109	2.90	375	145.1	937	2.39
200	138.5	1110	2.92				

A-5.2 Experimental Run CK017.

TABLE A5.3						
COOKING CONDITIONS AND RESULTS						
COOK NUMBER		CK017		MAXIMUM TEMPERATURE		130°C
WOOD LOAD		7.0 Kg		LIQUOR LOAD		46 litre
WOOD MOISTURE		30 %		TOTAL COOK TIME		8h15
Liquor Sample Analysis			Pulp Sample Analysis			
Elapsed Time	Total SO ₂	Combined SO ₂	Elapsed Time	Pulp Viscosity	K Number	S18
LOAD	8.70 %	1.24 %	7h00	150	5.47	6.51
0h00	7.71 %	1.18 %	7h15	120	5.11	6.32
1h30	7.39 %	1.09 %	7h30	105	4.40	6.25
2h00	7.31 %	1.01 %	7h45	96	4.05	6.04
3h30	7.10 %	0.81 %	8h00	93	3.69	6.14
4h30	6.75 %	0.51 %	8h15	81	3.37	5.70
6h30	6.42%	0.30 %				

TABLE A5.4**COOK DATA FOR CK017**

TIME (mins)	TEMPERATURE °C	PRESSURE (kPa)	MEASURED pH	TIME (mins)	TEMPERATURE °C	PRESSURE (kPa)	MEASURED pH
0	51	646	1.96	260	130.4	1104	2.70
10	58.6	698	2.00	270	130.9	1103	2.70
20	66.8	782	2.04	280	130.1	1082	2.69
30	74.2	889	2.07	290	130.9	1087	2.68
40	81.4	1011	2.12	300	130.4	1090	2.68
50	87.5	1120	2.17	310	130.8	1089	2.67
60	93.9	1104	2.24	320	130.1	1092	2.67
70	99.6	1148	2.31	330	130.7	1099	2.66
80	104.5	1112	2.38	340	130.2	1095	2.66
90	109.8	1118	2.44	350	130.2	1102	2.65
100	113.6	969	2.51	360	130.5	1101	2.65
110	116.4	1020	2.56	370	130.5	1103	2.64
120	119.1	1056	2.60	380	130.3	1110	2.63
130	121.9	1106	2.63	390	130.2	1089	2.63
140	124.7	1116	2.67	400	130.4	1091	2.62
150	127.5	1108	2.70	410	130.6	1095	2.62
160	128.3	1101	2.72	420	130.3	1100	2.61
170	128.3	1094	2.73	430	129.7	1087	2.59
180	128.9	1107	2.73	440	130.9	1102	2.59
190	129.2	1117	2.74	450	130.3	1112	2.59
200	130.4	1127	2.74	460	130.6	1105	2.58
210	129.9	1110	2.74	470	129.9	1121	2.56
220	130.1	1109	2.73	480	130.3	1152	2.56
230	130.2	1113	2.72	490	130.7	1129	2.56
240	130.6	1105	2.72	495	130.0	1108	2.54
250	130.0	1106	2.71				

A-5.3 Experimental Run CK018.

TABLE A5.5						
COOKING CONDITIONS AND RESULTS						
COOK NUMBER		CK018		MAXIMUM TEMPERATURE		140°C
WOOD LOAD		7.0 Kg		LIQUOR LOAD		46 litre
WOOD MOISTURE		30 %		TOTAL COOK TIME		6h45
Liquor Sample Analysis			Pulp Sample Analysis			
Elapsed Time	Total SO ₂	Combined SO ₂	Elapsed Time	Pulp Viscosity	K Number	S18
LOAD	7.92 %	1.26 %	5h30	88	4.51	5.95
0h00	7.03 %	1.14 %	5h45	79	4.12	5.91
1h30	6.64 %	1.04 %	6h00	68	3.44	5.69
2h00	6.63 %	1.01 %	6h15	61	3.02	5.58
2h30	6.60 %	0.96 %	6h30	53	2.95	5.38
3h30	6.16 %	0.68 %	6h45	48	2.56	5.36
4h30	5.72 %	0.34 %				
5h30	5.24 %	0.00 %				

TABLE A5.6**COOK DATA FOR CK018**

TIME (mins)	TEMPERATURE °C	PRESSURE (kPa)	MEASURED pH	TIME (mins)	TEMPERATURE °C	PRESSURE (kPa)	MEASURED pH
0	51.7	686	2.01	210	140.1	1123	2.90
10	58.3	713	2.06	220	139.2	1106	2.89
20	66.3	779	2.09	230	139.5	1113	2.88
30	74.6	860	2.12	240	139.2	1120	2.86
40	81.6	954	2.18	250	139.5	1110	2.85
50	88.4	1043	2.24	260	139.1	1106	2.84
60	94.6	1101	2.31	270	140.0	1116	2.83
70	100.6	1129	2.37	280	139.7	1102	2.82
80	105.7	1148	2.44	290	139.7	1114	2.81
90	111.0	945	2.50	300	139.6	1119	2.80
100	114.1	1004	2.56	310	139.3	1126	2.78
110	116.6	1047	2.61	320	139.6	1128	2.76
120	119.6	1086	2.65	330	139.7	1126	2.70
130	122.3	1098	2.69	340	139.6	1118	2.68
140	124.7	1119	2.72	350	139.8	1118	2.67
150	127.3	1111	2.76	360	139.6	1116	2.65
160	129.4	1102	2.79	370	140.1	1111	2.63
170	131.3	1112	2.80	380	139.8	1117	2.62
180	133.7	1109	2.84	390	139.8	1140	2.59
190	135.2	1116	2.86	400	140.1	1120	2.56
200	137.6	1097	2.88				

A-5.4 Experimental Run CK019.

TABLE A5.7						
COOKING CONDITIONS AND RESULTS						
COOK NUMBER	CK019		MAXIMUM TEMPERATURE	150°c		
WOOD LOAD	7.0 Kg		LIQUOR LOAD	46 litre		
WOOD MOISTURE	32 %		TOTAL COOK TIME	5h15		
Liquor Sample Analysis			Pulp Sample Analysis			
Elapsed Time	Total SO ₂	Combined SO ₂	Elapsed Time	Pulp Viscosity	K Number	S18
LOAD	7.80 %	1.30 %	4h15	128	6.53	6.90
0h00	6.79 %	1.16 %	4h29	94	4.76	6.66
1h30	6.51 %	1.08 %	4h44	69	4.05	6.15
2h00	6.47 %	1.07 %	4h59	55	2.98	5.83
2h30	6.41 %	0.99 %	5h14	39	2.63	5.50
3h30	6.16 %	0.74 %	5h28	24	2.09	5.38

TABLE A5.8**COOK DATA FOR CK019**

TIME (mins)	TEMPERATURE °C	PRESSURE (kPa)	MEASURED pH	TIME (mins)	TEMPERATURE °C	PRESSURE (kPa)	MEASURED pH
0	52.4	722	2.02	170	133.3	1119	2.85
10	58.8	743	2.11	180	136.3	1122	2.89
20	66.9	848	2.13	190	139.7	1093	2.93
30	75.1	984	2.16	200	143.4	1125	2.97
40	82.0	1098	2.21	210	146.6	1135	3.02
50	88.4	1140	2.27	220	148.6	1136	3.04
60	94.6	1123	2.34	230	150.3	1131	3.05
70	100.0	1130	2.41	240	150.1	1104	3.05
80	105.3	1095	2.47	250	150.5	1110	3.04
90	110.0	1127	2.54	260	150.0	1100	3.01
100	114.1	922	2.60	270	149.9	1111	2.99
110	116.9	963	2.65	280	149.6	1106	2.96
120	119.3	1004	2.69	290	150.0	1107	2.92
130	122.1	1050	2.72	300	150.1	1117	2.86
140	125.0	1106	2.76	310	150.4	1109	2.72
150	127.5	1127	2.79	320	150.3	1110	2.35
160	130.1	1141	2.82	328	150.1	1101	2.10

A-5.5 Experimental Run CK020.

TABLE A5.9						
COOKING CONDITIONS AND RESULTS						
COOK NUMBER	CK020		MAXIMUM TEMPERATURE	145°C		
WOOD LOAD	7.0 Kg		LIQUOR LOAD	46 litre		
WOOD MOISTURE	36 %		TOTAL COOK TIME	6h00		
Liquor Sample Analysis			Pulp Sample Analysis			
Elapsed Time	Total SO ₂	Combined SO ₂	Elapsed Time	Pulp Viscosity	K Number	S18
LOAD	8.67 %	1.26 %	4h45	111	5.15	6.39
0h00	7.50 %	1.14 %	5h00	76	4.08	6.05
1h30	7.20 %	1.08 %	5h15	61	3.40	5.62
2h00	7.19 %	1.04 %	5h30	50	3.05	5.96
2h30	7.14 %	1.00 %	5h45	41	2.66	5.37
3h30	6.70 %	0.72 %	6h00	30	2.31	5.48
4h45	5.83 %	0.31 %				

TABLE A5.10
COOK DATA FOR CK020

TIME (mins)	TEMPERATURE °C	PRESSURE (kPa)	MEASURED pH	TIME (mins)	TEMPERATURE °C	PRESSURE (kPa)	MEASURED pH
0	51.3	661	2.05	190	138.0	1128	2.84
10	58.4	721	2.07	200	140.4	1136	2.87
20	66.5	832	2.08	210	142.5	1109	2.90
30	74.0	982	2.11	220	144.1	1111	2.92
40	81.3	1117	2.15	230	144.9	1103	2.93
50	88.0	1117	2.21	240	144.9	1101	2.92
60	94.0	1112	2.27	250	144.9	1104	2.91
70	99.7	1100	2.34	260	144.9	1105	2.90
80	104.7	1118	2.41	270	144.9	1107	2.88
90	109.5	966	2.47	280	144.9	1109	2.87
100	113.7	946	2.53	290	144.9	1109	2.85
110	116.6	995	2.58	300	144.9	1111	2.83
120	119.2	1045	2.61	310	144.9	1107	2.81
130	121.8	1087	2.65	320	144.9	1110	2.77
140	124.6	1142	2.69	330	144.9	1114	2.71
150	127.3	1096	2.72	340	144.9	1107	2.60
160	130.1	1113	2.75	350	144.9	1128	2.37
170	132.9	1123	2.78	359	144.0	925	2.13
180	135.4	1104	2.82				

A-5.6 Experimental Run CK021.

<p style="text-align: center;">TABLE A5.11</p> <p style="text-align: center;">COOKING CONDITIONS AND RESULTS</p>						
COOK NUMBER	CK021		MAXIMUM TEMPERATURE	140°C		
WOOD LOAD	9.5 Kg		LIQUOR LOAD	44 litre		
WOOD MOISTURE	51 %		TOTAL COOK TIME	6h45		
Liquor Sample Analysis			Pulp Sample Analysis			
Elapsed Time	Total SO ₂	Combined SO ₂	Elapsed Time	Pulp Viscosity	K Number	S18
LOAD	9.07 %	1.27 %	5h30	111	5.11	5.96
0h00	7.73 %	1.10 %	5h45	72	3.40	5.36
1h30	7.14 %	0.99 %	6h00	60	3.02	5.30
2h00	7.10 %	0.95 %	6h15	48	2.91	5.35
2h30	7.05 %	0.90 %	6h30	43	2.63	5.30
3h30	6.67 %	0.64 %	6h45	40	2.48	4.80
4h30	5.25 %	0.34 %				

TABLE A5.12**COOK DATA FOR CK021**

TIME (mins)	TEMPERATURE °C	PRESSURE (kPa)	MEASURED pH	TIME (mins)	TEMPERATURE °C	PRESSURE (kPa)	MEASURED pH
0	52.8	706	2.07	210	139.7	1115	2.86
10	59.2	752	2.10	220	139.7	1093	2.86
20	67.5	888	2.10	230	139.7	1101	2.85
30	75.4	1082	2.12	240	139.7	1101	2.84
40	82.2	1109	2.17	250	139.7	1109	2.83
50	88.6	1097	2.23	260	139.7	1124	2.82
60	95.0	1098	2.29	270	139.7	1111	2.81
70	100.1	1128	2.36	280	139.7	1122	2.80
80	105.3	1109	2.42	290	139.7	1116	2.79
90	110.2	948	2.49	300	139.7	1129	2.78
100	113.9	939	2.54	310	139.7	1112	2.77
110	116.7	985	2.58	320	139.7	1117	2.76
120	119.2	1030	2.62	330	139.7	1125	2.74
130	121.9	1084	2.66	340	139.7	1126	2.72
140	124.9	1131	2.69	350	139.7	1109	2.71
150	127.5	1116	2.73	360	139.7	1124	2.68
160	129.4	1098	2.76	370	139.7	1127	2.65
170	131.3	1111	2.78	380	139.7	1141	2.62
180	133.3	1132	2.80	390	139.7	1127	2.58
190	135.4	1101	2.82	400	139.7	1116	2.52
200	137.7	1117	2.84	405	139.7	1004	2.49

A-5.7 Experimental Run CK022.

TABLE A5.13						
COOKING CONDITIONS AND RESULTS						
COOK NUMBER	CK022		MAXIMUM TEMPERATURE	150°C		
WOOD LOAD	7.0 Kg		LIQUOR LOAD	46 litre		
WOOD MOISTURE	36 %		TOTAL COOK TIME	5h30		
Liquor Sample Analysis			Pulp Sample Analysis			
Elapsed Time	Total SO ₂	Combined SO ₂	Elapsed Time	Pulp Viscosity	K Number	S18
LOAD	7.80 %	1.25 %	4h15	104	6.53	6.99
0h00	7.32 %	1.22 %	4h30	90	4.22	6.01
1h30	7.10 %	1.13 %	4h45	72	4.05	5.81
2h00	7.04 %	1.11 %	5h00	64	3.34	5.21
2h30	6.90 %	1.07 %	5h15	50	3.16	5.69
3h30	6.46 %	0.77 %	5h30	20	2.27	5.30
4h30	5.26 %	0.40 %				

TABLE A5.14**COOK DATA FOR CK022**

TIME (mins)	TEMPERATURE °C	PRESSURE (kPa)	MEASURED pH	TIME (mins)	TEMPERATURE °C	PRESSURE (kPa)	MEASURED pH
0	51.3	657	2.11	170	133.3	1122	2.91
10	58.3	751	2.15	180	136.4	1100	2.95
20	66.5	855	2.18	190	139.1	1127	2.99
30	74.2	1003	2.21	200	142.4	1097	3.03
40	81.3	1112	2.26	210	146.0	1135	3.08
50	88.2	1128	2.32	220	148.0	1104	3.13
60	94.2	1113	2.37	230	149.4	1114	3.14
70	99.7	1114	2.43	240	149.5	1113	3.14
80	104.9	1112	2.50	250	149.5	1105	3.12
90	109.9	1065	2.56	260	149.5	1102	3.11
100	114.0	930	2.63	270	149.5	1105	3.09
110	116.6	971	2.68	280	149.5	1103	3.07
120	119.2	1019	2.72	290	149.7	1110	3.03
130	121.9	1065	2.76	300	149.5	1115	2.95
140	124.5	1120	2.79	310	149.8	1101	2.72
150	127.1	1112	2.83	320	150.2	1113	2.27
160	130.2	1132	2.87	330	150.4	1012	2.10

A-5.8 Experimental Run CK023.

<p style="text-align: center;">TABLE A5.15</p> <p style="text-align: center;">COOKING CONDITIONS AND RESULTS</p>						
COOK NUMBER		CK023		MAXIMUM TEMPERATURE		135°C
WOOD LOAD		7.0 Kg		LIQUOR LOAD		46 litre
WOOD MOISTURE		35 %		TOTAL COOK TIME		7h30
Liquor Sample Analysis			Pulp Sample Analysis			
Elapsed Time	Total SO ₂	Combined SO ₂	Elapsed Time	Pulp Viscosity	K Number	S18
LOAD	9.11 %	1.27 %	6h15	82	3.73	6.38
0h00	7.88 %	1.20 %	6h30	70	3.66	6.35
1h30	7.76 %	1.11 %	6h45	61	2.98	6.25
2h00	7.72 %	1.05 %	7h00	66	2.73	6.20
2h30	7.70 %	1.00 %	7h15	55	2.66	6.19
3h30	7.31 %	0.74 %	7h30	46	2.59	5.85
4h30	6.99 %	0.51 %				
5h30	6.68 %	0.30 %				

TABLE A5.16**COOK DATA FOR CK023**

TIME (mins)	TEMPERATURE °C	PRESSURE (kPa)	MEASURED pH	TIME (mins)	TEMPERATURE °C	PRESSURE (kPa)	MEASURED pH
0	51.3	638	2.29	230	135.8	1072	2.90
10	57.8	679	2.28	240	136.1	1076	2.90
20	66.1	796	2.26	250	135.7	1069	2.89
30	73.8	972	2.26	260	135.8	1078	2.88
40	81.3	1104	2.27	270	135.8	1078	2.88
50	88.1	1060	2.31	280	136.1	1068	2.87
60	94.2	1051	2.37	290	135.8	1075	2.86
70	100.1	1092	2.42	300	135.9	1074	2.85
80	105.4	1053	2.48	310	135.8	1078	2.85
90	110.4	1062	2.54	320	135.7	1080	2.84
100	114.3	948	2.60	330	135.9	1088	2.83
110	117.4	995	2.64	340	136.3	1081	2.82
120	119.7	1045	2.68	350	135.9	1078	2.82
130	122.2	1016	2.72	360	135.8	1081	2.80
140	124.8	1040	2.76	370	135.9	1080	2.78
150	127.4	1068	2.80	380	135.8	1084	2.77
160	129.0	1040	2.83	390	135.8	1077	2.76
170	130.3	1068	2.85	400	135.9	1077	2.74
180	131.6	1072	2.86	410	136.3	1074	2.72
190	132.8	1072	2.88	420	135.9	1070	2.69
200	134.2	1082	2.89	430	136.6	1083	2.65
210	136.1	1107	2.90	440	137.4	1145	2.60
220	135.9	1074	2.91	450	136.1	1046	2.51

A-5.9 Experimental Run CK024.

<p style="text-align: center;">TABLE A5.17</p> <p style="text-align: center;">COOKING CONDITIONS AND RESULTS</p>						
COOK NUMBER		CK024		MAXIMUM TEMPERATURE		135°C
WOOD LOAD		7.0 Kg		LIQUOR LOAD		48 litre
WOOD MOISTURE		37 %		TOTAL COOK TIME		7h30
Liquor Sample Analysis			Pulp Sample Analysis			
Elapsed Time	Total SO ₂	Combined SO ₂	Elapsed Time	Pulp Viscosity	K Number	S18
LOAD	8.44 %	1.35 %	6h15	90	4.08	6.41
0h00	7.53 %	1.13 %	6h30	84	3.61	5.46
1h30	7.35 %	1.07 %	6h45	69	3.34	6.05
2h00	7.31 %	1.06 %	7h00	68	3.27	5.66
2h30	7.18 %	0.96 %	7h15	63	2.91	4.94
3h30	6.81 %	0.70 %	7h30	55	2.91	5.69
4h30	6.42 %	0.42 %				
5h30	6.25%	0.26 %				

TABLE A5.18**COOK DATA FOR CK024**

TIME (mins)	TEMPERATURE °C	PRESSURE (kPa)	MEASURED pH	TIME (mins)	TEMPERATURE °C	PRESSURE (kPa)	MEASURED pH
0	52.0	660	2.25	230	135.8	1098	3.00
10	58.4	701	2.27	240	135.6	1109	2.99
20	66.4	805	2.36	250	135.7	1105	2.99
30	74.0	946	2.33	260	135.7	1099	2.97
40	81.0	1094	2.38	270	135.7	1110	2.97
50	87.5	1117	2.41	280	135.7	1090	2.96
60	93.4	1129	2.46	290	135.8	1095	2.96
70	99.1	1111	2.52	300	135.8	1107	2.95
80	104.2	1122	2.57	310	135.6	1100	2.94
90	108.9	1050	2.63	320	135.8	1106	2.93
100	113.1	931	2.68	330	135.8	1100	2.93
110	116.5	990	2.72	340	135.8	1097	2.92
120	119.3	1039	2.77	350	135.8	1108	2.90
130	121.9	1090	2.80	360	135.8	1119	2.89
140	124.5	1121	2.84	370	135.9	1116	2.88
150	127.0	1074	2.88	380	136.2	1127	2.88
160	128.8	1097	2.94	390	135.8	1112	2.86
170	130.1	1099	2.95	400	136.0	1117	2.85
180	131.4	1108	2.97	410	136.1	1099	2.84
190	132.8	1103	2.98	420	136.3	1129	2.82
200	134.1	1119	2.99	430	135.2	1111	2.79
210	135.4	1123	3.00	440	134.9	1146	2.76
220	135.6	1098	3.01	450	134.9	1107	2.74

APPENDIX 6

SAMPLE CALCULATIONS OF CHEMICAL CONCENTRATIONS

<u>SECTION</u>	<u>TITLE</u>
A6.1	CALCULATIONS FOR TIME $t \leq 120$ minutes
A6.2	CALCULATIONS FOR TIME $t > 120$ minutes

A6.1) SAMPLE CALCULATIONS OF CHEMICAL CONCENTRATIONS FOR CK019 – TIME $t \leq 120$ minutes

NOTE :-

These calculations are based on the assumption that during this period [SA-] = 0.

MEASURED DATA

Concentrations measured by the Palmrose method and interpolated between samples

Calculated using Equation 3-9 cf. Section 3.3.1

See calculation of pH correction factor illustrated at $t = 120$ minutes

TIME (Minutes)	TEMPERATURE (Degrees C)	PRESSURE (kPa)	LIQUOR pH
1	52.4	722	2.02
2	52.7	706	2.03
3	53.5	706	2.03
4	54.0	706	2.04
5	55.0	710	2.05
6	55.6	716	2.06
7	56.1	721	2.06
8	57.3	728	2.10
9	57.8	732	2.11
10	58.8	743	2.11
11	59.5	753	2.11
12	60.4	760	2.11
13	61.4	766	2.11
14	62.0	779	2.11
15	63.1	792	2.12
16	63.6	800	2.12
17	64.4	808	2.12
18	65.4	818	2.12
19	66.3	835	2.12
20	66.9	848	2.13
21	67.8	853	2.13
22	68.2	864	2.13
23	69.2	885	2.14
24	69.8	895	2.14
25	71.0	911	2.14
26	72.0	913	2.14
27	72.6	944	2.15
28	73.3	944	2.15
29	73.9	970	2.15
30	75.1	984	2.16
31	75.5	998	2.16
32	76.4	1014	2.17
33	76.5	1030	2.17
34	77.6	1044	2.18
35	78.5	1061	2.18
36	78.9	1079	2.19
37	79.7	1097	2.19
38	80.5	1112	2.20
39	81.4	1133	2.20
40	82.0	1098	2.21
41	82.3	1103	2.21
42	83.4	1104	2.22
43	83.9	1107	2.23
44	84.6	1107	2.23
45	85.6	1115	2.24
46	85.8	1120	2.24
47	86.5	1125	2.25
48	87.2	1127	2.26
49	87.8	1133	2.26
50	88.4	1140	2.27
51	89.2	1114	2.28
52	90.1	1115	2.28
53	90.3	1112	2.29
54	91.1	1111	2.29
55	91.6	1106	2.30
56	92.0	1113	2.31
57	92.7	1108	2.32
58	93.1	1115	2.32
59	94.0	1113	2.33
60	94.6	1123	2.34

COMBINED SO2 mo/l	TOTAL SO2 mo/l
0.1812	1.0608
0.1810	1.0603
0.1809	1.0598
0.1808	1.0593
0.1806	1.0588
0.1805	1.0584
0.1803	1.0579
0.1802	1.0574
0.1801	1.0569
0.1799	1.0564
0.1798	1.0559
0.1796	1.0554
0.1795	1.0550
0.1794	1.0545
0.1792	1.0540
0.1791	1.0535
0.1789	1.0530
0.1788	1.0525
0.1787	1.0520
0.1785	1.0516
0.1784	1.0511
0.1783	1.0506
0.1781	1.0501
0.1780	1.0496
0.1778	1.0491
0.1777	1.0486
0.1776	1.0481
0.1774	1.0477
0.1773	1.0472
0.1771	1.0467
0.1770	1.0462
0.1769	1.0457
0.1767	1.0452
0.1766	1.0447
0.1764	1.0443
0.1763	1.0438
0.1762	1.0433
0.1760	1.0428
0.1759	1.0423
0.1758	1.0418
0.1756	1.0413
0.1755	1.0409
0.1753	1.0404
0.1752	1.0399
0.1751	1.0394
0.1749	1.0389
0.1748	1.0384
0.1746	1.0379
0.1745	1.0374
0.1744	1.0370
0.1742	1.0365
0.1741	1.0360
0.1739	1.0355
0.1738	1.0350
0.1737	1.0345
0.1735	1.0340
0.1734	1.0336
0.1732	1.0331
0.1731	1.0326
0.1730	1.0321

[HSO3-] mol/l
0.3748
0.3744
0.3739
0.3735
0.3730
0.3726
0.3722
0.3718
0.3712
0.3707
0.3703
0.3698
0.3693
0.3689
0.3684
0.3681
0.3676
0.3672
0.3667
0.3663
0.3659
0.3656
0.3651
0.3647
0.3642
0.3638
0.3634
0.3630
0.3627
0.3622
0.3619
0.3615
0.3612
0.3607
0.3603
0.3600
0.3596
0.3595
0.3590
0.3586
0.3582
0.3577
0.3574
0.3569
0.3565
0.3562
0.3558
0.3554
0.3550
0.3546
0.3542
0.3538
0.3535
0.3530
0.3527
0.3524
0.3520
0.3516
0.3512
0.3509

Corrected Liquor pH
1.91
1.92
1.92
1.93
1.94
1.95
1.95
1.99
2.00
2.00
2.00
2.00
2.00
2.01
2.01
2.01
2.01
2.02
2.02
2.02
2.03
2.03
2.03
2.04
2.04
2.04
2.04
2.05
2.05
2.06
2.06
2.07
2.07
2.08
2.08
2.09
2.09
2.10
2.10
2.11
2.12
2.12
2.13
2.13
2.14
2.15
2.15
2.16
2.17
2.17
2.18
2.18
2.19
2.20
2.21
2.21
2.22
2.23

TIME (Minutes)	TEMPERATURE (Degrees C)	PRESSURE (kPa)	LIQUOR pH	COMBINED SO2 mol/l	TOTAL SO2 mol/l	[HSO3-] mol/l	Corrected Liquor pH
61	95.0	1127	2.35	0.1728	1.0316	0.3506	2.24
62	95.3	1131	2.35	0.1727	1.0311	0.3502	2.24
63	95.8	1119	2.36	0.1726	1.0306	0.3499	2.25
64	96.4	1102	2.37	0.1724	1.0302	0.3495	2.26
65	97.4	1109	2.37	0.1723	1.0297	0.3491	2.26
66	98.0	1112	2.38	0.1721	1.0292	0.3488	2.27
67	98.1	1112	2.39	0.1720	1.0287	0.3485	2.28
68	98.6	1119	2.40	0.1719	1.0282	0.3482	2.29
69	99.3	1130	2.40	0.1717	1.0277	0.3478	2.29
70	100.0	1130	2.41	0.1716	1.0272	0.3474	2.30
71	100.6	1105	2.41	0.1714	1.0268	0.3471	2.30
72	101.0	1101	2.42	0.1713	1.0263	0.3468	2.31
73	101.3	1108	2.43	0.1712	1.0258	0.3465	2.32
74	101.9	1111	2.43	0.1710	1.0253	0.3461	2.32
75	102.7	1115	2.44	0.1709	1.0248	0.3458	2.33
76	103.4	1121	2.45	0.1707	1.0243	0.3454	2.34
77	103.8	1125	2.45	0.1706	1.0238	0.3451	2.34
78	104.3	1111	2.46	0.1705	1.0233	0.3448	2.35
79	104.7	1093	2.47	0.1703	1.0229	0.3444	2.36
80	105.3	1095	2.47	0.1702	1.0224	0.3441	2.36
81	105.3	1099	2.48	0.1701	1.0219	0.3438	2.37
82	105.9	1107	2.49	0.1699	1.0214	0.3435	2.38
83	106.5	1116	2.49	0.1698	1.0209	0.3431	2.38
84	107.1	1119	2.50	0.1696	1.0204	0.3428	2.39
85	107.4	1113	2.50	0.1695	1.0199	0.3425	2.39
86	108.3	1112	2.51	0.1694	1.0195	0.3422	2.40
87	108.4	1108	2.52	0.1692	1.0190	0.3419	2.41
88	108.9	1115	2.52	0.1691	1.0185	0.3416	2.41
89	109.6	1121	2.53	0.1689	1.0180	0.3412	2.42
90	110.0	1127	2.54	0.1688	1.0175	0.3409	2.43
91	110.5	940	2.54	0.1687	1.0170	0.3406	2.43
92	110.9	873	2.55	0.1680	1.0174	0.3393	2.44
93	111.4	867	2.56	0.1681	1.0172	0.3394	2.45
94	111.5	877	2.56	0.1682	1.0169	0.3396	2.45
95	112.2	887	2.57	0.1663	1.0167	0.3396	2.46
96	112.4	895	2.57	0.1683	1.0164	0.3397	2.46
97	112.8	904	2.58	0.1684	1.0162	0.3398	2.47
98	113.6	909	2.59	0.1684	1.0159	0.3398	2.48
99	113.5	915	2.59	0.1685	1.0157	0.3399	2.48
100	114.1	922	2.60	0.1685	1.0154	0.3399	2.49
101	114.0	929	2.60	0.1685	1.0152	0.3400	2.49
102	114.7	933	2.61	0.1685	1.0149	0.3399	2.50
103	115.2	935	2.61	0.1685	1.0146	0.3399	2.50
104	115.5	941	2.62	0.1685	1.0143	0.3398	2.51
105	115.7	949	2.62	0.1685	1.0141	0.3398	2.51
106	115.6	948	2.63	0.1684	1.0138	0.3397	2.52
107	116.1	956	2.63	0.1684	1.0135	0.3396	2.52
108	116.0	957	2.64	0.1683	1.0132	0.3395	2.53
109	116.4	964	2.64	0.1683	1.0129	0.3393	2.53
110	116.9	963	2.65	0.1682	1.0126	0.3392	2.54
111	117.2	976	2.65	0.1681	1.0123	0.3390	2.54
112	117.1	978	2.65	0.1680	1.0120	0.3388	2.54
113	117.3	978	2.66	0.1679	1.0117	0.3386	2.55
114	117.8	982	2.66	0.1678	1.0114	0.3383	2.55
115	118.3	986	2.67	0.1677	1.0110	0.3381	2.56
116	118.4	990	2.67	0.1676	1.0107	0.3378	2.56
117	118.7	997	2.67	0.1674	1.0104	0.3375	2.56
118	118.6	999	2.68	0.1673	1.0100	0.3372	2.57
119	119.0	1010	2.68	0.1671	1.0097	0.3369	2.57
120	119.3	1004	2.69	0.1670	1.0094	0.3366	2.58

Taken as [Initial Combined SO2]

Calculated pH value at time t = 120 minutes
obtained using Equation 5-4 cf. Section 5.3.2
 $[H^+] = [HSO_3^-] - 2 * [Initial Combined SO_2]$

The pH correction factor is calculated
as follows

$$pH_{err} = pH_{meas} - pH_{calc}$$

The corrected pH values for the cook
can then be calculated using:-

A6.2) SAMPLE CALCULATIONS OF CHEMICAL CONCENTRATIONS FOR CK019 – TIME t > 120 minutes

NOTE :-

These calculations are based on the following assumptions:-

- 1) Combined SO₂ value at t = 120 minutes used as the [Initial Combined SO₂] – See A6.1.
- 2) The corrected value of [H⁺] is used in all calculations.

Calculated using Equation 5-2
cf. Section 5.3.1

$$[SA^-] = [H^+] + 2 * [Initial Combined SO_2] - [HSO_3^-]$$

See calculation of pH correction factor
illustrated at t = 120 minutes

Calculated using Equation 5-1
cf. Section 5.3.1

Concentrations measured by the
Palmrose method and interpolated
between samples

MEASURED DATA

TIME (Minutes)	TEMPERATURE (Degrees C)	PRESSURE (kPa)	LIQUOR pH	COMBINED SO ₂ mol/l	TOTAL SO ₂ mol/l	[HSO ₃ ⁻] mol/l	Corrected Liquor pH	[SA ⁻] mol/l
121	119.8	1012	2.68	0.1668	1.0090	0.3281	2.57	0.0085
122	119.7	1015	2.69	0.1666	1.0087	0.3338	2.58	0.0028
123	120.2	1024	2.70	0.1664	1.0083	0.3333	2.59	0.0032
124	120.3	1030	2.70	0.1662	1.0080	0.3327	2.59	0.0038
125	121.0	1026	2.70	0.1660	1.0076	0.3278	2.59	0.0087
126	121.1	1037	2.71	0.1658	1.0072	0.3319	2.60	0.0046
127	121.4	1043	2.71	0.1656	1.0069	0.3296	2.60	0.0069
128	121.7	1040	2.71	0.1653	1.0065	0.3277	2.60	0.0087
129	121.7	1054	2.72	0.1651	1.0061	0.3323	2.61	0.0041
130	122.1	1050	2.72	0.1648	1.0057	0.3299	2.61	0.0065
131	122.6	1057	2.72	0.1645	1.0053	0.3259	2.61	0.0105
132	122.3	1059	2.73	0.1643	1.0049	0.3330	2.62	0.0033
133	122.7	1067	2.73	0.1640	1.0046	0.3303	2.62	0.0060
134	123.4	1074	2.74	0.1637	1.0042	0.3305	2.63	0.0058
135	123.7	1083	2.74	0.1634	1.0038	0.3282	2.63	0.0081
136	123.8	1087	2.74	0.1630	1.0033	0.3276	2.63	0.0087
137	124.0	1082	2.74	0.1627	1.0029	0.3257	2.63	0.0106
138	124.2	1089	2.75	0.1624	1.0025	0.3293	2.64	0.0069
139	124.7	1097	2.75	0.1620	1.0021	0.3258	2.64	0.0104
140	125.0	1106	2.76	0.1617	1.0017	0.3290	2.65	0.0072
141	125.0	1104	2.76	0.1613	1.0012	0.3284	2.65	0.0077
142	125.4	1112	2.76	0.1609	1.0008	0.3261	2.65	0.0100
143	125.5	1114	2.77	0.1606	1.0004	0.3303	2.66	0.0059
144	126.0	1119	2.77	0.1602	0.9999	0.3267	2.66	0.0095
145	126.0	1124	2.77	0.1598	0.9995	0.3265	2.66	0.0096
146	126.4	1129	2.77	0.1593	0.9991	0.3239	2.66	0.0123
147	126.6	1136	2.78	0.1589	0.9986	0.3271	2.67	0.0090
148	126.7	1132	2.78	0.1585	0.9981	0.3265	2.67	0.0096
149	127.0	1138	2.78	0.1580	0.9977	0.3243	2.67	0.0118
150	127.5	1127	2.79	0.1576	0.9972	0.3261	2.68	0.0099
151	127.7	1093	2.79	0.1571	0.9968	0.3244	2.68	0.0117
152	127.9	1096	2.80	0.1567	0.9963	0.3280	2.69	0.0080
153	128.1	1100	2.80	0.1562	0.9958	0.3262	2.69	0.0098
154	128.5	1108	2.80	0.1557	0.9953	0.3235	2.69	0.0125
155	128.7	1112	2.80	0.1552	0.9948	0.3225	2.69	0.0135
158	129.2	1115	2.81	0.1547	0.9944	0.3240	2.70	0.0119
157	129.3	1125	2.81	0.1542	0.9939	0.3231	2.70	0.0129
158	130.1	1124	2.82	0.1537	0.9934	0.3225	2.71	0.0134
159	130.2	1130	2.82	0.1531	0.9929	0.3219	2.71	0.0139
160	130.1	1141	2.82	0.1526	0.9924	0.3222	2.71	0.0137
161	130.7	1120	2.82	0.1520	0.9919	0.3179	2.71	0.0180

The format of the calculations shown
above is applied to the end of the cook

APPENDIX 7

DEFINITION OF THE pH VALUE

The following explanation is an excerpt from the book issued by the company Ingold Messtechnik AG, called "Practice and Theory of pH Measurement"⁵³.

Determining pH Values

The pH is defined as the negative (decade) logarithm of the H⁺ ion concentration, i.e.:

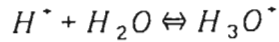
$$pH = -\log c_H.$$

If the H⁺ ion concentration changes by the factor of ten, the pH value changes by one unit. This illustrates how important it is to be able to measure the pH value to a tenth of a unit (or even a hundredth of a unit in critical cases).

The above definition of the pH value is sufficiently accurate only for dilute solutions, since only then are the solution's concentration and activity equal.

In many cases, however, the activity coefficient is smaller than one (the activity coefficient of the hydrogen ion is not measurable in real solutions). In order to overcome these difficulties, the pH values of a number of buffer solutions were, with the help of theoretically substantiated provisions and precision readings, defined, and thus the conventional pH scale was established. The corresponding work was mainly carried out by Bates at the National Bureau of Standards in the U.S.A.

It is common to refer to H^+ ions in connection with pH values, although the correct term is the hydronium (oxonium) ion (H_3O^+):



The hydrogen ion normally exists in its associated form:

$$\frac{a_{H^+} \cdot a_{OH^-}}{a_{H_2O}} = \text{constant}$$

Due to the low dissociation degree of water, a_{H_2O} may be considered a constant in the above equation, thus:

$$a_{H^+} \cdot a_{OH^-} = K_w = 10^{-14} (\text{mol/l})$$

whereby K_w is known as the **ion product** of water.

When $a_{H^+} = a_{OH^-}$ a solution is neutral, which corresponds to a pH of 7.

Very soon it was found that not the H^+ concentration, but its activity is decisive in determining the pH value.

The activity of the hydrogen ion can be defined by its relation to the concentration (molarity $c = \text{mol/l}$; molality $b = \text{mol/kg}$ solvent) and to the activity coefficient (γ_{H^+}):

$$a_{H^+} = \gamma_{H^+} \cdot b_{H^+}$$

In dilute solutions, $a_{H^+} = b_{H^+}$.

Temperature (T), ion strength (I), dielectric constant, ion charge (z), the size of the ions (in Angstroms), as well as the density (d) of the medium are factors which influence the activity constant.

All these factors link ion activity with ion concentration through two effects. One is the so-called salt effect γ_{H^+} , which is expressed as follows:

$$\log \gamma_{H^+} = \frac{-0.5I^{\frac{1}{2}}}{1 + 3I^{\frac{1}{2}}}$$

whereby:- $I = \text{total ionic strength} = \frac{1}{2} \sum c_i z_i^2$.

If we assume that both the anion as well as the hydrogen ion are monovalent, z_i will be equal to 1. Thus the molality remains the main factor in calculating the ion strength.

The following table shows the influence of the salt effect on the activity coefficient at different molalities.

Approximate Salt Effect (γ_{H^+})					
Molality	0.001	0.005	0.01	0.05	0.1
Activity Coefficient	0.964	0.935	0.915	0.857	0.829

Examples:

0.01m HCl solution :-

$$\begin{aligned} \text{pH} &= -\log(b_{H^+} \cdot \gamma_{H^+}) \\ &= -\log(0.01 * 0.915) \\ &= -\log(9.15 \cdot 10^{-3}) \\ &= 2.04 \end{aligned}$$

0.01m HCl solution with 0.09m KCl:-

$$\begin{aligned}
\text{pH} &= -\log(b_{H^+} \cdot \gamma_{H^+}^x) \\
&= -\log(0.01 * 0.829) \\
&= -\log(8.29 \cdot 10^{-3}) \\
&= 2.08
\end{aligned}$$

Hence the pH value increases by 0.04 pH units (the H⁺ activity decreases) in solutions with a higher ion strength. This explains why solutions with the same H⁺ concentration may show different pH values if their ion strengths are different.

The second effect which links activity to concentration is the so-called medium effect: $\gamma_{H^+}^m$. This effect shows what influence the medium (solvent, etc) will have on the H⁺ ion activity. Here electrostatic and chemical interactions play an important role. For instance, the H⁺ activity is 200 times greater in ethanol than in water.

Aqueous standard buffers are generally used to calibrate pH measuring chains. Therefore, it is not possible to find a correlation between the H⁺ activity in an aqueous and in a non-aqueous solution.

The next equation shows the relationship amongst activity, concentration, salt effect and medium effect:

$$a_{H^+} = \gamma_{H^+}^x \cdot \gamma_{H^+}^m \cdot b_m$$

CONCLUSION

THE MORE ACCURATELY DEFINED THE MEASURING CONDITIONS ARE, THE MORE REPRODUCIBLE ARE THE pH VALUES OBTAINED.